The Role of Hoxa2 and Characterization of its New Downstream Targets in Murine Palatogenesis

A Thesis Submitted to the College of Graduate Studies and Research

in Partial Fulfillment of the Requirements for the Degree of Doctor of

Philosophy in the College of Pharmacy and Nutrition

University of Saskatchewan

Saskatoon

By Tara Marie Smith

PERMISSION TO USE

In presenting this thesis in partial fulfillment of the requirements for a Doctor of Philosophy degree from the University of Saskatchewan, I agree that the Libraries of this University may make it freely available for inspection. I further agree that permission for copying this thesis in any manner, in whole or in part, for scholarly purposes may be granted by Dr. Adil J. Nazarali, the professor who supervised my thesis work, or in their absence, by the Dean of the College of Pharmacy and Nutrition in which my thesis work was done. It is understood that any copying or publication, or use of this thesis or parts thereof for financial gain shall not be allowed without my written permission. It is also understood that due recognition shall be given to me and to the University of Saskatchewan in any scholarly use which may be made of any material in my thesis.

Requests for permission to copy or to make use of material in this thesis in whole or in part should be addressed to:

Dean of the College of Pharmacy and Nutrition

University of Saskatchewan

110 Science Place

Saskatoon, Saskatchewan

S7N 5C9

Abstract

*Hoxa*2 null embryos display a high incidence of cleft secondary palate which has previously been described as secondary to altered tongue development. The experiments described in this thesis demonstrate that expression of *Hoxa*2 does occur within the developing palate, with the highest levels appearing in the early stages of palatogenesis (E12.5 and E13.5). Increased cell proliferation was observed throughout the palate in the absence of *Hoxa*2, without a detectable difference in apoptosis or the ability of the shelves to fuse. In addition, the palate shelves of the null embryos failed to elevate above the tongue, suggesting a mechanism by which the increased cell proliferation results in cleft palate.

Numerous downstream targets of Hoxa2 were also identified in the palate (*Msx1*, *Bmp4*, *Barx1*, *Ptx1*, *Six2*, *Lef1* and *Tbx1*). In all cases, Hoxa2 appears to act as a transcriptional repressor. Increases in palatal Msx1, Bmp4 and Barx1 expression have all been previously described to lead to increases in cell proliferation. Hoxa2, Ptx1, Lef1 and Tbx1 may be involved in a novel pathway that regulates proliferation in the palate. In addition, three novel gene targets were identified in the palate, Six2, Fgf8 and Htra3.

Together these data show that there is a direct role for Hoxa2 in regulating palate development, apparently through regulating the expression of downstream genes involved in maintaining normal cell proliferation rates.

Acknowledgments

This thesis would not have been possible without the support of many individuals. I would like to thank Dr. Adil Nazarali for his guidance and support over the past five years, in both my professional and personal life. I would also like to thank my committee members, Dr. William Kulyk, Dr. Baljit Singh and Dr. Phyllis Paterson for their support and suggestions throughout this process. Also thanks to my external examiner Dr. Scott Lozanoff for taking time out of his busy schedule to review my research and act on my committee.

I would like to thank the members of my lab especially LaRhonda Sobchishin. She provided constant encouragement and support and acted as a wealth of technical information. Thank you to my fellow graduate students especially Erin Prosser-Loose and Barbara McEwen with whom I have developed a special friendship due to the incredible ups and downs that grad school as put us through together.

Dedication

This is dedicated to my ever supportive family. To my mother, Elaine Smith, who taught me how to be a strong, confident woman that when she puts her mind to it can do anything. To my father, Curt Smith, who has been behind me everyday with love and encouragement. To my sister, Shari Smith, who constantly reminds me what is important in life. Finally to my husband, Scott Caswell, who has been there for me through all the ups and downs of the past couple of years, and whose confidence in me has never waivered.

Table of Contents

List of Figures

List of Abbreviations

Alk	Activin receptor-like kinase
ANOVA	Analysis of variance
AP	Activating protein
BA	Branchial Arch
Barx	BarH-like homeobox
Bmp	Bone morphogenic protein
BGJb	Biggers, Gwatkin and Judah Media, Fitton-Jackson Modification
bp	Base pairs
BrdU	5-Bromo-2'-deoxyuridine
C	Celsius
cDNA	complementary DNA
ChIP	Chromatin Immunoprecipitation
c-myc	myelocytomatosis viral oncogene homolog
CNCC	Cranial neural crest cell
CO_2	Carbon dioxide
Ct	Threshold cycle
DMEM	Dublecco's modified eagle medium
Dlx	Distal-less homeobox
DNA	Deoxyribonucleic acid
dNTP	Deoxyribonucleotide triphosphate
dUTP	2'-deoxyuridine
E	Embryonic day

EDTA	Ethylenediamine tetraacetic acid
EGF	Epidermal growth factor
EMSA	Electrophoretic Mobility Shift Assay
ERK	Extracellular signal-regulated kinase
Etv	ETS variant
Eya	Eyes absent
Fgfs	Fibroblast growth factors
Fgfr	Fibroblast growth factor receptor
Fig.	Figure
FNP	Frontonasal prominence
GABA	γ-aminobutyric acid
Gad 67	Glutamic acid decarboxylase 67
Gdnf	Glial-cell-line derived neurotropic factor
Gli	Gli-Kruppel family zinc finger
h	hours
HCl	Hydrochloric Acid
HEPES	N-2-Hydroxyethylpiperazine-N′-2-Ethanesulfonic acid
HOM-C	Homeotic complex in *Drosophila*
Hox	Homeobox
Htra	High temperature requirement factor a
IDV	Integrated density value
i.e.	id est “that is”

IgG	Immunoglobulin G
kDa	kiloDalton
kg	kilogram
KO	Knockout genotype
Lef	Lymphoid enhancer factor
Lhx	LIM homeobox factor
LNP	Lateral nasal prominence
M	Molar
mM	Millimolar
MAPK	Mitogen-activated protein kinase
MDP	Mandibular prominence
MEF2C	Myocyte enchancer factor 2C
MEK	MAPK/ERK kinase
Meis	Myeloid ecotropic insertion site genes
Meox	Mesenchyme homeobox
MES	Medial epithelial seam
mg	milligrams
min	Minutes
MNP	Medial nasal prominence
mRNA	messenger ribonucleic acid
Msx	msh-like
MXP	Maxillary prominence

n	Number of samples
ng	Nanogram
nM	Nanomolar
NaCl	Sodium chloride
NCC	Neural crest cell
OCT	Optimal cutting temperature
Pax	Paired box gene
PBS	Phosphate buffered saline
Pbx	pre-leukocyte B cell homeobox
PCR	Polymerase chain reaction
pg	Page
Prep	Pbx regulating protein
Ptc	Patched
Ptx	Paired like homeodomain transcription factor
PVDF	Polyvinylidene difluoride
r	rhombomere
RIPA	Radio immuno precipitation assay buffer
RNA	Ribonucleic acid
Ror	Receptor tyrosine kinase-like orphan receptor
RQ	Relative quantification
RT	Reverse transcription
RT-PCR	Reverse transcriptase polymerase chain reaction

s	Seconds
SARA	Smad anchor for receptor activation
SDS	Sodium dodecylsulphate
SEM	Standard error of the mean
Shh	Sonic hedgehog
Shox	Short stature homeobox
siRNA	Small interfering ribonucleic acid
Six	Sine oculis homeobox homolog
Smo	Smoothened
SM-PBS	Skim milk in phosphate buffered saline
SM-PBST	Skim milk in phosphate buffered saline with 1% Triton X-100
Sox	SRY-like HMG-box gene
Spry	Sprouty
Tbx	T-box protein
Tβr	Transmembrane serine/threonine kinase receptor
Tgf	Transforming growth factor
TGF-β	Transforming growth factor β
Tp63	Tumor protein p63
TUNEL	Terminal deoxynucleotidyl transferase-mediated dUTP nick end labeling
U	Units
µl	Microlitre

µm	Micrometer
µM	Micromolar
UV	Ultraviolet
Wnt	Wingless
Wt	Wild-type
Italics	Denotes the gene or mRNA form
Normal	Denotes the protein form

1.0 Introduction

Cleft palate is one of the most common congenital birth defects in the human population, occurring with a frequency of 1:400-1000 (Gorlin et al., 2001). A complex network of interaction between signalling molecules is required for the proper growth and development of the palate shelves. In the embryonic mouse, secondary palate development begins at E11.5 with the palate shelves budding out of the maxillary prominences. From that point until E14.0 the palate shelves grow vertically down either side of the tongue. At E14.0, the tongue drops and the palates undergo a rapid elevation to become oriented horizontally above the tongue and then grow together and contact at E14.5 at which point the palate shelves fuse together to form a complete palate (Ferguson, 1988). Defects at any stage of this tightly regulated developmental process can result in a cleft secondary palate.

Hoxa2 has been shown to be the selector gene for the second branchial arch (Grammatopoulos et al., 2000; Hunter and Prince, 2002; Pasqualetti et al., 2000; Santagati et al., 2005) while being completely absent from the first branchial arch from which the secondary palate is derived (Prince and Lumsden, 1994). The absence of *Hoxa2* expression in the first branchial arch suggested that it could not play a direct role in palatogenesis despite an 81% incidence of cleft palate in *Hoxa*2 null embryos. Therefore, altered tongue musculature was suggested as the defect resulting in the observed cleft (Barrow and Cappechi, 1999; Gendron-Maguire et al., 1993; Rijli et al., 1993).

Recently, *Hoxa2* expression was reported in the developing palate suggesting a more direct role for the gene in regulating palatogenesis (Nazarali et al., 2000). Further analysis of any potential role of *Hoxa2* in the development of the palate is required.

The regulation of the growth and development of the secondary palate has been shown to be dependent on a complex network of signalling pathways that have been intensely investigated (reviewed in Gritli-Linde, 2007). The expression of many of these genes display closely regulated localized expression. In many cases these genes are epithelial or mesenchymal specific. In addition, a number of genes display specific localization along the anteroposterior axis of the palate. Distinct pathways have been shown to be involved in regulating the growth, elevation and the fusion of the palate shelves. There is a possible role for *Hoxa*2 in the regulation of these complex pathways but this has not previously been investigated and has been addressed in this thesis.

2.0 Hypothesis

*Hoxa*2 has one or more downstream targets within the developing murine palate, and through regulating the expression of these genes, *Hoxa*2 acts to maintain normal cell proliferation within the palate.

Objectives

1. To determine whether *Hoxa*2 plays an important role in the regulation of any or all of the following processes within the developing murine palate:
    - Cell proliferation
    - Cell survival or apoptosis
    - Fusion and degradation of the medial edge epithelium
2. To determine putative downstream targets of *Hoxa*2 in the murine palate involved in one or more of the processes outlined in objective 1.
3. To determine if *Hoxa*2 affects the expression of its putative downstream target genes in the developing palate.

3. Literature Review

3.1 Overview of Craniofacial Development

Development of the face requires precise coordination of the growth, differentiation and convergence of numerous populations of cells called facial prominences/processes (Helms et al., 2005). The patterning of the face begins significantly before the overt growth of these facial prominences. Early in vertebrate development the anterior region of the neural tube differentiates into the forebrain (prosencephalon), midbrain (mesencephalon) and the hindbrain (rhombencephalon) (Gilbert, 2003; Lumsden and Keynes, 1989). The ectodermal neural folds of the neural tube located between the neuroectoderm and the epidermis then undergo a transition from ectoderm to mesenchyme. These ectomesenchymal cells, called neural crest cells (NCC), are pluripotent and as such can give rise to a range of diverse tissue types (reviewed in Gammill and Bronner-Fraser, 2003; Le Douarin and Kalcheim, 1999) (Fig. 1). As embryonic development proceeds the hindbrain becomes further segmented into smaller compartments called rhombomeres. The rhombomeres represent distinct populations of cells that do not mix with cells from other compartments (Guthrie and Lumsden, 1991; Guthrie et al., 1993). These cells also express distinct subsets of genes that lead to different developmental fates (Fraser et al., 1990).

3.2 Cranial Neural Crest Cell Migration

Migration of cranial neural crest cells (CNCC) gives rise to the bulk of the

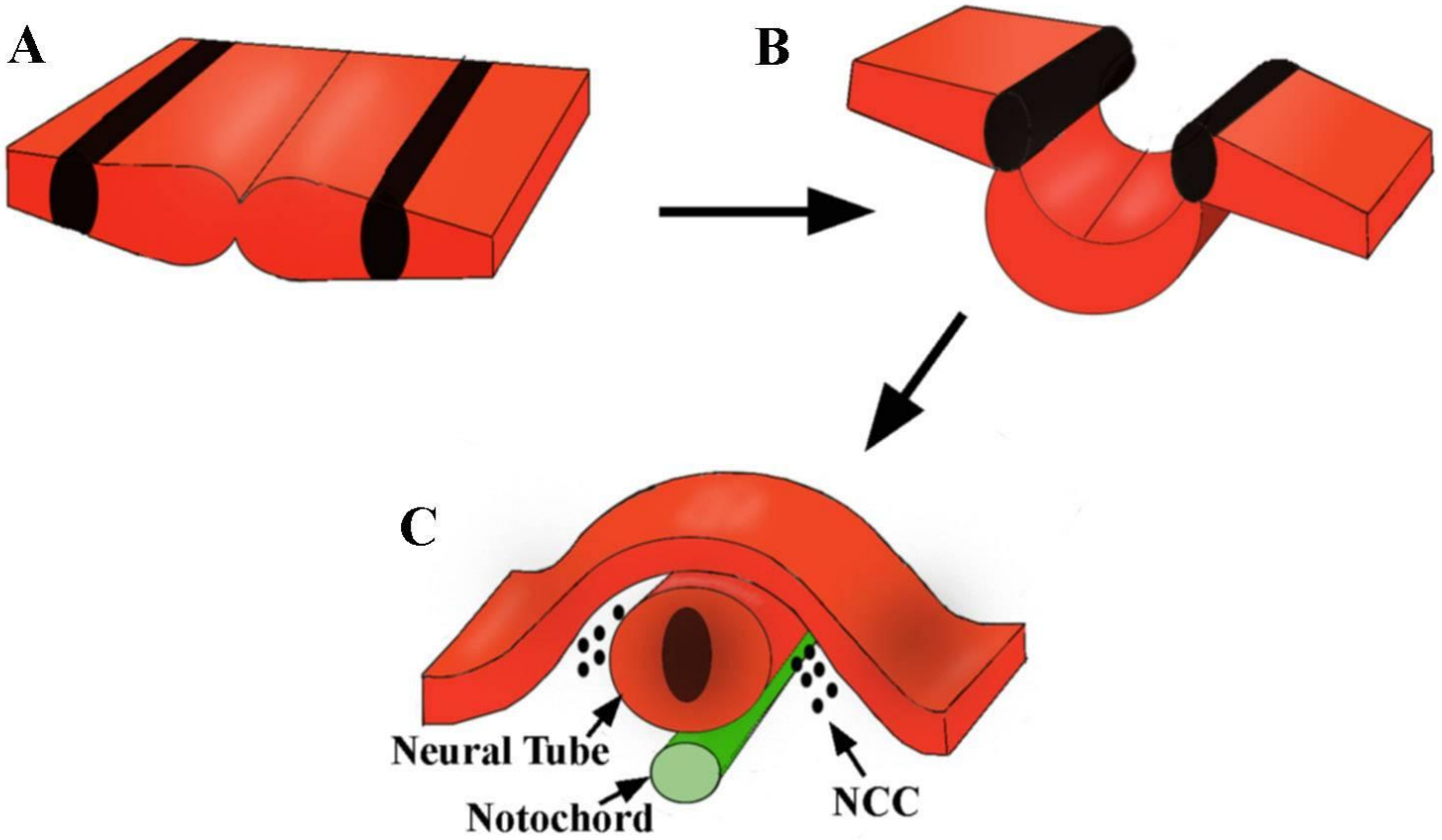
A
B
C
Neural Tube
Notochord
NCC

Figure 1. Schematic Representation of Neural Crest Formation.

The above is a schematic representation of an amniote embryo. A) Represents the stage following the development of the primitive streak denoted by the depression in the center. The area in between the black represents the neuroectoderm. B) The neuroectoderm then fold at the neural folds (black), which contact one another and fuse forming the neural tube. C) The neural crest cells originate from the junction between the epidermal ectoderm and the presumptive neural ectoderm, and then migrate away from the neural tube to form a variety of structures throughout the developing embryo. Adapted from Gilbert, 2003.

cells that compose the face (Gammill and Bronner-Fraser, 2003). Establishment of the anteroposterior axis of the embryo as well as directing the migration of CNCC is believed to be regulated by the expression of homeobox (*Hox*) genes (reviewed in Noden and Trainor, 2005; Santagati and Rijli, 2003; Trainor and Krumlauf, 2001). *Hox* genes are differentially expressed between rhombomeres and in general migrating CNCC express the same subset of *Hox* genes as the rhombomeres from which they arose (Helms et al., 2005; Le Douarin et al., 2004; Noden and Trainor, 2005). Further description of the expression and function of *Hox* genes will be discussed in section 3.5 (pg. 46).

Five facial prominences/processes [the frontonasal process (FNP), a pair of maxillary processes (MXP) and a pair of mandibular processes (MDP)] act as the building blocks of the vertebrate face (Fig. 2). Each of these processes is composed of migrating CNCC with a core of mesoderm cells and is overlaid by surface ectoderm. CNCC will go on to become the facial skeleton while the mesoderm cells will eventually compose the facial musculature (Noden, 1983; Noden, 1988; Noden and Trainor, 2005). The FNP is comprised of CNCC from the mesencephalon migrating over the prosencephalon. Migrating CNCC from the posterior mesencephalon as well as rhombomeres form the six branchial (pharyngeal) arches (Fig. 2). These arches are separated externally by visible ectodermal grooves as well as internally by endodermal pharyngeal pouches (Sperber and Sperber, 2009). CNCC from the posterior mesencephalon and rhombomeres 1 and 2 populate the first


r1
r2
r3
r4
r5
r6
r7
BA1
BA2
BA3

Figure 2. Schematic Representation of Facial Development

Schematic representation of the development of the murine face, from the stage of branchial arch (BA) development to the completed face. The face is developed from the growth and convergence of five facial prominences. The frontonasal prominence (yellow) originates from the mesencephalon and forms the forehead and portions of the nose. The maxillary prominence (green) is derived from rhombomere 1 & 2 contributes to the formation of the upper lip and primary palate. The mandibular prominence (blue) forms the lower lip, mandible and the anterior portion of the tongue. The nose is composed primarily of the medial nasal prominence (purple) and the lateral nasal prominence (red) which are differentiated from the FNP.

branchial arch. The first branchial arch gives rise to the MXP and MDP. The second branchial arch is populated from CNCC migrating from the fourth rhombomere and goes on to form the stapes and styloid process (bones of the middle ear) and the hyoid bone to which the tongue muscles attach. The third and fourth branchial arches are composed of CNCC from rhombomeres 6-8 (Bronner-Fraser, 1993; Lumsden and Krumlauf, 1996; Osumi-Yamashita et al., 1990; Selleck et al., 1993; Serbedzija et al., 1992). The cells in rhombomeres 3 and 5 undergo massive apoptosis prior to migration and therefore do not significantly contribute to populating any of the branchial arches (Graham et al., 1993).

3.3 Facial Development

The convergence of the facial prominences is responsible for forming the embryonic face (reviewed by Jiang et al., 2006; Sperber and Sperber, 2009). The center of the developing face is the primitive mouth or stomodeum. The stomodeum is a central depression lined by the oropharyngeal membrane. This membrane marks the boundary between the endoderm of the future throat and the ectoderm of the future mouth. This central feature of the face is surrounded by the outgrowths of the facial prominences. Rostrally the stomodeum is bordered by the FNP, laterally it is the MXPs and caudally the MDPs (Ferguson et al., 2000; Hinrichsen, 1985)(Fig. 2).

The FNP contributes to the formation of the embryonic forehead and nose. This process begins with the development of bilateral nasal placodes

formed from the inferolateral corners of the FNP. These nasal placodes then appear to sink as the medial nasal prominences (MNP) and lateral nasal prominences (LNP) elevate forming a horseshoe shaped structure that surrounds the bilateral nasal pits (Hinrichsen, 1985; Sperber, 2002b). As development proceeds the LNPs will continue to elevate to form sides (alae) of the nose (Ohbayashi and Eto, 1986). Growth of the MXPs acts to force together the MNPs and LNPs resulting in the nasal pits appearing more like slits than the widely spaced nostrils. Fusion of the MNPs and the LNPs completes the formation of the nostrils (Gaare and Langman, 1977; Hinrichsen, 1985; O'Rahilly, 1967). The posterior portion of each of the nasal pits is originally separated from the oral cavity by the presence of a transient oronasal membrane. At the end of the fifth week of human embryonic development this membrane disappears, allowing the nostrils to be connected to the posterior oral cavity (Sperber, 2002b).

Growth of the MXPs towards the midline results in fusion between the MNPs and the MXPs and in the formations of the tip of the nose, the upper lip and the primary palate (Hinrichsen, 1985; Ohbayashi and Eto, 1986; Sperber, 2002b; Trasler, 1968)(Fig. 2). Closure of the wide stomodeum results from the growth and fusion of the MXPs and the MDPs, which form the corners of the embryonic mouth. Fusion of the MDPs is responsible for the formation of the lower lip, mandible and the anterior part of the tongue (Hinrichsen, 1985; Yoon et al., 2000). The bilateral lens placodes are the result of invaginations of the

optic placodes and evaginations of the diencephalon. CNCC migrate around these placodes forming the sclera and choroid optic coats as well as the FNP (Adler and Canto-Soler, 2007) . Narrowing of the FNP in conjunction with expansion of the lateral areas of the face leads to migration of the eyes towards the midline (Sperber, 2002a). Bones and cartilage of the inner ear are the result of migration of CNCC from the first and second branchial arches (Gendron-Maguire et al., 1993; Noden, 1983; Rijli et al., 1993).

3.3.1 Secondary Palate Development

Along with the primary palate, the secondary palate acts to form a barrier between the oral and nasal chambers. This separation is an evolutionary advancement over the single chamber seen in reptiles and birds (Chong el al., 2002; Sperber et al., 2002). Bilateral palate shelves first develop as outgrowths from the inner side of maxillary processes at embryonic day 11.5 (E11.5) in mice (6^{th} week of gestation in humans), extending along the lateral walls of the stomodeal chamber (Fig. 3). The shelves then grow vertically down either side of the tongue until E14.0 (8^{th} week of gestation in humans) (Ferguson, 1988; Berkovitz,et al., 2002). At this point the shelves undergo a rapid elevation to become horizontally oriented towards one another above the tongue (Brinkley, 1980; Ferguson, 1978). Growth of the stomodeum, as well as functional neuromuscular and jaw joint activity makes it possible for the embryo to have mouth opening reflexes. These movements allow the tongue to flatten and depress to a point below the edges of the downward positioned palate shelves

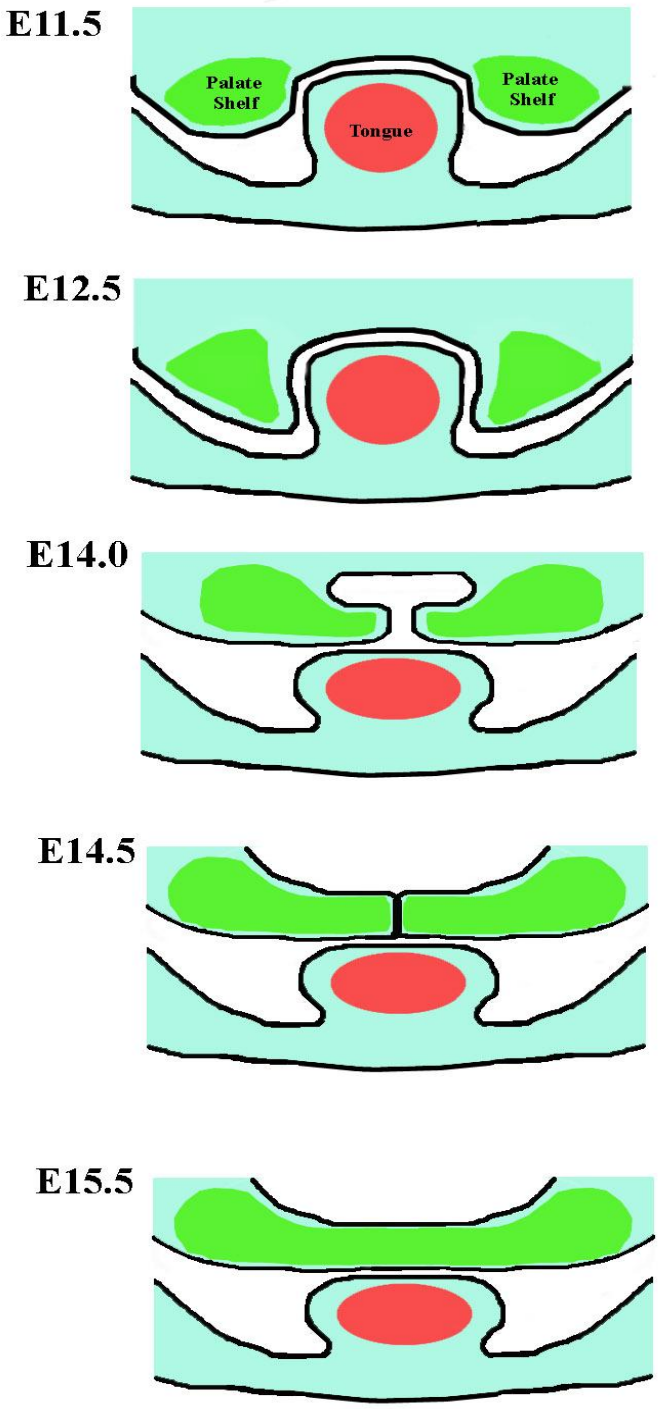
E11.5
Palate Shelf
Palate Shelf
Tongue
E12.5
E14.0
E14.5
E15.5

Figure 3. Schematic Diagram of the Stages of Palatogenesis

Palate shelves are denoted by the green colour while the tongue is coloured red. Embryonic ages reflect the timing of the events in the developing mouse embryo. Palate shelves arise out of the maxillary prominences (E11.5), they grow vertically down the sides of the tongue before elevating above the tongue at E14.0 and then contacting one another and fusing.

allowing them to reorient (Diewert, 1980; Humphrey, 1969). The palate shelves also undergo a number of changes in order to facilitate the move from a vertical position to a horizontal position. The mechanism of elevation of the palate shelves is unclear, some of the predicted mechanisms are: a change in the consistency of the palate shelves through an increase in extracellular matrix components including hyaluronic acid (Brinkley and Morris-Wiman, 1984; Brinkley and Morris-Wiman, 1987; Ferguson, 1978; Larsson et al., 1959; Pratt et al., 1973; Singh et al., 1994; Singh et al., 1997), variations in blood flow to the palate shelves (Amin et al., 1994), increased cell proliferation and change in morphology in specific regions of the mesenchyme (Babiarz et al., 1979; Brinkley, 1980; Brinkley and Bookstein, 1986; Bulleit and Zimmerman, 1985; Greene and Pratt, 1976; Greene and Pratt, 1976; Innes, 1978). The elevated palatal shelves then grow towards one another until the medial edge epithelium from each shelf contacts to form the midline epithelial seam (MES) at E14.5. In addition to growth of the palate shelves, a change in the relative dimensions of the head (vertical dimensions of the head increases while the lateral maxillary width remain constant) allows the palate shelves to contact one another at the midline (Diewert, 1978; Diewert, 1983). Epithelial cells from opposing palate shelves adhere to one another through glycoproteins on their surface (Greene and Kochhar, 1974; Greene and Pratt, 1976; Pratt and Hassell, 1975; Souchon, 1975) as well as through desmosomes (De Angelis and Nalbandian, 1968; Morgan and Pratt, 1977). Contact of the palate shelves and their subsequent

fusion begins in the mid-palate regions and precedes both anteriorly and posteriorly like a zipper (Ferguson, 1988; Morgan and Pratt, 1977). The MES then undergoes a rapid degradation to form a secondary palate with complete mesenchymal confluence (Berkovitz et al., 2002; Ferguson, 1988). The mechanism of midline epithelial seam degradation is still unclear and may require any or all of the following: epithelial apoptosis (Farbman, 1968; Martinez-Alvarez et al., 2000; Pourtois, 1966; Saunders, 1966; Shuler, 1995; Xu et al., 2006), migration (Carette and Ferguson, 1992; Martinez-Alvarez et al., 2000; Shuler et al., 1992), and epithelial-mesenchymal transformation (Cui et al., 2005; Fitchett and Hay, 1989; Griffith and Hay, 1992; Kaartinen et al., 1995; Proetzel et al., 1995; Shuler et al., 1992; Sun et al., 1998). Mesenchymal confluence signals the end of palatogenesis at E15.5 (Ferguson, 1988). In addition to fusion to one another, the anterior secondary palate fuses to the primary palate and the dorsal portions of the secondary palate fuses with the nasal septum (Ferguson, 1988).

After the palate shelves have fused, the area undergoes further differentiation to form the completed palate. The dorsal or nasal surface of the palate will be lined with ciliated columnar respiratory epithelial cells, while the ventral or oral side of the palate will develop stratified squamous epithelial cells (Carette et al., 1991). Anterior and posterior regions of the palate also undergo distinct differentiation. The anterior portion of the palate undergoes ossification beginning during the 8^{th} week post fertilization in humans (E14 in mice).

Intramembranous ossification begins at primary centers in the maxillae and palatine bones and proceeds out centrifugally, eventually creating the entire hard palate (Kjaer, 1992; Sildu et al., 1994). The posterior palate does not ossify and is known as the soft palate (Cohen et al., 1993)

Defects at any step in the developing palate have been shown to result in cleft palate. In addition to problems with development of the palate proper, defects in the development of other craniofacial elements including the tongue and mandible can result in a cleft palate.

3.3.1.1 Cleft Palate

Cleft palate is one of the most common congenital birth defects in the human population occurring with a frequency of 1:400 to 1:1000 live births (Gorlin et al., 2001). A cleft secondary palate can occur as an isolated birth defect (non-syndromic), in conjunction with a cleft lip or as a part of another syndrome (syndromic).

Altered aesthetics is far from the only problem facing individuals born with a cleft secondary palate. Breathing, eating and speaking are all challenging for these individuals. Numerous surgeries are often required to repair the cleft, as well as improve the general aesthetics of these individuals. In later years, teeth are regularly absent or their development is altered and speaking properly can continue to be an issue. Recent studies have shown numerous other side effects of being born with a cleft palate exist. Individuals with a cleft palate have a significantly shorter lifespan with an increased risk for

all major causes of death (Christensen et al., 2004). Hospitalization for psychiatric illness in adults is also increased in these individuals (Christensen and Mortensen, 2002). It has been speculated that there may be a link between abnormal facial development and abnormal brain development, which would explain the increased incidence of psychiatric illness (Nopoulos et al., 2007). This is supported by the finding that problems with signalling during forebrain development can lead to craniofacial malformations (Marcucio et al., 2005). Clearly the effects of this birth defect are diverse and complex and will require intensive research to help understand and treat the range of associated problems.

A number of genetic and environmental factors have been reported to play a role in the development of cleft palate. Normal palate development requires a tightly regulated and complex network of interactions within and between the epithelium and mesenchyme. Extensive research into the expression and interaction of genes within the developing palate has been conducted by researchers but a complete understanding of their regulation is unclear (reviewed in Gritli-Linde, 2007; Gritli-Linde, 2008).

Cleft palate can occur as a result of defects at numerous stages of development including: (1) failure of the palate shelves to form properly; (2) failure of the palate shelves to grow together and contact at the midline epithelial seam due to altered cell proliferation or apoptosis; (3) failure of the contacted palate shelves to fuse and gain mesenchymal confluence; (4) failure

of the palate shelves to contact one another due to a physical barrier, such as the tongue, obstructing their access to one another (Ferguson, 1987).

3.4 Molecular Signalling within the Palate

During mammalian embryogenesis the development of the secondary palate is regulated by a complex network of signalling pathways (Fig. 4). These pathways work together to tightly regulate critical cellular processes in the palate including: cell proliferation, apoptosis, migration and epithelial-mesenchymal transdifferentiation. It has been well reported that there are numerous pathways that display reciprocal signalling between the epithelium and mesenchyme (reviewed in Gritli-Linde, 2007). Many genes known to be expressed in the palate show specific expression in either the epithelium or mesenchyme but their function is in regulating cellular processes in the other cell population such that there is to and fro signalling between the epithelium and mesenchyme (Nawshad et al., 2007; Rice et al., 2004; Yamamoto et al., 2003; Zhang et al., 2002). In recent years, it has become increasingly evident that gene expression does not only display epithelial-mesenchymal specificity but can also have anterior-posterior or medial-lateral specific expression. In addition to their specifically localized expression, genes have been reported to elicit different responses in different regions of the palate. For example, while Fgf10 acts to promote proliferation in the anterior palate it has no affect on proliferation in the posterior region of the palate (Rice et al., 2004). Due to the number of genes involved in the development of the palate that display very

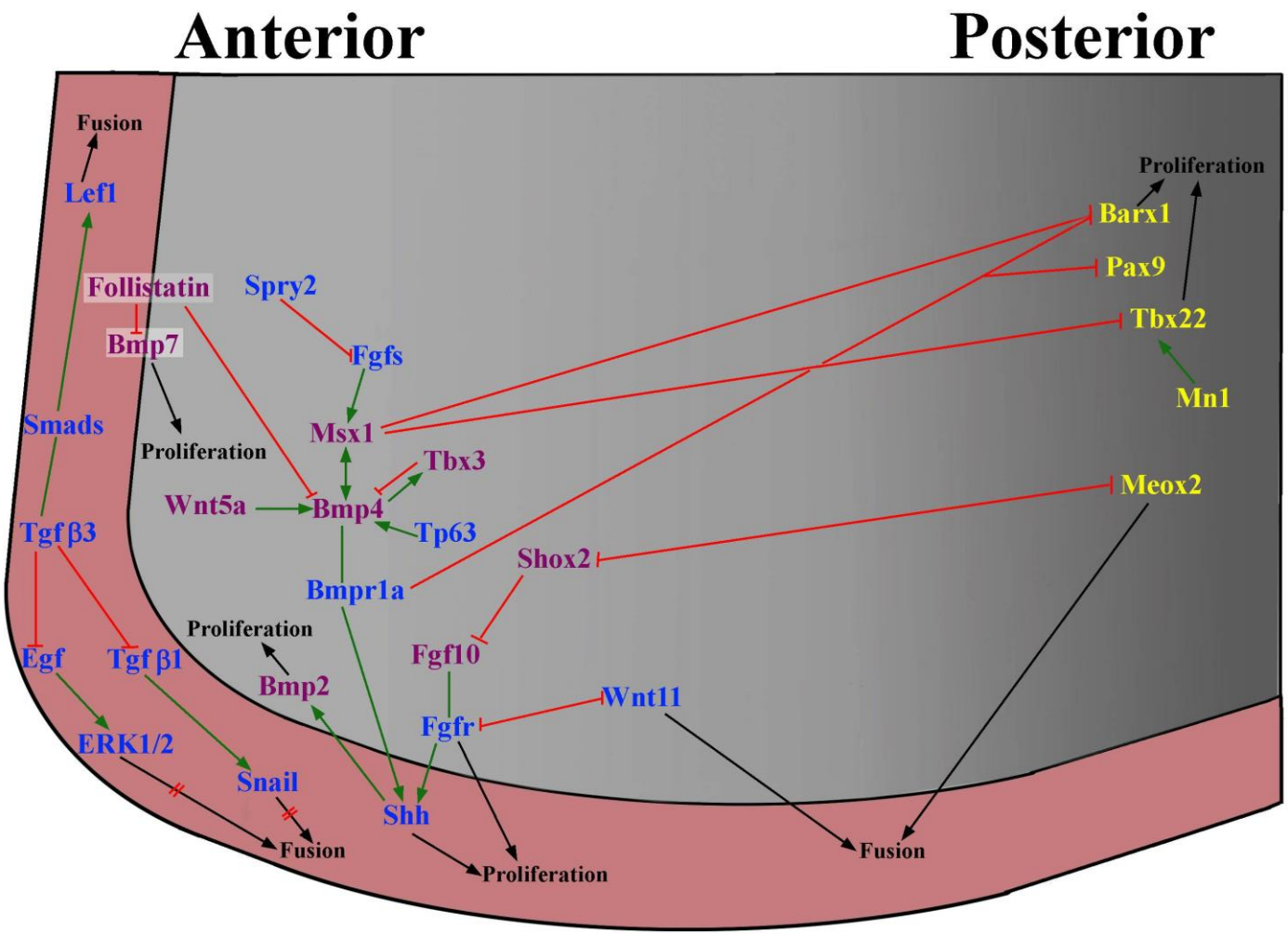
Anterior
Posterior
Fusion
Lef1
Follistatin
Spry2
Bmp7
Fgfs
Smads
Proliferation
Msx1
Tbx3
Wnt5a
Bmp4
Tp63
Tgf β3
Bmpr1a
Shox2
Proliferation
Egf
Tgf β1
Bmp2
Fgf10
Wnt11
Fgfr
ERK1/2
Snail
Shh
Fusion
Proliferation
Proliferation
Barx1
Pax9
Tbx22
Mn1
Meox2
Fusion

Figure 4. Overview of the Signalling Pathways Involved in Regulating Palatogenesis

Schematic representation of the major signalling pathways known to be involved in regulating murine palatogenesis. Green arrows denote activation, while red lines denote repression of one factor on another. Black lines represent the effects of that factor on the denoted process (proliferation or fusion), if crossed by red lines the process is inhibited by the factor. The pink area representing the epithelium, grey represents the mesenchyme. Factors are shown in their relative anteroposterior region of expression, with factors with an exclusively anterior expression pattern in purple, posterior expression indicated in yellow. Expression patterns that are not region specific or are confirmed are shown in blue.

specific regional expression, it is clear that regional differentiation must be occurring within the palate. Although the morphological differences have long been recognized between the different regions of the palate, these localized expression and function phenomena clearly highlight the importance of regional patterning and differentiation within the palate at the molecular level.

Regulation of proliferation, apoptosis, fusion, and cell migration has all been examined in the palate. Each of these processes has been shown to be controlled by a tightly regulated network of genes including signalling molecules, growth factors and transcription factors. The role of a particular gene or signalling pathway can vary depending on the stage of palate development and the location within the palate. It is clear that there is not a single straightforward pathway sufficient to regulate palatogenesis; instead an intricate regulation takes place between all of these signalling pathways in order to ensure palate development occurs normally (Li and Ding, 2007).

3.4.1 Gene Signalling that Regulates Proliferation within the Palate

3.4.1.1 Msx1 Signalling Pathway

The first pathway to be described to play a role in regulating proliferation within the developing palate involves the homeobox transcription factor Msx1. Mutations in the human *MSX1* gene have been linked to isolated non-syndromic cleft palate (Lidral et al., 1998; Van den Boogaard et al., 2000; Vastardis et al., 1996). *Msx*1 deficient mice display neonatal lethality due to a wide open cleft

secondary palate (Houzelstein et al., 1997; Satokata and Maas, 1994). Expression of *Msx*1 is localized exclusively to the anterior mesenchyme during the early stages of palate development. It has been shown to function through regulating the expression of *Bmp4*, *Shh*, and *Bmp2* in the anterior palate. *Msx1* appears to directly activate *Bmp4* expression in the anterior mesenchyme which subsequently signals to the epithelium and activates the expression of *Shh* which then signals back to the mesenchyme and activates *Bmp2* expression (Zhang et al., 2002). In addition to this pathway, it was also shown that *Bmp4* is involved in a reciprocal regulatory cycle controlling the expression of *Msx*1. The main function of *Msx1* and its subsequent signalling pathway appears to be in regulating cell proliferation within the anterior mesenchyme (Zhang et al., 2002). Since this pathway was originally reported, numerous studies have investigated the expression and function of the genes in this pathway. All studies performed to date have confirmed that this pathway is important in anterior mesenchyme proliferation. However, they have determined that the regulation of each of these genes is far more complex than the original pathway suggested.

The regulation of *Msx*1 expression has been linked to many other factors in the palate. Loss of the Fgf antagonist *Spry2* was shown to result in increased *Msx1* expression as well as a posterior expansion of its expression border. This increased expression led to an increase in proliferation within the palate (Welsh et al., 2007). *Msx1* has been shown to be Fgf-responsive in other regions of craniofacial development (Alappat et al., 2003; Bei and Maas, 1998). However,

Fgf10 null palates do not display altered Msx1 expression (Alappat et al., 2005). These data suggest that other Fgfs are likely acting in the palate to regulate *Msx1* expression. It has been proposed Fgf9 may play an active role in palate development (Colvin et al., 1999; Colvin et al., 2001) and that loss of Spry2 may relieve the antagonism of Fgf9 resulting in the observed upregulated and expanded *Msx*1 expression (Welsh et al., 2007). Fgf7 has also been shown to be expressed within the palate mesenchyme (Rice et al., 2004) and could therefore also be involved in regulating *Msx1* expression and may be altered by loss of *Spry2*.

The transcriptional activity of *Msx1* can be altered by other proteins in the palate. *Msx1* has been shown to undergo post-translation modification by sumoylation *in vivo*. This modification was shown to occur in a region of the protein which is responsible for regulating interactions between *Msx1* and other proteins (Gupta and Bei, 2006). Therefore, sumoylation of *Msx1* may help control its ability to interact with other transcription factors and therefore regulate its ability to regulate the expression of other genes. Haplosufficiency of the *SUMO1* gene has been shown to result in cleft palate through altering the sumoylation status of various proteins (*Eya1, Pax9* and *Msx1*) in the palate (Alkuraya et al., 2006).

In addition to regulating *Bmp4* and *Bmp2, Msx*1 has recently been shown to regulate the expression of *Bmp7*. Loss of *Msx*1 leads to a decrease in the anterior palatal expression of *Bmp7*, but an increase in its expression in the

posterior palate. The Bmp antagonist Follistatin is primarily expressed in the anterior palate in a restricted dorsal domain that does not overlap the regions of *Bmp4* and *Bmp2* expression. These restricted expression patterns appear to be the result of Follistatin repressing *Bmp4* and *Bmp2* and regulating its region of action. In addition to increased *Bmp7* expression, *Msx1* null mice also exhibit a decrease in the level of Follistatin expression (Levi et al., 2006). Together, these data highlight the important role for *Msx*1 in the regulation of the Bmp family and their antagonists in the palate and provides another mechanism by which it may regulate the level of proliferation in the anterior palate.

Mutations in the *Dlx5* gene have recently been shown to result in a cleft secondary palate despite the fact that it does not appear to be expressed within the palate proper (Levi et al., 2006). In addition, loss of the transcription factor MEF2C consequently leads to loss of *Dlx*5 expression in the branchial arches resulting in a cleft palate (Verzi et al., 2007). It is known that despite an absence of *Dlx*5 expression within the palate, *Dlx5/Msx1* double knockouts show a partial rescue of the *Msx1* null cleft palate phenotype. It appears that loss of *Dlx5* in *Msx*1 null embryos alters the expression of *Bmp7* and *Follistatin* in the anterior palate in a non-cell autonomous fashion. These data also show that increased *Bmp*7 and decreased *Follistatin* in the anterior palate appear to be able to compensate for the loss of *Bmp4* expression and partially rescue the cleft palate phenotype seen in *Msx*1 null mice, likely through allowing for somewhat normal proliferation to take place in the anterior palate (Levi et al.,

2006). It is unclear whether *Dlx*5 plays a role in regulating the growth and development of other craniofacial structures which impact palate development.

3.4.1.2 Bone Morphogenic Protein Signalling Pathways

Bmp4 has been known to be downstream of *Msx*1 in the palate for many years (Zhang et al., 2002), and as with *Msx1,* many alternative regulatory pathways have been elucidated for *Bmp4* in recent years. The transcription factor *Tbx*3 shows an overlapping expression pattern with *Bmp4* in the developing anterior palate mesenchyme. These two genes have been reported to regulate each others expression in the palate whereby *Tbx*3 can act to inhibit the expression of *Bmp4* while *Bmp4* acts by inducing the expression of *Tbx*3. As expected based on the previously reported role of Bmp4 in the palate, this regulatory loop acts by regulating the levels of cell proliferation in the anterior palatal mesenchyme (Lee et al., 2007). In the limb, it has previously been reported that *Tbx3* expression is dependent on *Bmp*4 (Tumpel et al., 2002) and that it plays an important role in maintaining normal proliferation in the region (Davenport et al., 2003). *Tbx*3 null embryos, however, do not display a cleft palate and therefore its ability to repress *Bmp4* expression and subsequently regulate proliferation may be redundant with another regulatory mechanism in the palate.

At the initial onset of palate development the transcription factor Tp63 was found to regulate the expression of *Bmp4* in the anterior palate. Loss of the *Tp63* gene leads to cleft palate through altering the expression of a variety

of genes (including *Bmp4*) in the maxillary processes from which the palatal shelves emanate. This altered gene expression results in defects of the anterior-posterior axis as well as the onset of palate development (Thomason et al., 2008). These results show that regulation of gene expression during and prior to the overt growth of the palate shelves can influence palate development and patterning.

Bmp4 acts upstream of *Shh* and *Bmp2* within the palate (Zhang et al., 2002). Recently it was shown that the Wnt5a signalling molecule is involved in regulating the anterior-posterior axis in the palate, including the expression of *Bmp4*. In the absence of the Wnt5a signalling, *Bmp4* expression is downregulated in the anterior palate while being ectopically upregulated in the posterior palate. As expected, similar changes were observed in the expression profile of *Shh*. Two interesting findings involving this pathway were also reported. The first is that *Bmp2* expression was unaltered in the *Wnt5a* null mutants. These data implied that *Bmp2* expression in the palate must be regulated by an alternative mechanism than the one described previously (section 3.4.1.1, page 22). The second finding was that despite a decrease in *Bmp4* and *Shh* expression, proliferation was increased in the anterior mesenchyme (He et al., 2008). This once again suggests that the regulation of anterior palate development is more complex than initially reported and involves the cooperation of multiple signalling pathways.

It has been well recognized that the Bmp family plays an important role in maintaining the anterior-posterior axis of the palate shelves as well as regulating proliferation. The Bmp ligands are not the only members of the family that are important in palatal development, but they also regulate expression and cell processes through binding to cellular receptors. The Bmp receptor Bmpr1a has been reported to be essential in the regulation of proliferation and patterning in the palate. Loss of the *Bmpr1a* gene leads to decreased proliferation as well as an anterior shift in the expression patterns of the posterior specific genes *Pax9* and *Barx*1. The expression of *Msx1* was unaltered in the *Bmpr1a* mutants (Liu et al., 2005). This suggests that other Bmp receptors function in the palate which allow for the regulation of *Msx*1 by Bmp4. Additionally, a novel role for *Bmp4* and potentially other Bmps acting through the *Bmpr1a* receptor is to regulate the spatial expression of posterior specific genes.

3.4.1.3 Sonic Hedgehog Signalling Pathway

Sonic hedgehog (Shh) is expressed in the epithelium throughout palatogenesis. Expression is restricted to a striped pattern that corresponds to the areas of the epithelium that thickened (Rice et al., 2006). These areas go on to form the rugae on the oral surface of the palate. It has been suggested that these rugae act as centers that coordinate patterning within the palate (Rice et al., 2004). This implies an important role for Shh in the patterning of

the developing palate. Shh is a known downstream target of the Msx1 signalling pathway that has been shown to regulate cell proliferation in the anterior palate (Zhang et al., 2002).

Regulation of the Shh signal is crucial for normal palate development to occur. Loss of the *Spry2* gene leads to a disorganization in the expression pattern of Shh which ultimately leads to deformities in the rugae of these knockout animals (Welsh et al., 2007).

Gli3 is a protein shown to be expressed in the epithelium and mesenchyme along the entire anterior-posterior axis of the palate, and is capable of acting as both an activator and repressor of *Shh* signalling (Huang et al., 2008). In the absence of the Shh signal, the Gli3 protein is processed by protein kinase A allowing it to enter the nucleus and repress the expression of Shh target genes. The presence of the Shh signal prevents the processing of the Gli3 protein and therefore, prevents Gli3 from being capable of repressing the expression of the Shh target genes (Litingtung et al., 2002; Wang et al., 2000). In the limb, the antagonistic relationship between Shh and Gli3 is crucial in setting up the anterior- posterior axis. Gli3 is expressed in the anterior region of the developing limb, where it represses the expression of Shh. dHAND is a posterior specific protein that in the limb that is also repressed by Gli3 but is a known activator of Shh expression. Together this pathway sets up an anterior-posterior axis in the limb that ensures proper development

(Niswander, 2003). The important role of the interaction between Gli3 and Shh plays in the limb, in combination with the expression of both genes in the palate, suggested that there may be a role for Gli3 in the palate. It was therefore not surprising when *Gli3* null mice were found to display a cleft secondary palate. It was however surprising that this cleft palate phenotype does not appear to be the result of changes within the palate itself, but rather due to a defective growth of the tongue (Huang et al., 2008). Clearly, these results show that signalling pathways are not conserved between areas of the developing embryos. Hence, by simply lining up the expression of all of the players in a pathway within the palate does not necessarily imply that they function by a similar mechanism described in other areas of the developing embryo.

3.4.1.4 Sprouty2 Signalling Pathway

In addition to the Bmp family of signalling molecules, the Fgf family plays an important role in palate development. Mutations in numerous members of the Fgf family have been shown to be linked to cleft palate in the human population (Riley et al., 2007). Loss of the Fgf antagonist *Spry2* leads to a cleft palate due to alterations in the level of cell proliferation within the palate, as well as the expression profiles of numerous genes including *Msx1*. This mutation also leads to clear defects in the anterior-posterior patterning of the palate. The posterior expansion of *Msx*1 coincides with a loss of the anterior expansion of the posterior specific transcription factor *Tbx22*. While *Tbx22* expression fails to

reach its normal anterior expression boundary, *Etv5* and *Barx1* which are primarily expressed in the posterior palate expand their domains anteriorly (Welsh et al., 2007). This would suggest that antagonism of Fgfs by *Spry2* affects a number of signalling pathways in the palate leading to gross changes in their expression patterns. Although Fgf signalling is necessary for palate development, it appears that its action must be fine-tuned by repressors in order for proper palatogenesis to occur.

3.4.1.5 Barx1 Signalling Pathway

Barx1 expression has been demonstrated to have a predominantly posterior expression profile which is complementary to the anterior expression of *Msx1*. This region specific expression is initially set up in the branchial arches where *Msx*1 expression is localized to the distal regions of the first brachial arch while *Barx1* expression is localized proximally (Barlow et al., 1999). It is believed that the anterior-posterior axis derived from the region expression of *Barx1* and *Msx1* is the result of the relative strength of Bmp and Fgf signalling (Welsh et al., 2007). The expression of *Barx1* has been shown to be altered in a number of knockout mouse lines. Loss of *Spry2* not only affects *Msx*1 and *Tbx22* expression. It also leads to an anterior expansion of *Barx1* expression which is believed to be involved in the increased cell proliferation seen in these palates (Welsh et al., 2007). The loss of the Bmp receptor *Bmpr1a* also led to an expansion of the region in the palate expressing *Barx1*

(Liu et al., 2005). The fact that alterations in both Fgf and Bmp signalling causes altered *Barx*1 expression supports the theory that regulation of the regional expression of *Barx1* involves both of the families of signalling molecules.

3.4.1.6 Tbx22 Signalling Pathway

Tbx22 has also been described to have a posterior specific expression profile within the developing palate (Herr et al., 2003). The *Tbx22* gene is a T-box protein that acts as a transcription factor regulating the expression of downstream genes. It has been reported that alterations in the *Tbx22* gene can lead to a cleft palate. This has been identified as the most common single cause of cleft palate known to date (Marcano et al., 2004). It has also been shown that a missense mutation in the *Tbx22* gene is responsible for X-linked cleft palate (Marcano et al., 2004). The missense mutation in individuals with X-linked cleft palate has been found to affect the ability of Tbx22 to bind DNA and subsequently act as a transcriptional repressor. It is believed that this mutation prevents the SUMO-1 enzyme from sumoylating the Tbx22 protein. In the absence of this post-translational modification, Tbx22 has a much lower affinity for its DNA binding sequence (Andreou et al., 2007). If Tbx22 can not recognize and bind to its target binding sequence appropriately it is not possible for it to perform its normal repressor functions. Once again an important role in regulating palatogenesis has been assigned to SUMO-1. Based on the number

of important genes known to require sumoylation to function properly, it is not surprising that haploinsufficiency of SUMO-1 leads to a cleft palate (Alkuraya et al., 2006).

Tbx22 expression in the *Spry2* mutants is significantly restricted in *Spry2* mutants. In the absence of this Fgf antagonist the expression of *Tbx22* failed to expand from the most posterior regions of the palate. This altered expression profile coincided with a posterior shift in the expression of *Msx*1 as well as an increase in proliferation throughout the palate shelves (Welsh et al., 2007). It has previously been reported that the 5' regulatory region of the *Tbx22* gene contained putative Msx1 binding sites (Herr et al., 2003). These data suggest that Msx1 is likely involved in repressing the expression of *Tbx22* in the anterior palate, leading to a posterior specific expression pattern in wild-type palate shelves.

A novel molecular pathway involving the *Tbx22* gene was recently described (Liu et al., 2008). Loss of one or both copies of the gene encoding the transcription factor *Mn1* leads to craniofacial abnormalities including a cleft secondary palate. *Mn1* has a medial-posterior specific expression profile that generally overlaps the *Tbx22* expression profile. In the *Mn1* null embryos the expression of the *Tbx22* gene was decreased in the posterior region of the palate and it was determined that Mn1 directly regulates the expression of *Tbx22* in the palate. In addition to a decrease in *Tbx22* expression, there was

also a marked decrease in proliferation in the medial and posterior palate shelves. However, this is believed to be due, at least in part, to the regulation of a separate gene target (*Ccnd2*) by *Mn1* (Liu et al., 2008). This represents the first pathway that specifically regulates the level of proliferation in the posterior palate. Tbx22 expression therefore appears to be regulated by at least two factors within the palate. Msx1 acts as a repressor, while Mn1 acts as an activator and together they determine the specific expression domain of Tbx22 in the posterior region of the palate.

3.4.1.7 Fgf10 signalling pathway

The best understood Fgf-dependent pathway in the palate involves Fgf10 and its receptor Fgf2rb. *Fgf10* null mice exhibit a wide open cleft palate that appears to be due to abnormal palate shelf morphology and size, preventing the shelves from contacting at the midline epithelial seam. In addition, ectopic fusion of the palate shelves to the oral epithelium was observed in some animals, preventing proper shelf elevation (Alappat et al., 2005). Similar to *Msx*1 expression, *Fgf10* is expressed primarily in the anterior palate mesenchyme at the early stages of palatogenesis. The *Fgf10* ligand acts through the receptor *Fgfr2b,* which also shows an anterior specific expression pattern in areas of epithelium adjacent to mesenchyme expressing *Fgf10* (Alappat et al., 2005; Rice et al., 2004). *Shh* expression is downregulated in the epithelium of both *Fgf10* and *Fgfr2b* null embryos. This downregulation directly

leads to a severe reduction in epithelial cell proliferation and consequently a thin epithelial layer. Mesenchymal cell proliferation was also significantly decreased due to a lack of reciprocal *Shh* signalling through its receptor *Ptc*1 (Alappat et al., 2005; Rice et al., 2004). *Msx*1 expression was not altered in Fgf10 null mutants (Alappat et al., 2005), clearly demonstrating that the altered *Shh* expression in the Fgf10 or Fgfr2b null mice is directly due to the loss of Fgf signalling, and not through alterations in the *Msx*1 pathway. Therefore, like all the other members of the *Msx*1 pathway, *Shh* expression is regulated by more than one mechanism. Additionally, regulation of cell proliferation in the anterior mesenchyme is regulated by this pathway as well as the others discussed. Loss of *Fgf*10 signalling altered other cellular processes including apoptosis suggesting it also plays a role in cell survival. Fgf10 null mice exhibited premature and ectopic fusion suggesting it also plays a role in ensuring proper fusion (Rice et al., 2004).

Fgf10 clearly regulates cell proliferation within the anterior palate. It is interesting to note that if the posterior palate is exposed to ectopic *Fgf10* there is not a noticeable effect on the level of proliferation (Rice et al., 2004). Therefore, the downstream effectors of Fgf10 expression must not be present within the posterior region of the palate. This implies that distinct pathways are responsible for the regulation of anterior and posterior cell proliferation.

3.4.1.8 Fgf Receptors

The Fgf receptor Fgfr1b has also been described to have an anterior and medial specific expression pattern within the developing palate. As with other members of the Fgf family, its expression was linked to the regulation of proliferation within the anterior palate. Expression of Fgfr1b was shown to be negatively regulated by the Wnt11 signalling molecule. In return, Fgfr1b was shown to negatively regulate the expression of Wnt11. At early stages of palate development the balance is tilted towards Fgfr1b allowing the palate to undergo cell proliferation. As palate development proceeds however, the expression balance is shifted away from Fgfr1b. At this stage it has been shown to be important for proliferation to temporarily halt in order for the individual palate shelves to fuse and form a complete palate (Lee et al., 2008). Again, this shows that although the most obvious role for the Fgf family is in regulating the level of proliferation within the palate it also plays a role in regulating events like fusion through maintain low expression of certain genes until the appropriate time.

3.4.1.9 Shox2 Signalling Pathway

Fgf10 expression has been shown to be downstream of the homeobox transcription factor *Shox2*. The *Shox2* gene is expressed solely in the anterior mesenchyme region of the developing secondary palate, with its highest expression seen during the early stages of palate development. When mice are

deficient in the *Shox2* gene they exhibit a rare form of cleft palate where the cleft only occurs in the anterior part of the secondary palate. In these *Shox2* null mice it was reported that the expression domains of both *Fgf10* and *Fgfr2c* were altered. This altered expression corresponds with a decrease in proliferation and increase in apoptosis within the anterior palate (Yu et al., 2005). These data show that it is possible that altering the expression of genes only in one area of the palate can lead to clefting only in a specific area.

The regulation of the *Shox2* gene has also been investigated. Although a complete understanding of *Shox2* regulation is far from being achieved, it was shown that blocking Bmp signalling with the antagonist Noggin resulted in a downregulation of *Shox2* expression within the exposed anterior mesenchyme. Exposure of the palatal mesenchyme to *Bmp4, Bmp2* and *Shh* was not sufficient to induce *Shox2* expression. These data suggests that while Bmp signalling does not appear to be capable of inducing *Shox2* expression on its own, it is necessary for normal *Shox2* gene expression (Yu et al., 2005).

3.4.2 Regulation of Palatal Shelf Fusion

The mechanism by which the palate shelves fuse together to create a complete secondary palate has been a matter of dispute for many years. Apoptosis (Martinez-Alvarez et al., 2000; Xu et al., 2006), migration (Martinez-Alvarez et al., 2000), and epithelial-mesenchymal transformation (Cui et al., 2005; Fitchett and Hay, 1989; Griffith and Hay, 1992; Kaartinen et al., 1995;

Proetzel et al., 1995; Shuler et al., 1992; Sun et al., 1998) have all been suggested as potential mechanisms. It is becoming apparent that fusion of the palate shelves likely requires a combination of all three of these processes and can not be explained by a single mechanism.

3.4.2.1 Transforming Growth Factors Signalling Pathways

TGF-β3 has been shown to be essential in the fusion of the palate shelves. TGF-β3 null mutant mice exhibit a cleft secondary palate due to failure of the elevated palate shelves to adhere and fuse (Fitchett and Hay, 1989; Griffith and Hay, 1992; Shuler et al., 1992; Sun et al., 1998). Numerous members of the TGF-β family of genes have been shown to be involved in several regulatory processes during palatogenesis including: cell migration, epithelial-mesenchymal transformation, extracellular matrix synthesis and deposition, degradation of the basement membrane, cell proliferation and apoptosis (reviewed in Kaartinen et al., 1997; Pelton et al., 1990). TGF-β3 expression is first detected at E11.0 in palatal epithelium and remains restricted to the epithelium with increasing intensity as development progresses. At E14 there is distinct localization of intense TGF-β3 expression to the medial epithelial edge, with expression lost only after palatal fusion when the cells lose their epithelial phenotype (Fitzpatrick et al., 1990; Pelton et al., 1990).

It has been demonstrated fairly convincingly that in the palate, TGF-β3 signals through Smad-dependent pathways. TGF-β3 has been shown to act through a transmembrane serine/threonine kinase receptor (Tβr) (Cui and

Shuler, 2000). Upon binding of TGF-β3 to its receptor, Alk5 is phosphorylated and both Alk5 and the receptor-ligand complex are internalized. Smad anchor for receptor activation (SARA), a cytoplasmic protein, interacts with Smad 2/3 and brings it to the internalized activated receptor where Smad 2/3 is phosphorylated (Tsukzaki et al., 1998), allowing it to form a complex with Smad4 and be translocated to the nucleus where the complex activates transcription of genes such as lymphoid enhancer factor 1 (*Lef*1). *Lef*1 has been shown to induce midline epithelial seam degradation (Nawshad and Hay, 2003; Nawshad et al., 2007). Overexpression of the Smad2 protein in the medial epithelial edge of TGF-β3 null mutant mice partially rescues the cleft palate phenotype, although fusion was not observed at the junction between the primary and secondary palates or at the most posterior region of the secondary palate. These data clearly suggest that although Smad2 phosphorylation is critical for proper palate fusion, there are other unknown factors that are required in palatal fusion involving *TGF-β*3 (Cui et al., 2005).

A downregulation or absence in the expression of TGF-β3 results in an upregulation in the expression of TGF-β1, which consequently leads to ectopic activation of Snail (a zinc-finger transcription factor) in the epithelium. Snail activation in the epithelium is known to promote cell survival, therefore inhibiting the action of TGF-β3 in degrading the epithelial seam (Martinez-Alvarez et al., 2004). TGF-β1's exact role in palatogenesis has been very difficult to decipher as embryos die at E11.0, prior to the beginning of palate development (Brunet

et al., 1995). TGF-β1 expression is first detected in the developing murine palate at E12.0-12.5 in the epithelium. TGF-β1 expression continues to be localized to the epithelium, both in cells expressing and those not expressing TGF-β3 (Fitzpatrick et al., 1990). Expression remains in the epithelial cells until E15.5 when they lose their epithelial phenotype (Fitzpatrick et al., 1990; Pelton et al., 1990). At this stage, a low level of mesenchymal TGF-β1 expression is also observed. Later in development TGF-β1 expression is limited to areas of the palate undergoing ossification (Pelton et al., 1990). TGF-β1 has also been described as a potent inducer of apoptosis, and is hypothesized to be responsible for the apoptosis observed in the periderm prior to shelf contact. Once the periderm has been sloughed off, the underlying layer of medial epithelial edge cells that are exposed are able to form the adherent seam (Nawshad et al., 2004).

3.4.2.2 Epidermal Growth Factor Signalling Pathway

Epidermal growth factor (EGF) has also been shown to play a key role in maintaining cell proliferation and survival in the epithelium of the developing palate. EGF signalling must be tightly regulated however, as the medial epithelial edge cells must stop DNA synthesis and cell proliferation prior to the palate shelves initially contacting one another, and EGF has been shown to inhibit these cessations (Yamamoto et al., 2003). EGF is known to signal through binding to and activating its receptor tyrosine kinase (Hackel et al., 1999). This activation starts a three kinase pathway, whereby Raf, a mitogen-

activated protein kinase (MAPK) phosphorylates MEK1/2, a MAPK kinase, which in turn phosphorylates the MAPK extracellular signal regulated kinase1/2 (ERK1/2) (Graves et al., 2000; Marshall, 1995). Upon phosphorylation, ERK1/2 translocates from the cytoplasm to the nucleus where it acts to phosphorylate transcription factors, causing them to become activated and change the expression of a variety of target genes involved in cell survival and proliferation (Brunet et al., 1999; Khokhlatchev et al., 1998). Phosphorylated ERK1/2 was found to be localized to the medial epithelial edge cells within the palate, with none detected within the mesenchyme (Yamamoto *et al*., 2003). It is important to note that ERK1/2 is the only known target of MEK1/2 (Pearson et al., 2001). When palatal organ cultures were grown in the presence of exogenous EGF, an increase in DNA synthesis, and therefore cell proliferation was observed. These cultures also showed that although the treated palate shelves appear to adhere to one another normally, the midline epithelial seam never degraded and therefore palate fusion was never complete (Yamamoto et al., 2003). When a MEK1/2 specific inhibitor was introduced into these palate organ cultures, the levels of phosphorylated ERK1/2 and DNA synthesis returned to normal and the cleft palate phenotype was rescued (Yamamoto et al., 2003). It has also been shown that phosphorylated ERK1/2 can elicit one of two effects on cells. Depending on the location and duration of the activated ERK, this can either result in differentiation or proliferation. It is believed, that retaining the phosphorylated ERK1/2 within the cytoplasm is sufficient to block the

proliferative effects (Brunet et al., 1999; Formstecher et al., 2001; Tohgo et al., 2002) and may play a crucial role in the degradation of the medial epithelial seam during palatogenesis (Yamamotto et al., 2003). TGF-β3 has been shown to be capable of overriding the proliferative effects of EGF in normal epithelial cells (Like and Massague, 1986; Massague, 1990). It has been hypothesized that one of the key roles of TGF-β3 is to prevent the translocation of ERK1/2 to the nucleus, preventing its proliferative effects and therefore allowing the fusion of the palate shelves through the degradation of the midline epithelial seam, although this has yet to be confirmed (Yamamotto et al., 2003).

3.4.2.3 Meox2 Signalling Pathway

Meox2 is a homeobox transcription factor shown to have a posterior specific expression pattern that becomes increasingly localized to the extreme posterior region as development proceeds (Jin and Ding, 2006; Li and Ding, 2007). Mice null in the *Meox2* gene exhibit a low penetrance of cleft palate that results from a novel mechanism. Palate shelves grow, elevate and fuse, however, fusion is weak and as the craniofacial region expands the palate shelves pull apart from one another leading to a cleft palate specifically in the posterior region. Histological analysis of the cleft palates showed clearly that the palate shelves were completely absent of the medial epithelial edge and were composed solely of mesenchyme. The defect in the palates that is responsible for the post-fusion cleft palate is not completely clear. It may be

that there is a palatal growth defect in the posterior palate which prevents the palates from being able to keep up with the rest of craniofacial development. Alternatively, it may be that loss of *Meox2* leads to improper palatal fusion leading to a weak seam that does not stand up to the mechanical forces of craniofacial development (Jin and Ding, 2006). Although the role of *Meox2* is not understood it expression does provide a molecular marker that specifically identifies posterior cells within the palate.

3.4.2.4 Fgf10 Signalling Pathway

As discussed in section 3.4.1.7 (pg 34) Fgf10 plays a role in regulating proper fusion of the palate shelves. Loss of the Fgf10 gene leads to ectopic fusion of the palate shelves to the oral epithelium in some cases. This ectopic fusion prevents the palate shelves for being able to reorient towards one another and therefore leads to a wide open cleft palate (Alappat et al., 2005). This shows that the palate shelves must not be able to fuse before they come into contact with one another or it can actually be detrimental to proper palate development.

3.4.3 Cell Migration

The importance of the migration of cells between regions of the palates has become an increasingly interesting phenomenon. In order for proper palate development to occur, it would appear that cells must be able to migrate within

the palate.

Although the expression of *Shox2* remains anterior specific throughout palatogenesis, it does display a dynamic expression pattern. At the initial stages of palate growth *Shox*2 expression is only detected in the most extreme anterior regions of the palate (less than 25% of the length of the palate). As the palate shelves continue to grow the expression of *Shox*2 expands until by E14.5 when it covers the entire anterior palate and most of the medial palate (60% of the length of the palate shelf). Concurrent with the expansion of *Shox2* expression, the region of the palate expressing the posterior specific gene *Meox2* was shown to shrink (Li and Ding, 2007). This phenomenon clearly shows that in order for the anterior palate to develop properly it must recruit cells from the posterior, which are converted into *Shox2* anterior specific cells. Initially, this was predicted to be due to a repression of *Meox2* by *Shox2* or a downstream target of the *Shox2* signalling pathway (Li and Ding, 2007).

Ror2 has been shown to regulate the expression of *Wnt5a* in anterior specific cells. The Wnt5a signal was shown to consequently act as a chemoattractant causing cells to migrate from the posterior region of the palate towards the anterior region. As discussed above, Wnt5a also was shown to regulate the expression of *Bmp4* and *Shh* both of which play important roles in the development and growth of the anterior palate (He et al., 2008). It is therefore possible that it is not that *Shox2* is simply being upregulated and

Meox2 downregulated that results in the conversion of posterior cells to anterior cells, but rather that the cells are migrating towards the higher Wnt5a signal. As cells enter the anterior region of the palate, Wnt5a and potentially other factors act to alter the expression profile of genes in the cells causing them to transdifferentiate into anterior specific palate cells.

Recently, it was shown that in addition to regulating proliferation, apoptosis and fusion, Fgf10 can also induce cell migration within the anterior palate. Fgf10 expression is not only localized to the anterior mesenchyme but it also exhibits higher expression in the lateral region of the anterior mesenchyme (Rice et al., 2004). Fgf10 has been shown to act as a chemoattractant in other cell types, and recently was shown to be able to induce the migration of anterior mesenchyme cells from the medial to the lateral side of the palate (He et al., 2008). The loss of Fgf10 was shown to cause palate shelves that are abnormal in shape (Alappat et al., 2005), which could be explained in part by the loss of lateral cell migration.

The new discoveries that cells migrate first from the posterior region of the palate to the anterior region of the palate, and then to the lateral region of the anterior palate underscores the dynamic processes directing palatal development. Although cells display a specific set of genes at any time that determine how they react to external stimuli, that set of factors is continually changing as development proceeds. Additionally, this migration to the anterior

region of the palate specifically lends further support to the theory that the anterior palate plays a role as a signalling center acting to regulate palatogenesis as a whole. This also demonstrates the importance of maintaining the proper anterior to posterior axis in the palate.

3.5 Homeobox Genes

Homeobox genes (Hox) genes were first described in *Drosophila* (Balkaschina, 1929; Bridges and Morgan, 1923; Bridges and Dobzhansky, 1933). This group of genes was of particular interest due to their ability to transform each segment of the body into the likeness of another. In *Drosophila,* these homeotic genes are localized on a single chromosome (chromosome #3) into a homeotic complex (HOM-C), which is separated into two separate clusters [Bithorax complex and Antennapedia complex] (Kaufman et al., 1990; Lewis, 1978; Scott et al., 1983). Homeobox genes are evolutionarily conserved, and found in all metazoans, plants and fungi examined to date (Burglin, 1997). Vertebrates express homeobox genes that share a high degree of sequence similarity to those in the *Drosophila* that play important roles in embryonic patterning and development (reviewed in Akin and Nazarali, 2005).

There are over 700 homeobox-containing genes identified to date in vertebrates (Zhong et al., 2008). A subset of these genes are called ‘clustered’ genes and are known as *Hox* genes. A common feature between the Antennapedia-class genes and *Hox* genes is a 180 base pair homeobox

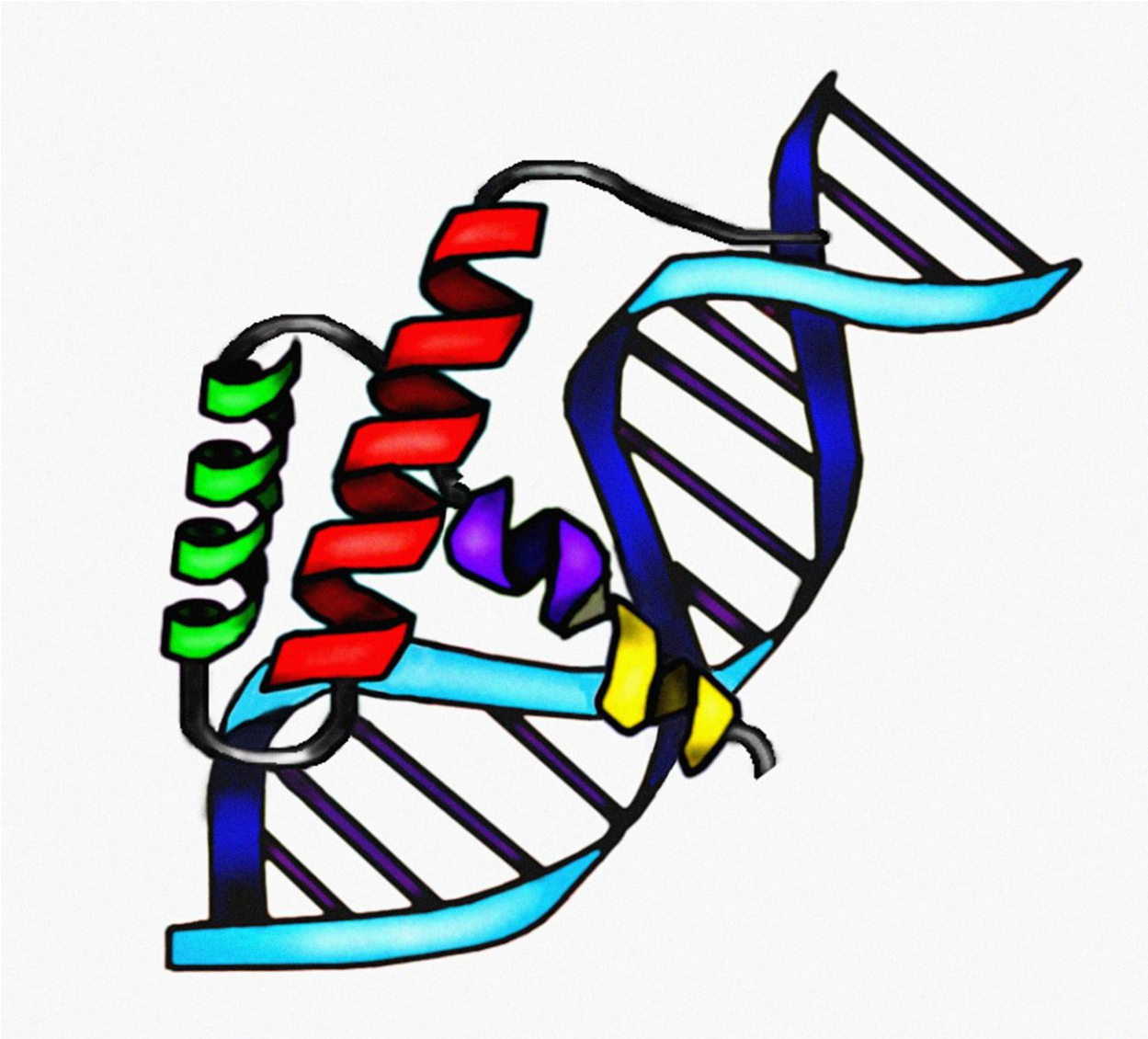

Figure 5. Schematic Diagram of the Homeodomain

Schematic representation of the interaction between the homeodomain of a Hox protein and DNA. The third helix (purple) acts as the recognition helix and interacts with the major groove of DNA. The fourth helix (yellow) acts as an extension of the third. The first (red) and second (green) helices interact with the DNA backbone to stabilize the interaction. The region N-terminal to the first helix allows the protein to interact with other protein cofactors.

sequence that encodes a 60 amino acid protein domain called the homeodomain. Four alpha helices are the core of this domain (Fig. 5). The first three alpha helices form a compact globular structure, while the fourth helix is more flexible and appears to be an extension of the third helix. N-terminal to the first helix, is a conserved flexible region of six amino acids that acts by allowing the Hox protein to interact with other protein co-factors. The second and third helices together form a helix-turn-helix motif that is capable of recognizing and binding to a specific sequence of nucleotides on DNA, providing them the ability to act as transcription factors and regulate the expression of downstream genes (Akin and Nazarali, 2005; Gehring et al., 1990; Graba et al., 1997; Kissinger et al., 1990; Li et al., 1990). The third helix is the recognition helix, which contacts the target DNA in the major groove. The first and second helices also make contact with the DNA backbone in order to stabilize the structure. A core binding site for *Hox* genes has been determined *in vitro* and consists of a 10-12 base pair regions with a core sequence of TAAT (Gehring et al., 1990; Kalionis and O'Farrell, 1993; Laughton, 1991).

In mice and humans there are 4 separate chromosomal *Hox* gene clusters called the HoxA, HoxB, HoxC and HoxD. In total there are 39 genes in these Hox clusters in mice and humans. Each cluster is arranged in a 3′ to 5′ order, which also reflects their homology to genes in the other *Hox* clusters as well as their level of similarity with the genes in the HOM-C complex in *Drosophila*. Each of the clusters contains multiple genes numbered based on

their linear position in the chromosomal cluster as well as their similarity to the HOM-C complex. There are 13 paralogous gene groups in mice and humans (Fig. 6). Paralogs exhibit a higher degree of sequence similarity with each other than with any of the genes in their cluster. Although there are 13 groups, none of the clusters actually contain genes in all 13 paralogous groups. Genes within each cluster exhibit spatial colinearity, that is they are expressed along the anterior-posterior axis of the embryo in the same order they appear along the chromosome, from the 3′ to 5′ (Dressler and Gruss, 1989; Duboule and Morata, 1994; Graham et al., 1989; Lewis, 1978). In general, there is also temporal colinearity of the gene clusters with the 3′ genes being expressed earlier in development than their more 5′ counterparts (Gaunt and Strachan, 1996; Izpisua-Belmonte et al., 1991) (Fig. 6). Spatial and temporal colinearity does not exist between the different chromosomal clusters. Paralogs are generally expressed in the same region and time frame in development suggesting that they may be functionally redundant (Gaunt et al., 1989; Manley and Capecchi, 1998; Rossel and Capecchi, 1999).

The *Hoxa2* gene is an exception to the spatial colinearity observed between of *Hox* genes. The anterior expression boundary of *Hoxa2* is the border between r1/r2. This is anterior to the *Hoxa1* expression boundary, which is only present in r4 and more posterior rhombomeres (Prince and Lumsden, 1994).

Expression of *Hox* genes is known to be fundamental in embryonic

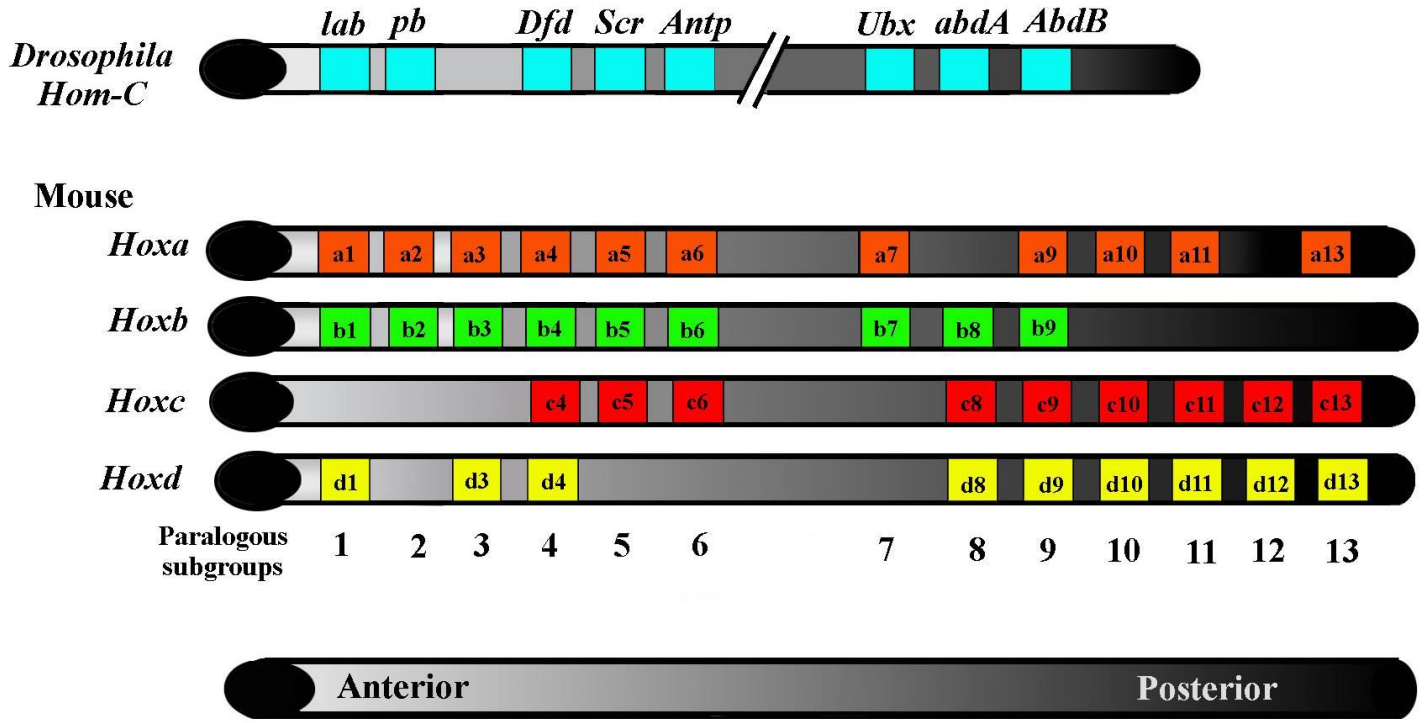
lab pb Dfd Scr Antp Ubx abdA AbdB
Drosophila Hom-C
Mouse
Hoxa
a1 a2 a3 a4 a5 a6 a7 a9 a10 a11 a13
Hoxb
b1 b2 b3 b4 b5 b6 b7 b8 b9
Hoxc
c4 c5 c6 c8 c9 c10 c11 c12 c13
Hoxd
d1 d3 d4 d8 d9 d10 d11 d12 d13
Paralogous subgroups
1 2 3 4 5 6 7 8 9 10 11 12 13
Anterior
Posterior

Figure 6. Organization of Hox Genes Along the Chromosome in the Fruit Fly and Mouse as well as their Relative Region of Expression during Embryogenesis

There is a clear conservation of the organization of the HOM-C complex in the fruit fly and the four gene clusters in mice. Paralogous groups share the same relative location along the cluster and expression pattern in the body. Spatial colinearity exists between members of the Hox clusters. The anterior-posterior expression of genes occurs from 3'-5' on the chromosome of both the mouse and fruit fly.

development, and in particular in patterning the body axis. Therefore, functional redundancy may act as a safeguard against developmental problems. Many *Hox* genes act as selector genes, controlling a cascade of events through "realizator" genes that is capable of determining the fate of an entire body segment.

3.5.1 Hoxa2

*Hoxa*2 belongs to the Hox A cluster of genes in both the mouse and human. The gene was originally cloned in 1992, and designated as *Hoxa1.11* (Nazarali *et al*., 1992). The *Hoxa*2 gene encodes a 41 kDa protein (Tan *et al*., 1992), which has been shown to act as a transcription factor in the murine central nervous system (Gendron-Maguire et al., 1993; Nazarali et al., 1992; Rijli et al., 1993; Tan et al., 1992). *Hoxa*2 is the most anteriorly expressed *Hox* gene (Gendron-Maguire et al.,1993; Nazarali et al., 1992; Rijli et al., 1993; Tan et al., 1992), and has been shown to act as the selector gene for second branchial arch patterning (Grammatopoulos et al., 2000; Hunter and Prince, 2002; Pasqualetti et al., 2000; Santagati et al., 2005). The rostral expression boundary of *Hoxa2* in the hindbrain is the rhombomere 1/2 boundary (Nonchev et al., 1996; Prince and Lumsden, 1994). Expression is detected as early as E8.25 in the neural folds of mice (Maconochie et al., 1999; Nonchev et al., 1996). As the CNCC migrate from the rhombomeres into the branchial arches, *Hoxa*2 is not expressed within the migrating CNCC of rhombomeres 2 and 3.

Therefore, the first branchial arch is free of *Hox* gene expression, while the more posterior arches express subsets of *Hox* genes which determine their developmental fates (Prince and Lumsden, 1994). Expression is also detected at E12.5 and E14 in the hindbrain, spinal cord, dorsal root ganglia, larynx, lungs, vertebrae, sternum, intestine and palate. Later in development *Hoxa2* expression is turned on in the diencephalon and forebrain (Tan et al., 1992; Wolf et al., 2001).

3.5.1.1 Regulation of *Hoxa*2 Expression

The importance of *Hox* gene expression in patterning the body, and in particular the expression of *Hoxa2*, the selector of the second pharyngeal arch, has led to an interest in the genes responsible for regulating the expression of this group. Due to the intricate temporal and spatial regulation of *Hoxa*2 in multiple cells types, it is clear that regulation of *Hoxa*2 expression is likely to involve a network of regulatory elements. *Hoxa2* being the sole *Hox* gene expressed within rhombomere 2 led researchers to examine if a unique regulatory element exists within the *Hoxa2* gene which acts to allow expression. A *cis*-regulatory module, embedded in the second coding exon of *Hoxa*2, was located that allowed expression in rhombomere 2. This module is a conserved enhancer sequence that contains 2 consensus Sox binding sites, as well as several other elements, that act together to regulate expression (Tumpel et al., 2002; Tumpel et al., 2007). Interestingly, Sox1, Sox2 and Sox3 all exhibit high levels of expression in rhombomeres 2 and 4 (Wood and Episkopou, 1999).

Elements that are responsible for regulating the expression of *Hoxa2* within NCC specifically have also been identified. A region located 5′ to the gene contains multiple *cis*-acting elements were described that work in conjunction with one another to regulate *Hoxa2* expression in NCC and restrict its expression to the cells of the second branchial arch as well as more posterior arches. Although these elements are known to be critical for regulation, it is not clear what factors are binding. One of the elements was shown to bind to members of the AP-2 family of transcription factors (Maconochie et al., 1999).

In rhombomere 4, it was shown that the regulatory element responsible for *Hoxa2* expression is located in the first intron of the gene. This region contains 4 separate binding sites, that based on their sequences, are bound by *Hox*-genes as well as their cofactors in coordination with the transcription factors Pbx and Prep/Meis. It was also shown that this regulatory element allows *Hoxa2* expression to be responsive to *Hoxb1*. This confirms that there is a regulatory network that exists between the *Hox* genes and is likely responsible for maintaining the proper expression of the correct *Hox* genes at the right anteroposterior regions of the embryo ensuring proper development (Tumpel et al., 2007).

Krox-20 is a transcription factor that has been shown to regulate the expression of both *Hoxa2* and its paralog *Hoxb2*. The 5′ flanking region of the *Hoxa*2 gene has an enhancer region that is responsible for the expression of *Hoxa2* in the third and fifth rhombomeres. This enhancer site has two binding

sites for Krox-20. In *Krox-20* null mice there is a complete loss of *Hoxa2* expression in the rhombomere 3. Hence, different areas of *Hoxa*2 expression are regulated by different mechanisms. Krox-20 regulates *Hoxa2* expression within the cells of rhombomeres 3 and 5, but not in the migrating NCC or mesoderm (Nonchev et al., 1996). These data also provide support to the theory that there are common elements that regulate different members of the *Hox* gene family.

3.5.1.2 *Hoxa2* Mutant Phenotypes

Mice lacking *Hoxa*2 expression in the NCC that have migrated to the second branchial arch display a homeotic transformation of the second branchial arch hyoid structures to mandibular arch skeletal derivatives of the first branchial arch (Gendron-Maguire et al., 1993; Rijli et al., 1993; Santagati et al., 2005). This transformation results in numerous craniofacial abnormalities, leading to postnatal mortality within 24 hours of birth. One of the numerous facial abnormalities *Hoxa*2 null embryos exhibit is a cleft secondary palate in 81-82% of embryos (Gendron-Maguire *et al*., 1993; Rijli et al., 1993; Barrow and Cappechi, 1999). Cleft palate leads to problems with feeding for these embryos. Small amounts of milk, along with large amounts of air, were found in the abdomen of these animals suggesting that they started to feed postnatally, but could not continue due to the build up of air resulting from a lack of separation in the oral and nasal cavities (Gendron-Maguire et al., 1993). During normal embryonic development, the first branchial arch gives rise to Meckel's

cartilage which goes on to form the malleus and incus (first two bones of the middle ear). The second branchial arch cells form Reichert's cartilage which goes on to form the stapes (third bone of the middle ear), styloid process of the temporal bone and the lesser horn and superior portion of the hyoid bone (Noden, 1983). *Hoxa2* null embryos display a complete lack of the Reichert's cartilage derivatives and a duplication of the primordial of the malleus and incus (Gendron-Maguire et al., 1993). Embryos that lack both *Hoxa2* and *Hoxa1* actually display a decreased penetrance of cleft palate which was explained by the authors as a restoration of the tongue musculature in the double knockouts, allowing the tongue to flatten normally (Barrow and Capecchi, 1999).

Overexpression of the *Hoxa2* gene in the first branchial arch of chicks leads to a transformation of first branchial arch structures (Meckel's cartilage, quadrate and entoglossum) into structures from the second branchial arch (basihyoid skeleton). This results in duplication of a number of second arch structures, with these duplicate structures being fused to their normally occurring counterparts (Grammatopoulos et al., 2000).

Loss of *Hoxa2* exclusively from the CNCC and not the overlying epithelium of the second branchial arch was shown sufficient to yield to knockout phenotype. This would suggest that *Hoxa*2 expression in the epithelium alone is not capable of directing the developmental fate of the second arch (Santagati et al., 2005). Conversely, *Hoxa2* was also shown to be required in both the CNCC and the surrounding tissue to get the complete

duplication of the first arch structures into second arch structures. CNCC overexpression of *Hoxa2* alone resulted only in a loss of first arch structures. Therefore, although the CNCC contain a portion of the required patterning information they require cues from the overlying epithelium to develop normally. However, expression within the surrounding tissue is not sufficient for development. Also demonstrated with this finding was the fact that the role of *Hoxa2* is relatively late in development, controlling the differentiation of cartilage and not the migration of CNCC (Grammatopoulos et al., 2000).

3.5.1.3 *Hoxa2*'s involvement in Palate Development

The palate is a derivative of the first branchial arch, which is known to lack *Hox* gene expression. As the NCC migrate into the branchial arches *Hoxa*2 is absent from the cells of the first branchial arch (Prince and Lumsden, 1994), suggesting that it could not play a direct role in the cleft secondary palate in the *Hoxa*2 null mice. This led to the original hypothesis that the cleft secondary palate was the result of alterations in the hyoid structure, leading to a defect in tongue musculature. This defect was believed to cause the tongue to act as a physical barrier between the palate shelves, preventing them from contacting and fusing (Barrow and Capecchi, 1999). The recent discovery of *Hoxa*2 expression within the developing palate suggests a more direct role in palatogenesis (Nazarali et al., 2000). *Hoxa*2 expression is first detectable by immunohistochemical analysis at E12 within the palate epithelium. Expression levels continue to increase expanding to include the mesenchyme at E13,

reaching its peak at E13.5. At E14 *Hoxa*2 expression becomes localized to the medial edge epithelium, and remains localized to the epithelium at E14.5 before expression is downregulated (Nazarali et al., 2000).

Whole palate organ cultures grown in the absence of the tongue showed a shorter palate length, and a significantly lower fusion rate (44%) in the *Hoxa*2 null mutant embryos than in its heterozygous or wild-type counterparts (78% and 90%, respectively) (Zhang, 2003). In addition, data collected from retroviral infection of whole organ palate cultures with anti-sense *Hoxa*2 showed a decrease in fusion rates compared to the control infections (Wang, 2006). Together, these data provide strong support that *Hoxa*2 plays a critical role in regulating palatogenesis without completely negating the importance of the abnormal positioning of the tongue. The first step in confirming the role of *Hoxa*2 in palatogenesis is to determine which processes of palatogenesis (i.e. cell proliferation, apoptosis and/or fusion), if any, are altered in the absence of Hoxa2. Once this information is collected, the search for downstream targets of *Hoxa*2 in the palate can be focused towards those genes known to be involved in that aspect of palate development.

3.5.1.4 Putative Downstream Targets of *Hoxa2* in Palate Development

3.5.1.4.1 Msx1

*Hoxa*2 has recently been reported to be upstream of *Msx*1 in the murine second branchial arch neural crest cells. Wild-type mice show broad *Msx*1

expression in the second arch hyoid structures, and less intensely in the mandibular arch, or first arch at E10.5. Expression was greatly reduced in the second branchial arch of *Hoxa*2 null mice taking on a first arch-like pattern of expression (Santagati et al., 2005). Due to the importance of *Msx*1 in regulating normal proliferation within the developing palate, and the effect *Hoxa*2 has on its expression in the branchial arches, it is an attractive putative downstream target of *Hoxa*2 in the developing palate.

3.5.1.4.2 Htra3

The high temperature requirement A3 (*Htra*3) protein has recently been described to be capable of binding to and inactivating a number of members of the TGF-β family including: *TGF-β*1, *TGF-β*2, *Bmp*4 and *Bmp*2. *TGF-β*3 was not tested, and therefore the ability of *Htra*3 to inhibit its action is still unknown. Although the mechanism of this inactivation remains unknown, protease activity is an absolute requirement (Tocharus et al., 2004). *Htra*3 is an extracellular protein, whose primary targets are hypothesized to be extracellular matrix proteoglycans, including decorin and biglycan (Tocharus *et al*., 2004). The breakdown and remodeling of the extracellular matrix is known to be a crucial part of many embryonic development processes. *Htra*3 may also inhibit TGF-β signalling through its degradation of the extracellular matrix.

*Htra*3 has been shown to be a putative downstream target of *Hoxa2* in the murine spinal cord and hindbrain (Akin, 2004). Data showed that Hoxa2 protein bound specifically to a region of the *Htra*3 genomic sequence *in vivo*. A

significant upregulation in the expression of *Htra*3 in the *Hoxa2* null embryos was also observed (Akin, 2004), suggesting *Hoxa*2 acts as a direct inhibitor of *Htra*3 expression in the spinal cord and hindbrain. These data, together with the ability of *Htra*3 to degrade numerous genes important in palatogenesis, make *Htra*3 a possible downstream target of *Hoxa*2 in the developing palate.

3.5.1.4.3 Six2

Six2 is a homeodomain containing transcription factor that has been shown to be involved in regulating craniofacial and kidney development (Fogelgren et al., 2008; Fogelgren et al., 2009; Lozanoff, 1993; Lozanoff et al., 2001; Ma and Lozanoff, 1996; Ma and Lozanoff, 1999; McBratney et al., 2003; Singh et al., 1998). Six2 expression has been reported in the mesenchyme of the nasal prominences of E11.5 mice (Brodbeck et al., 2004; Fogelgren et al., 2008; Ohto et al., 1998; Oliver et al., 1995). The *Brachyrrhine* mutation in mice was recently shown to involve the abnormal expression of *Six2* in both the kidney and the developing craniofacial region (Fogelgren et al., 2008). This mutation had previously been described to also result in the absence of the primary and secondary palates (McBratney et al., 2003; Singh et al., 1998). Interestingly, a Six2 knockout mouse was generated and reported to have similar kidney defects as the *Brachyrrhine* mutation, but did not exhibit any craniofacial defects (Self et al., 2006). At present, it is unclear what role if any Six2 does play in the development of the face and in particular in the palate.

*Six*2 has been shown to be a direct downstream target of *Hoxa*2 in the

murine branchial arches (Kutejova et al., 2005; Kutejova et al., 2008). Expression of *Six*2 in wild-type embryos is restricted to the first branchial arch mesenchyme. In *Hoxa*2 null mice, *Six2* expression expands to include the second branchial arch. This suggests that *Hoxa*2 expression is sufficient to repress the expression of *Six2* (Santagati et al., 2005). Interestingly, when *Six2* is overexpressed in the areas of the embryo controlled by *Hoxa*2 the result is a phenotype similar to the *Hoxa*2 mutant phenotype. Analysis of the promoter region of *Six*2 in combination with ChIP experiments suggests that *Hoxa*2 directly represses the expression of *Six*2 (Kutejova et al., 2005; Kutejova et al., 2008). These findings imply that *Six2* may be an important *in vivo* downstream target of *Hoxa*2, although its role in palate development has not been identified.

3.5.1.4.4 Ptx1

*Ptx*1 is a homeodomain containing transcription factor belonging to the *paired* family. In the developing mouse, *Ptx*1 is expressed in the first branchial arch as early as E9.0 (Bobola et al., 2003), with all derivatives of the first arch including the palate continuing to express *Ptx*1 until E15.5 (Lanctot et al., 1997). *Ptx*1 expression is expanded to include the second branchial arch mesenchyme in *Hoxa*2 null mice. In addition, transgenic *Hoxa*2 expression in the first branchial arch is sufficient to block *Ptx*1 expression. A partial reversion to the wild-type phenotype was observed in double mutants lacking both *Hoxa*2 and *Ptx*1. These data suggest that *Hoxa*2 plays a crucial role in inhibiting *Ptx*1 expression in the second branchial arch. *Ptx*1 appears to be an important

downstream target of *Hoxa2,* and therefore a good candidate for further investigation within the developing palate.

Mesenchymal expression of *Ptx*1 in the first branchial arch requires fibroblast growth factor 8 (*Fgf*8) signals from the epithelium. Removal of the epithelium from cultured first branchial arches of wild-type embryos or the second branchial arches of *Hoxa*2 null embryos *in vitro* results in a complete loss of mesenchymal *Ptx*1 expression. Expression can be rescued by introducing *Fgf*8 soaked beads to the culture. Lhx6, another Fgf8 target in the first branchial arch was also shown in *Hoxa2* null embryos to exhibit ectopic expression in the second branchial arch (Bobola et al., 2003). Although *Fgf*8 does not show an altered expression pattern in the second branchial arch of *Hoxa*2 null embryos, these data suggest that *Hoxa*2 regulates the expression of *Ptx*1 and *Lhx*6 through *Fgf*8.

3.6 Summary

The development of the secondary palate involves a complex interaction of different signalling networks. The expression and roles of numerous genes has been described in recent years. Despite all of this knowledge a complete understanding of palate development is still far from clear.

The *Hoxa2* gene has previously been shown to be expressed within the palate, and loss of expression leads to a high penetrance of cleft palate in embryos. Furthermore, whole organ culture data suggests an increased

incidence of cleft palate in *Hoxa*2 null palates grown in the absence of the tongue (Zhang, 2003). Together, these data suggest a direct role for *Hoxa*2 in regulating palatogenesis; however what that role may be has not been investigated. The purpose of my thesis is to examine the expression and function of *Hoxa2* in the palate. In order to elucidate its role, I will investigate cell proliferation, apoptosis and fusion of the palate shelves. In addition, the expression of putative downstream targets will be compared between wild-type and *Hoxa2* null palate shelves throughout development to determine if loss of the gene leads to altered expression. Together, these data will provide us with an understanding of the role of *Hoxa*2 in palate development.

4. Materials and Methods

4.1 Hoxa2 transgenic mice

Hoxa2 $^{+/+}$, *Hoxa2*$^{+/-}$ and *Hoxa2* $^{-/-}$ C57 black mice (Gendron-Maguire et al., 1993) were obtained by timed heterozygous matings. Heterozygous animals were obtained by backcrossing heterozygous males with wild-type females. After pups were weaned, animals were anaesthesized and an approximately 1 cm piece of the tail was docked. Genotypes were confirmed by polymerase chain reaction (PCR) analyses. Timed heterozygous matings were then performed, and were staged according to Kaufman with mice being considered E0 days pregnant on the day the vaginal plug was found (Kaufman, 1992).

4.1.1 PCR analysis of genotype

Tissue sample (tail or embryonic tissue) was digested overnight at 55°C in a 50mM Tris (pH 8.0), 100 mM EDTA, and 0.5% SDS solution containing 150 µg of proteinase K enzyme. Following the digestion, an equal volume of phenol/chloroform/ isolamyl alcohol (25:24:1) solution (Sigma) was added and the reactions were mixed vigorously to mix the phases completely before centrifugation for 10 min at max speed. The aqueous layer was transferred to a fresh tube and the phenol/chloroform/isoamyl alcohol and centrifugation steps were repeated. DNA was then precipitated using 100% ethanol containing 300 mM sodium acetate. Samples were washed with 70% ethanol and the DNA pellet was allowed to dry to remove any residual ethanol before being dissolved in sterile water. DNA was then analyzed by PCR to determine the genotype of

the animal. Each sample was amplified in two different PCR reactions, one to determine the presence of the wild-type *Hoxa2* allele (5´-GTTGGAACTGACCTCCTCTTG-3´ and 5´-GGGTCCGAGCAGGGTTATTCC-3´) and the other to detect the presence of the neomycin cassette that replaces part of exon 1, all of intron 1 and part of exon 2 in the knockout animals (5´-TCGCCTTCTATCGCCTTCTTG-3´ and 5´-GTTGGTGTACGCGGTTCTCAG-3´). 100 µl PCR reactions containing 1X amplification buffer (VWR), 2 mM dNTP mix (Sigma), 1µM of each primer (Invitrogen) and 2.5 U of taq (VWR) and 1 µg of DNA (VWR). Reactions were run on the BioRad MyCycler^{TM} using the temperature cycling conditions 95°C for 4 min followed by 35 cycles of 95°C for 30 s, 65°C for 3 min and 72°C for 7 min (Gendron-Maguire et al., 1993). PCR samples were then separated on a 1% agarose gel containing ethidium bromide and visualized using UV light. A sample of the PCR products is shown in figure 7.

4.2 Immunohistochemical analysis

4.2.1 Fgf8, Six2 and Active Caspase 3

Embryos were harvested from timed-pregnant mice, and heads were fixed in 4% paraformaldehyde in phosphate buffered saline (PBS). Embryo heads were then placed in 20% sucrose in PBS for at least 24 h before being embedded in optimal cutting temperature (OCT) compound (Tissue-Tek) and serially sectioned on to gelatin coated coverslips. Determination of anterior, medial and posterior was performed by matching to sections from each region

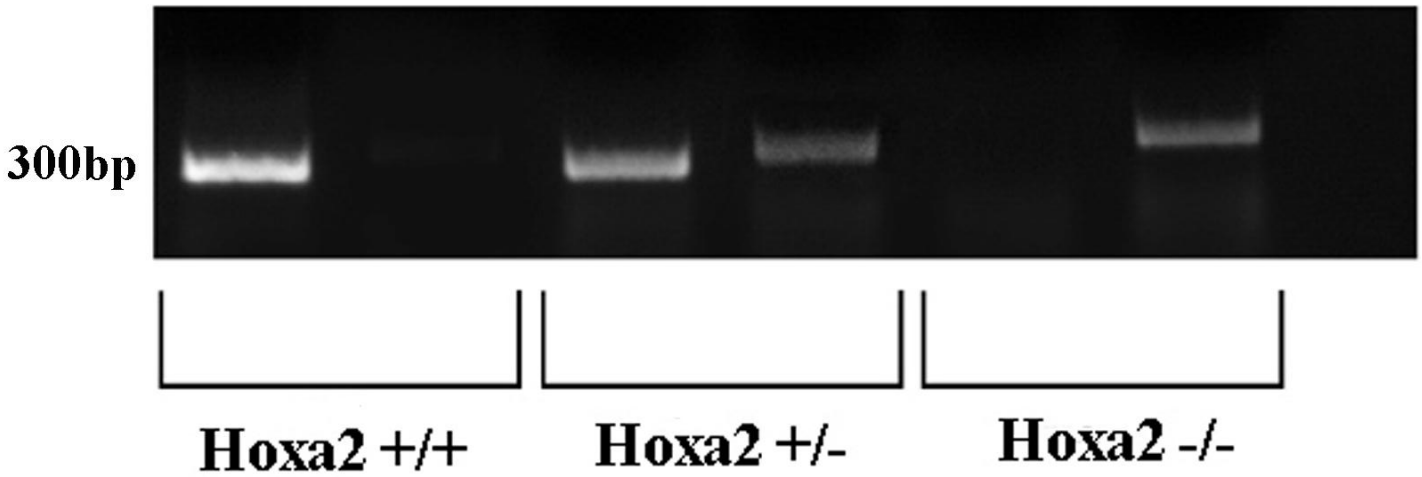
300bp
Hoxa2 +/+
Hoxa2 +/-
Hoxa2 -/-

Figure 7. Sample of the Genotyping Results of Hoxa2 Transgenic Mice

An ethidium bromide gel of the PCR analysis used in the genotyping of Hoxa2 transgenic mice. The presence of a band with the wild-type primers only (first well) confirms that the animal is wild-type. If a band is present only with the neomycin primers (second well) this confirms the embryo is Hoxa2 null. Presence of both bands indicates that the animal is a heterozygote.

in Rice et al 2004 paper. Sections were then allowed to dry at room temperature for at least 2 h. The 8 µm thick sections were then rehydrated with two 20 min washes in PBS and blocked in 3% skim milk powder and 1% Triton X-100 in PBS (3% SM-PBST) for 1h. Sections were exposed to the primary antibody diluted in 3% SM-PBST overnight at 4°C. Fgf8 was stained using a mouse monoclonal antibody (R&D, 1:200), Six2 was stained with a rabbit polyclonal antibody (Affinity BioReagents,1:200) and activated caspase 3 was stained with a rabbit polyclonal antibody (R&D, 1:500). Excess unbound primary antibody was rinsed off by two washes in PBS before being exposed to labeled secondary IgG Alexa 594 antibody (1:400, Invitrogen) for 45 min at room temperature. Sections were then rinsed twice in PBS before being exposed to Hoechst (a fluorescent stain that labels all nuclei). Finally, sections were rinsed two more times in PBS, mounted in Prolong (Molecular Probes) and viewed by fluorescence microscopy. To ensure that the signal observed was not the result of non-specific signal from the secondary antibody, negative controls were performed. These included staining in the absence of the primary antibody, and another set where the secondary antibody was omitted.

4.2.2 Htra3 and Hoxa2

Time staged embryos were fixed in 4% paraformaldehyde followed by immersion in 20% sucrose in PBS. Frozen embryos in embedding medium were sectioned (8 µm thick), and tissue sections were collected on gelatin-coated coverslips. The coverslips were dried for 2h at room temperature before

being subjected to immunohistochemical analysis with the TSA™ #22 (Invitrogen) using the following modified procedure. Coverslips with the tissue sections were incubated twice in PBS, 5 min each time, followed by a 1 h incubation in a 3% hydrogen peroxide solution. This was followed by two 5 min washes in PBS and then 30 min in the manufacturer provided block solution. After blocking, sections were incubated overnight at 4°C with the antigen specific primary antibody. The *Hoxa2* rabbit polyclonal antibody that was generated using oligopeptide, SPLTSNEKNLKHFQHQS (Hao et al., 1999; Nazarali et al., 2000) was used at a dilution of 1:5000 in the block solution. Htra3 staining was stained with a polyclonal rabbit antibody at 1:500 dilution (Tocharus *et al*., 2004). Sections were rinsed in PBS twice (5 min each) and then incubated in biotinylated anti-rabbit secondary antibody (Vector Laboratories) at 1:100 for 1 h at room temperature. Sections were then washed twice (5 min each) in PBS, followed by a 30 min incubation in the secondary avidin–horseradish peroxidase antibody at 1:100 dilution. The sections were washed twice in PBS for 5 min each and then incubated in the Alexa Fluor® 488-conjugated tyramide diluted to 1:200 in the amplification buffer for 10 min and then counterstained with Hoechst before being mounted in Prolong® (Molecular Probes).

4.3 Cell Proliferation Assay

Cell proliferation was assessed by intraperitoneal injection of timed pregnant mice with 5-Bromo-2'-deoxyuridine (BrdU) at a concentration of 100

mg/kg body weight. BrdU is a thymidine analogue that is taken up and incorporated into the DNA of proliferating cells, including those in the developing embryos. One and a half hours after injection, mice were sacrificed and the harvested embryos fixed and sectioned as described above. Tissue samples were taken from the body of each embryo and DNA was isolated and subjected to PCR analysis as outlined above. Wild-type and *Hoxa2* null embryos from the same mother were treated together to minimize variations. Sections were immunohistochemically stained with a monoclonal anti-BrdU antibody (Sigma) and the Mouse-on-Mouse staining kit (Vector Laboratories) to detect proliferating cells, using a modified procedure as follows: briefly, the sections were pretreated by rehydrating the tissue sections in PBS-0.1% Triton-X100 before being exposed to 1N HCl on ice for 10 min and then 2N HCl for 10 min at room temperature followed by a 40 min incubation in 2N HCl at 37°C. Sections were neutralized with 0.1M sodium borate, followed by three 5 min washes in PBS-1% Triton-X100. Endogenous biotin and avidin was blocked using the Avidin-Biotin blocking kit (Vector Laboratories) as per the manufacturer's protocol. After incubating the section in the blocking reagent overnight at 4°C the remainder of the procedure was as per the manufacturer's protocol. Finally, sections were counter stained with Hoechst and mounted in Prolong (Molecular Probes). Tissue from the anterior, medial and posterior palatal regions of wild-type and *Hoxa*2 null embryos at E12.5, E13.5 and E14.5 and 15.5 were used.

4.4 TUNEL Assay

Cell survival and apoptosis was measured using the DeadEnd Fluorometric TUNEL (terminal deoxynucleotidyl transferase-mediated dUTP nick-end labelling) System (Promega) as per the manufacturer's protocol. This kit exploits the property that, during programmed cell death, chromosomal DNA is fragmented. A recombinant terminal deoxynucleotidyl transferase enzyme is used to incorporate fluoroscein-12-dUTP to the free 3'-OH groups of fragmented DNA. The fluoroscein-12-dUTP labeled DNA can then be visualized directly by fluorescence microscopy. Tissue from the anterior, medial and posterior palatal regions of wild-type and *Hoxa*2 null embryos at E12.5, E13.5, and E14.5 were examined for apoptotic cell death. Positive controls were performed by staining E13.5 hindlimbs which are known to have high levels of apoptosis. Additionally. palatal sections were treated with DNase to fragment DNA and then stained with the TUNEL kit.

4.5 Whole Palate Organ Cultures

Numerous organ culture systems were attempted in order to develop a system that could be used to examine if loss of the *Hoxa2* gene altered the palate shelves ability to fuse with one another. First, a system was used that consisted of removing the tongue and tissue surrounding the palate shelves, leaving the snout attached to maintain the correct orientation and curvature of the palate shelves which had been reported to maximize the fusion rate (Cuervo et al., 2002). Palates were excised from E14 embryos in Hanks' Balanced Salts

or L-15. The explants were then placed on 13 mm nitrocellulose membrane filters, 0.8 µm pore size (Millipore), and the filters placed on Gelfoam surgical sponges (Pfizer) in Dublecco's modified eagle medium (DMEM) supplemented with 1% penicillin/streptomycin and allowed to grow for 72 h in a 5% CO_2 incubator at 37°C (Chai et al., 1998; Liu et al., 2005). Cultures were then observed under a light microscope to determine if the palate shelves fused. Using this technique, only a 60% fusion rate was ever achieved in the wild-type animals, which was not effective enough to examine the role of *Hoxa2* in fusion. A number of variations on this technique were tried, such as supplementing the media with HEPES or FBS, allowing a longer period of time for cultures to fuse, changing to BGJb media and removing more or less of the surrounding tissue. Additionally, Nucleoport Track-Etch membrane filters, 8µm pore size (Whatman) were also tried.

A previously described technique (Nakajima et al., 2007; Shiomi et al., 2006) with two modifications: the addition of 1M HEPES (4-(2-hydroxyethyl)-1-piperazineethanesulfonic acid) to a final concentration of 20 mM and addition of a penicillin-streptomycin antibiotic solution to a final concentration of 0.1% (Sigma-Aldrich) proved to be successful. Briefly, the E14.0 palate shelves were aseptically excised and arranged in pairs with their medial edges in contact and in proper anterior-posterior orientation on Nucleopore Polycarbonate Track-Etch filters (Whatman). Two filters were floated in a 35 mm tissue culture dish containing 1.4 mL of BGJb medium (Invitrogen), supplemented as detailed

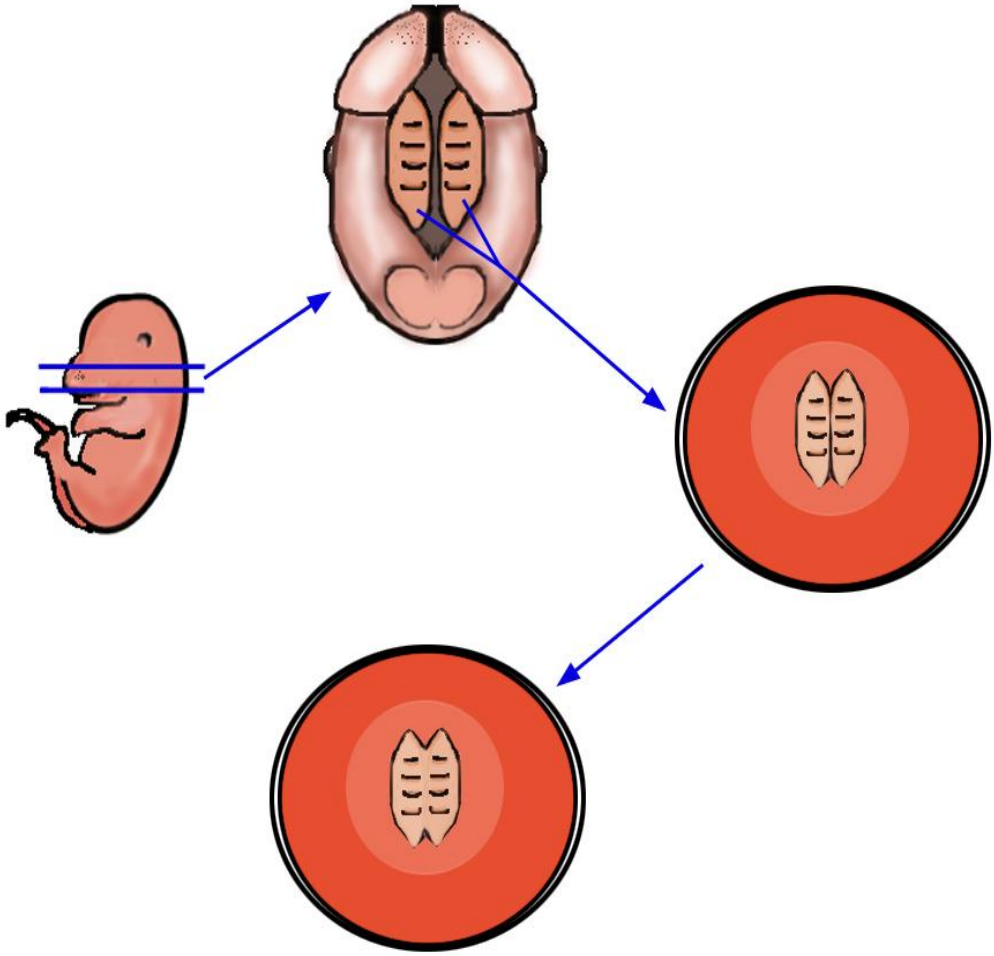

72 h, 37^{o}C, 5% CO_2

Figure 8. Schematic Representation of the Organ Culture Technique Used to Evaluate Fusion.

Palate shelves are excised from E14.0 embryos and placed on filters. The filters are floated on BGJb media for 72 h in a 5% CO_2 incubator after which palates were evaluated for fusion.

above, and incubated in 5% CO_2 at 37^{o}C for 72 h. Following incubation, cultures were observed under a light microscope to determine if the epithelial seam was lost and palate shelves fused (Fig. 8). Cultured palatal shelf explants were sectioned in a coronal plane and stained with cresyl violet to ensure that the midline epithelial seam had degraded. Fusion rates were compared among wild-type, heterozygous and *Hoxa*2 null mutant embryos to determine if *Hoxa*2 played a role in fusion.

4.6 Western Blot Analysis

Protein was isolated from wild-type and *Hoxa*2 null mutant embryonic palate shelves and pooled together prior to lysis in RIPA buffer (Radio Immuno Precipitation Assay Buffer, 150 mM NaCl, 10 mM Tris, 0.1%-SDS, 1% Triton X-100, 1% Deoxycholate, 5 mM EDTA). Protein was quantified using the Nanovue (General Electric) to ensure that equal loading was achieved. Samples were then boiled for 20 min with loading buffer and loaded on a 10% polyacrylamide-SDS gel. After gel separation, the proteins were transferred to a PolyScreen PVDF membrane, which was subsequently blocked by overnight incubation in 3% skim milk in PBS (SM-PBS) at 4°C. The membrane was then exposed to the primary antibody for either Msx1 (rabbit polyclonal, Developmental Studies Hybridoma Bank, 1:500), Fgf8 (mouse monoclonal, R&D, 1:500), Ptx1 (goat polyclonal, Santa Cruz, 1:100), Hoxa2 (rabbit polyclonal, Hao et al., 1999; Nazarali et al., 2000, 1:1000), Six2 (goat

polyclonal, Santa Cruz, 1:200), Bmp4 (goat polyclonal, Santa Cruz, 1:200), Barx1 (goat polyclonal, Santa Cruz, 1:200), or Htra3 (rabbit polyclonal, (Tocharus et al., 2004), 1:1000) and incubated for 1 h at room temperature. This was followed by 3 consecutive washes of 10 min each in PBS with 0.08% Tween-20. After the washes were complete, the membrane was incubated with a secondary antibody specific to the species of primary antibody production. In all cases, a species specific IgG horseradish peroxidase conjugate (Bio-Rad) was used and diluted to 1:3000 in SM-PBS for 1 h at room temperature. After 3 washes of 40 min each in PBS-Tween-20, membrane was exposed with a chemiluminescent reagent (DuPont NEN) and signal was detected by exposing to X-ray film. The membrane was then washed overnight at 4°C in PBS before being incubated with the anti-β-actin (Sigma) at a dilution of 1:1000, and incubated for 1 h at room temperature, followed by 3 washes in PBS with 0.08% Tween-20. After the washes, the membrane was exposed to the anti-mouse IgM horseradish peroxidase conjugate (Bio-Rad) in SM-PBS at a dilution of 1:1500, and then treated as indicated above.

Following exposure to film, semi-quantitative densitometry was performed using the AlphaImager (Alpha Innotech). The film was placed on the light source and an image was taken, which was then analyzed using the AlphaImagers densiometric software to determine an integrated density value (IDV) for each of band. Three separate western blots were performed for each of the proteins evaluated. The software allowed for the selection of a

representative background area and then to define an area around the bands of interest. Equal size boxes were used in all comparisons. To compare expression, relative IDV values were calculated by normalizing to β-actin levels from the same sample and then a sample from each gel was set as 1. Due to differences in the IDV values between different blots it was necessary to normalize each blot to a band on its own gel to accurately represent any changes in protein expression observed. This was done by normalizing all 3 western blots to the knockout band from the same age (E12.5, E13.5 or E14.5). In order to gain a complete picture, each set of western blots was analyzed three times, once normalized to each of the following: E12.5, E13.5 and E14.5 knock out samples. Student's T-tests were run to compare wild-type and knockout expression levels at each of the other two ages. In all cases where a statistically significant change in expression was observed it was significant when normalized to either of the two ages.

4.7 RNA Isolation and Reverse Transcription

Total RNA was isolated from excised wild-type and *Hoxa*2 null embryo palate shelves using the RNeasy® Protect Mini Kit (Qiagen) as per the manufacturer's protocol. RNA concentration was determined by optical density (Nanovue, General Electric). First strand DNA synthesis was performed using the SuperScript® first-strand synthesis system for RT-PCR (Invitrogen), using random decamer primers, as per the manufacturer's protocol. Final concentration of RNA for all RT reactions was 20 ng/µl.

4.8 Quantitative Real Time RT-PCR

Gene expression was quantified using the Taqman® primers and labeled probe system (Applied Biosystems) and a real time PCR machine (ABI 7300) from Applied Biosystems. Wild-type and *Hoxa*2 mutant embryo palates at E12.5, E13.5, E14.5 and E15.5 were tested for each gene, with the exception of *Hoxa*2, where only wild-type tissue was used. All reactions were performed using the Taqman Universal Master Mix (2X), FAM-labeled Taqman Gene Expression assays for gene of interest (*Msx*1, *Bmp*4, *Lef*1, *Six*2, *Ptx*1, *Hoxa*2, *Barx1*, *Tbx1*, *Lhx8, Fgf8* or *Htra*3), VIC-labeled Taqman Endogenous Control β-Actin, and 10ng of cDNA. All reactions were run in replicates of 4, and an n=4 was used for each gene with the exception of *Hoxa*2 (n=3). Thermocycling parameters were as follows: 2 min at 50^{o}C, 10 min at 95^{o}C, 40 cycles of 15s at 95^{o}C plus 70s at 60^{o}C. Taqman gene expression assays have all been tested to have efficiencies not significantly different from 1 (Applied Biosystems, 2004). However, in order to ensure that all primer sets were working properly and that multiplexing the gene specific and β-Actin primers did not result in altered amplification efficiencies all primer sets were examined individually and in complex with β-Actin. Standard curve reactions were run using 1 ng, 10 ng and 100 ng of palate cDNA and amplification efficiency was calculated using the equation $E=10^{(-1/\text{slope standard curve})} -1 \times 100\%$. In all cases the efficiency was required to be between 90-110% for both the gene specific and β-Actin primers

sets before analysis continued. In most cases the appropriate efficiencies were possible using 1 µl of the gene specific primer and probe solution and 0.25 µl of the β-Actin primer and probe set per reaction. For the reactions using the *Hoxa2* and *Lhx8* primer and probe sets it was necessary to increase the volume of these sets to 2 µl per reaction while leaving the concentration of the β-Actin primer and probe set at 0.25 µl. For the *Tbx1* gene specific reactions, it was not possible to achieve an acceptable efficiency for both *Tbx1* and β-Actin when multiplexing. In this case, the reactions were run in separate wells on the same plate. All comparisons were performed using the relative quantification (RQ) software (Applied Biosystems).

To ensure that the *Hoxa2* primers and probe set was specific, reactions were run on cDNA generated from *Hoxa2* null embryos and in all cases the Ct values generated were well above the acceptable cut off.

4.9 RT-PCR Analysis

RT-PCR was run on cDNA generated from wild-type and *Hoxa2* null embryos to ensure that *Hoxa2* mRNA message could not be detected in the null palate shelves. 100 µl PCR reactions contained 1X amplification buffer (VWR), 2 mM dNTP mix (Sigma), 1µM of each primer (Forward primer : 5' ctgg - atgaaggagaagaaggc and reverse primer : 5' cggttctgaaaccacactttc, Invitrogen) and 2.5 U of taq (VWR) and 2 µg of cDNA. Reactions were run on the Biorad MyCycler™ using the temperature cycling conditions 95°C for 4 min followed by 35 cycles of 95°C for 30 s, 65°C for 3 min and 72°C for 7 min. PCR samples

were then separated on a 1% agarose gel containing ethidium bromide and visualized using UV light.

4.10 Histological analysis

Time staged embryos were fixed in 4% paraformaldehyde followed by immersion in 20% sucrose in PBS. Frozen embryos in embedding medium were sectioned (8 μm thick), and tissue sections were collected on gelatin-coated coverslips. After sections were allowed to dry for at least two hours they were stained with hematoxylin and eosin.

4.11 Statistical Analysis

All statistical analysis and graphs were performed using the GraphPad 5.0 software package (GraphPad Prism). Statistical analysis on quantitative real time RT-PCR data for *Hoxa2* expression was evaluated using one way analysis of variance (ANOVA) followed by Bonferroni post-tests to compare ages. Quantitative real time RT-PCR of the expression levels of all putative downstream targets was first analyzed in the wild-type embryos to determine the normal trend of expression using one way ANOVA and a Bonferroni post-test. Comparisons of the expression of putative downstream targets between wild-type and *Hoxa2* null palates as well as the cell proliferation data were analyzed statistically by comparing mean values using two way ANOVA followed by Bonferroni post-hoc tests for comparing groups. Western blot densitometry values were compared using Student's T-Tests due to the lack of variance in the expression of the sample set to equal 1. A significant p-value of

less than or equal to 0.05 was adopted for all comparisons.

5.0 Results

5.1 Hoxa2 Expression

Hoxa2 expression in the palate has been previously described by our lab (Nazarali et al., 2000); however, expression within the palate shelves themselves has been disputed by other groups. To further support our claim that *Hoxa2* is expressed throughout the developing palate, real time RT-PCR, western blot and immunohistochemical reactions were performed.

Hoxa2 mRNA expression was detected at E12.5, E13.5, E14.5 and E15.5 and displays differential expression throughout palatogenesis ($p=0.0073$, $F=8.448$). Expression significantly increases between E12.5 and E13.5 ($p<0.05$) before *Hoxa2* levels decrease at E14.5 and remain low for the remainder of palatogenesis (Fig. 9 A). PCR reactions were also run on RNA samples isolated from *Hoxa2* null palate shelves to confirm the specificity of the signal, and as expected there was no detectable signal in these samples (Fig. 9 B).

Expression of the Hoxa2 protein was detected by western blot analysis at E12.5, E13.5, E14.5 and E15.5 (Fig. 10 A). Densitometry of the western blots (n=3) confirmed the trend that protein expression was highest early in development, reaching a peak at E13.5 (Fig 10 B). These results are in agreement with the mRNA expression observed after real-time RT-PCR. Confirmation that the Hoxa2 antibody is specific was determined by running

A)

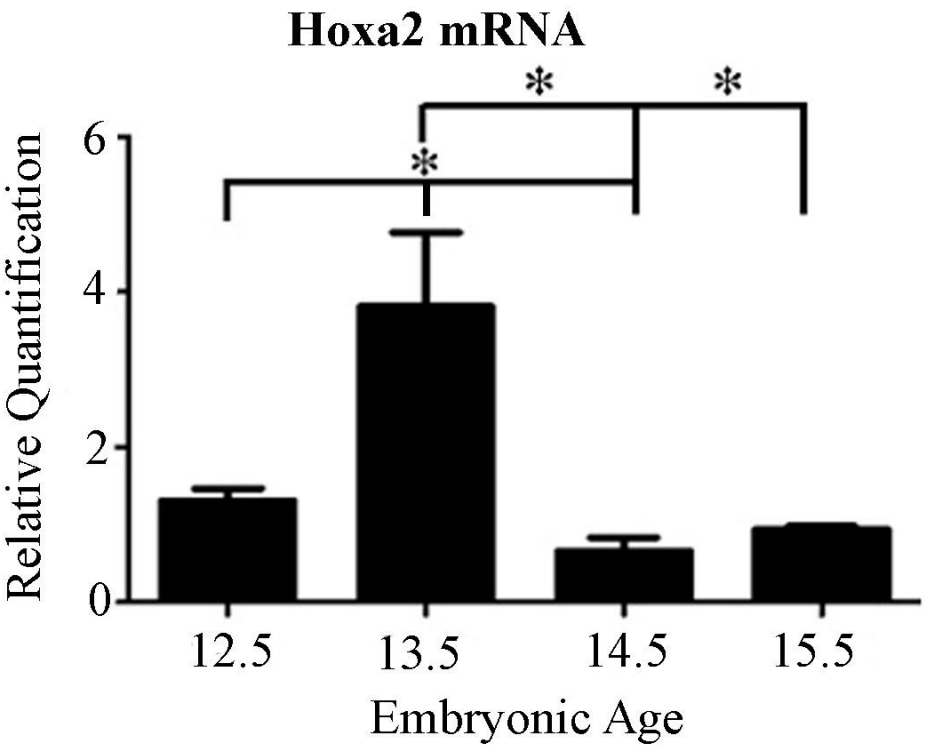
Hoxa2 mRNA
*
*
*
6
4
2
0
Relative Quantification
12.5
13.5
14.5
15.5
Embryonic Age

B)

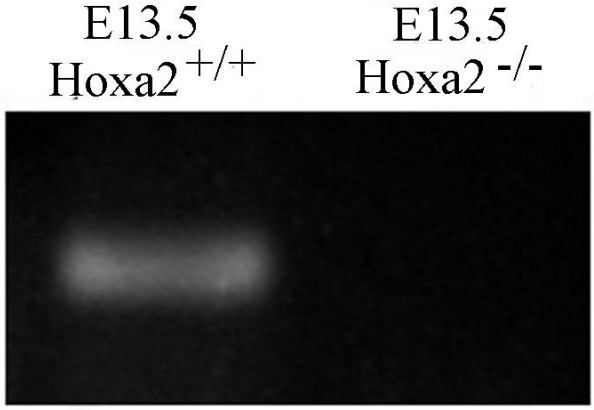
E13.5
Hoxa2 +/+
E13.5
Hoxa2 -/-

Figure 9. *Hoxa*2 mRNA Expression in the Developing Palate

A) Relative quantitative expression of the *Hoxa*2 gene throughout murine palatogenesis as determined by quantitative real time RT-PCR using Taqman primers and probes. Graph represents mean ± SEM, n=3. * represents a significance of $p<0.05$ between the bars indicated by the brackets. B) Ethidium bromide gel of *Hoxa*2 mRNA in the wild-type at E13.5 and absence signal was observed in *Hoxa2* null embryos implying a lack of amplification of *Hoxa2* mRNA.

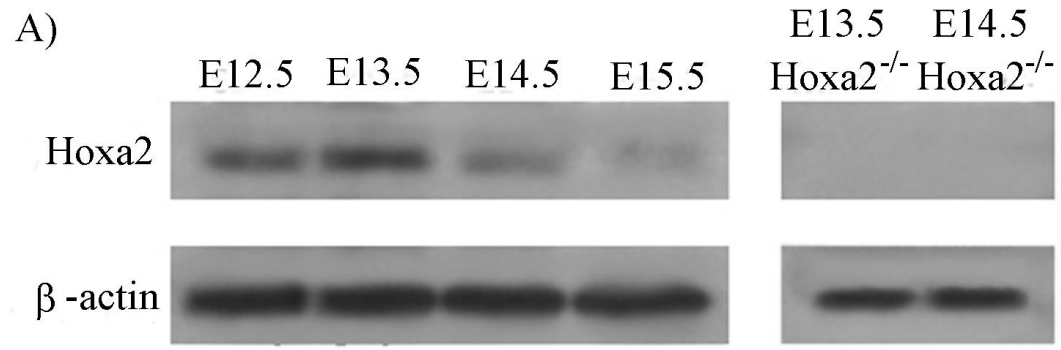
A)
E12.5
E13.5
E14.5
E15.5
E13.5 Hoxa2-/-
E14.5 Hoxa2-/-
Hoxa2
β -actin

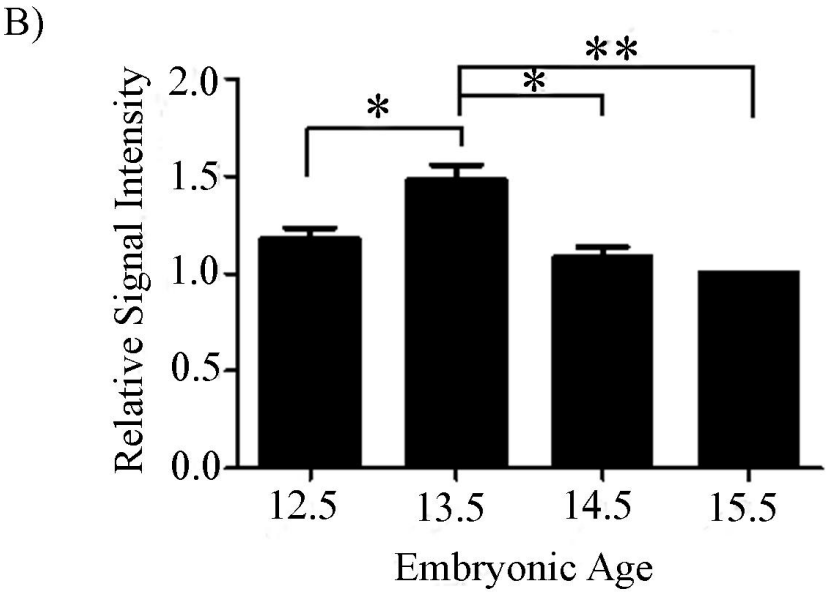
B)
Relative Signal Intensity
2.0
1.5
1.0
0.5
0.0
*
*
**
12.5
13.5
14.5
15.5
Embryonic Age

Figure 10. Hoxa2 Protein Expression in the Developing Palate

A) Western blot analysis of Hoxa2 protein expression levels in the developing palate at E12.5, E13.5, E14.5 and E15.5. Beta-actin levels are used to show equal loading of protein between wells. Hoxa2$^{-/-}$ protein samples are from an E13.5 and an E14.5 embryo and confirm the specificity of the antibody to the Hoxa2 protein. B) Densitometry was performed on the western blots (n=3) and the expression levels normalized to Beta-actin and relative to E15.5 are shown above. Graph represents mean ± SEM. * denotes $p<0.05$ and ** denotes $p<0.01$.

western blots on protein isolated from the palate shelves of E13.5 and E14.5 *Hoxa2* null embryos.

Anterior, medial and posterior sections from E12.5, E13.5, E14.5 and E15.5 embryos were analyzed for Hoxa2 protein. At E12.5 Hoxa2 was expressed in both the epithelium and the mesenchyme (Fig. 11 A-C). Hoxa2 protein expression increased in both the mesenchyme and epithelium of the palate at E13.5 (Fig. 11 E-G). By E14.5, overall Hoxa2 expression had declined throughout the palate with the highest expression observed in the midline epithelial seam (Fig. 11 I-K). At E15.5 the contacted palate shelves had fused to gain mesenchymal confluence and low levels of Hoxa2 expression was observed throughout the palate (Fig. 11 M-O). Hoxa2 null palate shelves did not show a detectable signal confirming that the antibody is specific for the Hoxa2 protein (Fig. 11 D,H,L,P). These data also correspond with the levels observed by real time RT-PCR and western blot analyses.

5.2 Histology

Wild-type and *Hoxa2* null embryos were sectioned in a coronal plane to examine if there was an alteration in the shape, size or orientation of the null palates compared to wild-type controls. Anterior, medial and posterior regions were examined between E12.5 and E15.5. Initially, there did not appear to be any gross differences in the appearance of the palate shelves in the *Hoxa2* null animals (Fig. 12 A-D). At E14.5 in wild-type animals, the palate shelves have flipped to be oriented horizontally above the tongue and by E15.5 they have

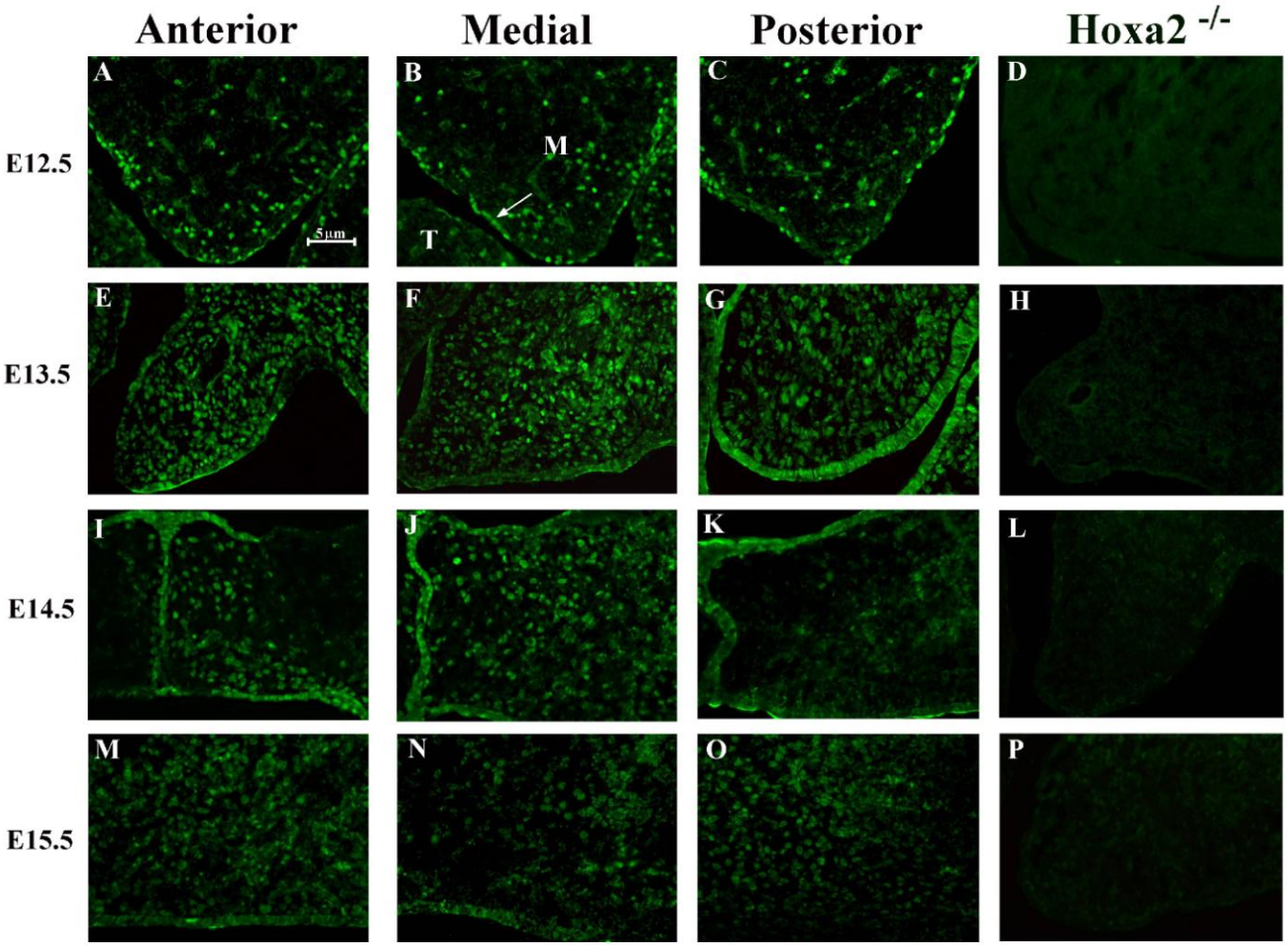
Anterior
Medial
Posterior
Hoxa2 -/-
E12.5
E13.5
E14.5
E15.5
A
B
C
D
E
F
G
H
I
J
K
L
M
N
O
P
M
T
5μm

Figure 11. Immunohistochemical Staining for Hoxa2 Protein in the Mouse Palate.

Anterior, medial and posterior palate sections are in the same orientation and from the same embryo. Green nuclear staining represents the expression of the Hoxa2 protein at E12.5 (A-C), E13.5 (E-G), E14.5 (I-K) and E15.5 (M-O). Sections of the Hoxa2$^{-/-}$ palates (D,H,L,P) are from the anterior palate regions at the ages denoted on the left. These sections clearly show a lack of staining in the Hoxa2$^{-/-}$ palates confirming the specificity of the antibody. Arrow is pointing the epithelium. M, mesenchyme, T, tongue.

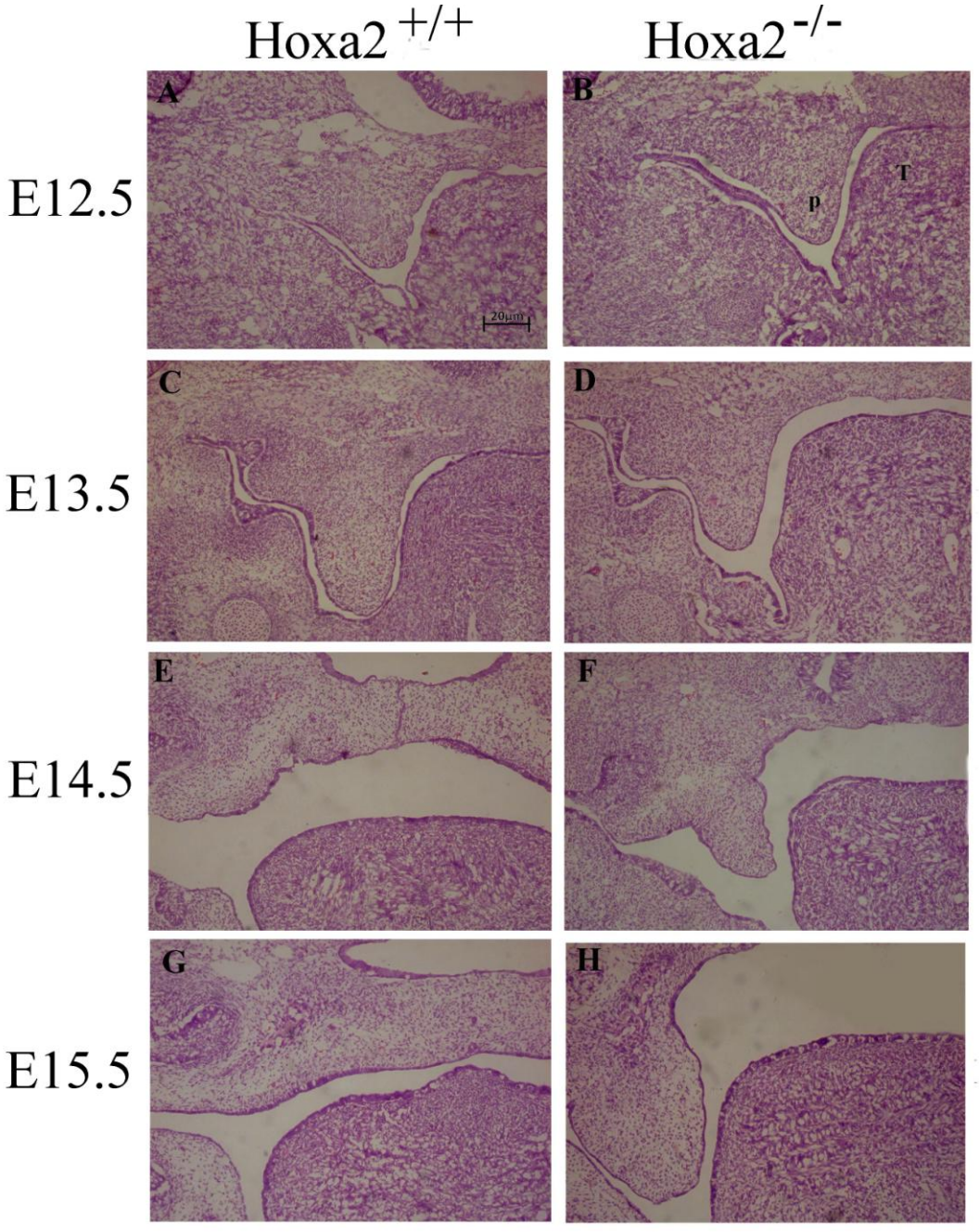
Hoxa2 +/+
Hoxa2 -/-
E12.5
E13.5
E14.5
E15.5
A
B
C
D
E
F
G
H
T
p
20µm

Figure 12. Histological Analysis of the Palate Shelves

Coronal sections of wild-type and *Hoxa*2 null palate shelves were stained with Hemotoxylin and Eosin to compare the gross morphology of the palate shelves. Representative medial sections are shown. Palate shelves fail to elevate above the tongue in *Hoxa2* null embryos. P=palate shelf, T=Tongue.

undergone fusion to form a confluent palate (Fig. 12.E,G). Loss of the *Hoxa2* gene appears to result in problems at this stage as palate shelves remain vertically oriented in most animals even at E15.5 (Fig. 12 F,H).

5.3 Cell Proliferation Assay

To determine whether a loss of *Hoxa*2 expression in the palate resulted in alterations in the growth of the palate primordia, cell proliferation rates were compared within the anterior, medial, and posterior regions of the palate in wild-type and *Hoxa*2 null palates at stages E12.5 through E15.5 (n=4) (Fig. 13 and 14). Two-way ANOVA analysis revealed that in all three regions of the palate, the interaction between the genotype and developmental stage was significant ($p<0.001$). An overall increase in proliferation rates in the *Hoxa*2 null palate shelves was observed. In the anterior of the palate, a significant increase in proliferation rates were observed at E12.5, E14.5 and E15.5 ($p<0.001$) (Fig. 14 A). A similar trend was also observed in the medial (Fig. 14 B) and posterior (Fig. 14 C) palate with a significant increase at E12.5 and E14.5 ($p<0.001$) in both regions.

5.4 Apoptosis analysis

To examine whether the survival of cells in the developing palate is changed in the absence of *Hoxa2,* the level of apoptosis was compared between wild-type and *Hoxa*2 null palates at E12.5, E13.5 and E14.5 using the DeadEnd Fluorometric TUNEL (terminal deoxynucleotidyl transferase-mediated dUTP nick-end labelling) System (Promega). The anterior, medial

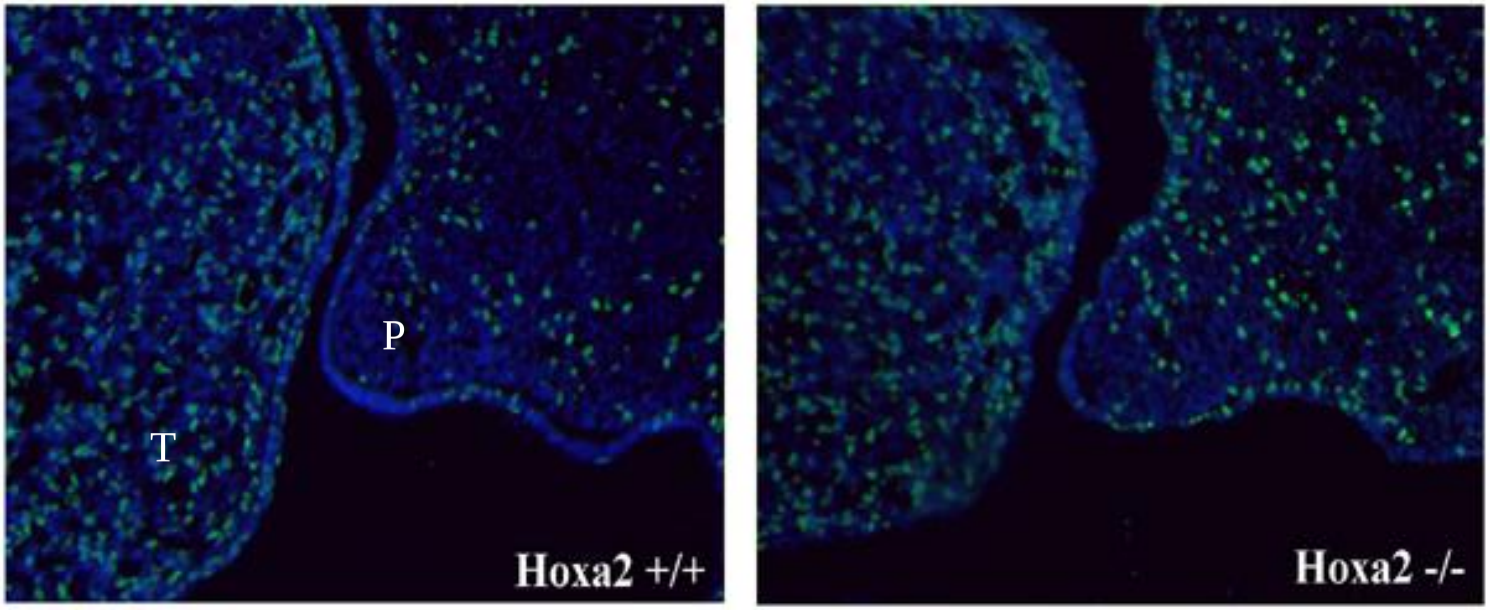
P
T
Hoxa2 +/+
Hoxa2 -/-

Figure 13. Immunohistochemical Analysis of BrdU Uptake to Compare Proliferation Rates between Wild-type and *Hoxa2* null palates

Representative medial sections from E12.5 embryos of wild-type (Hoxa2 +/+) and *Hoxa2* null (Hoxa2 -/-) palate shelves stained with a BrdU specific antibody (green), and Hoechst (blue). A clear increase in the number of BrdU positive cells can be seen in the *Hoxa*2 null sample indicative of an increase in proliferation in the absence of the *Hoxa*2 gene. P=palatal shelf, T=tongue.

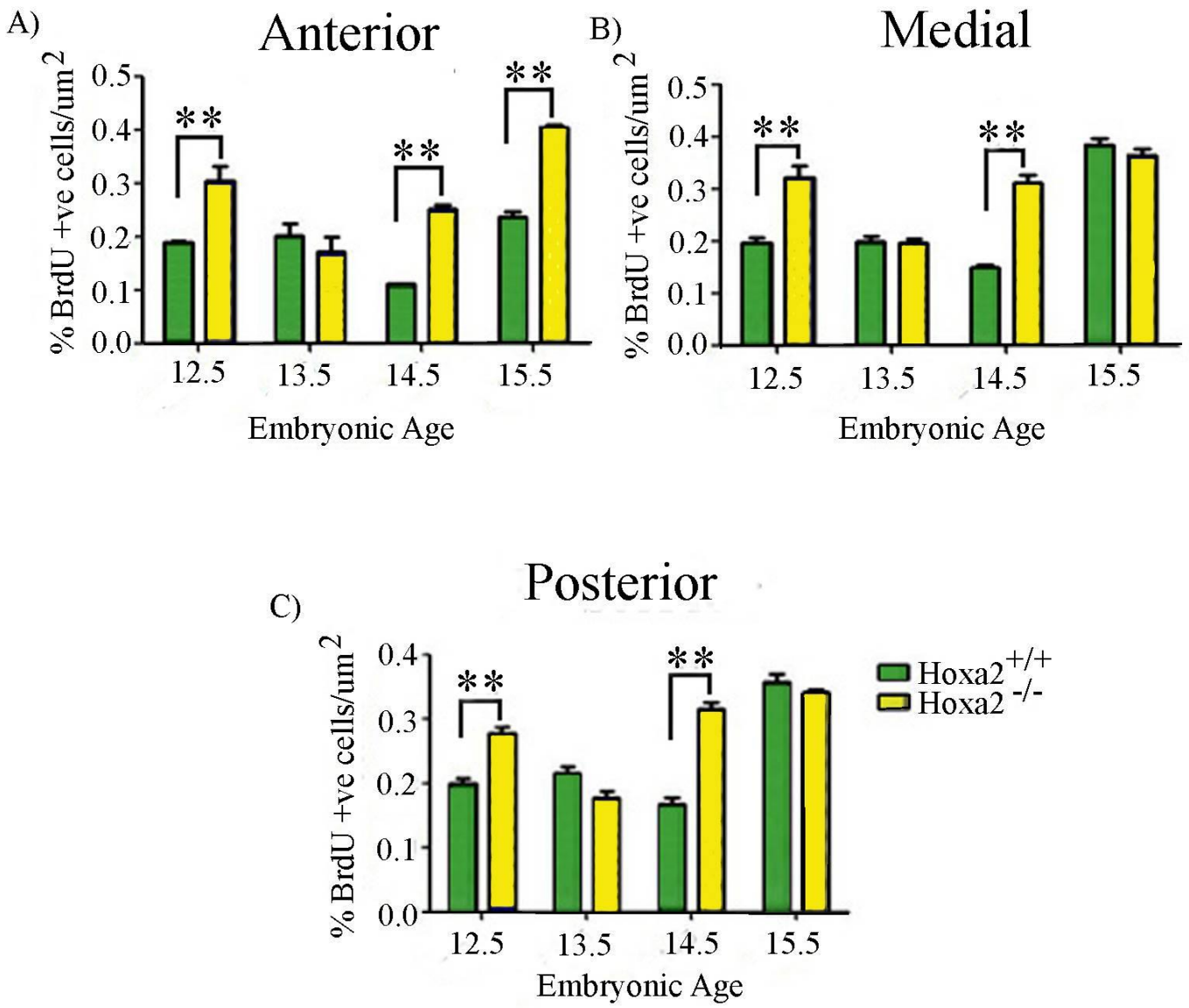
A)
Anterior
% BrdU +ve cells/um 2
0.5
0.4
0.3
0.2
0.1
0.0
**
**
**
12.5
13.5
14.5
15.5
Embryonic Age
B)
Medial
% BrdU +ve cells/um 2
0.5
0.4
0.3
0.2
0.1
0.0
**
**
12.5
13.5
14.5
15.5
Embryonic Age
C)
Posterior
% BrdU +ve cells/um 2
0.4
0.3
0.2
0.1
0.0
**
**
12.5
13.5
14.5
15.5
Embryonic Age
Hoxa2 +/+
Hoxa2 -/-

Figure 14. Increased Cell Proliferation Rates within *Hoxa2* null Palates

Cell proliferation rates within the developing palate shown as mean percentage of cells that are BrdU positive per μm^2 ± SEM. Sections from the anterior (A), medial (B) and posterior (C) regions of the palate were analyzed at E12.5, E13.5, E14.5 and E15.5 of wild-type and *Hoxa2* null palates (n=4).

and posterior was examined at each age (n=3). No difference was observed in the number of apoptotic cells at any developmental stage between the wild-type and *Hoxa*2 null palates (Fig. 15).

To confirm these findings, sections from the anterior, medial and posterior of E12.5, E13.5 and E14.5 of wild-type and *Hoxa*2 null palates were stained with an antibody specific for the activated caspase 3 protein, another hallmark of apoptosis (Fig. 16). Once again no difference was observed in the number of apoptotic cells in the palates of *Hoxa2* null embryos at any stage.

5.5 Organ Cultures

To determine whether *Hoxa2* null palates are capable of fusing together, an organ culture technique was employed. Palate shelves were placed in contact with one another and allowed 72 h to fuse. Fusion rates were not significantly different between wild-type, heterozygous and *Hoxa2* null palates (Fig. 17 B). Sections of the cultured palates were stained with cresyl violet to confirm mesenchymal confluence had occurred (Fig. 17 A). *Hoxa2* null palates were equally capable of fusing as their wild-type controls.

5.6 Msx1 Expression

*Msx*1 expression within the developing palate has been well characterized (Zhang et al., 2002). Quantitative real time RT-PCR showed expression at all stages of development in both the wild-type and *Hoxa*2 null palatal shelves (Fig. 18 A). Two-way ANOVA showed that there was a significant interaction between genotype and embryonic age ($p=0.0012$,

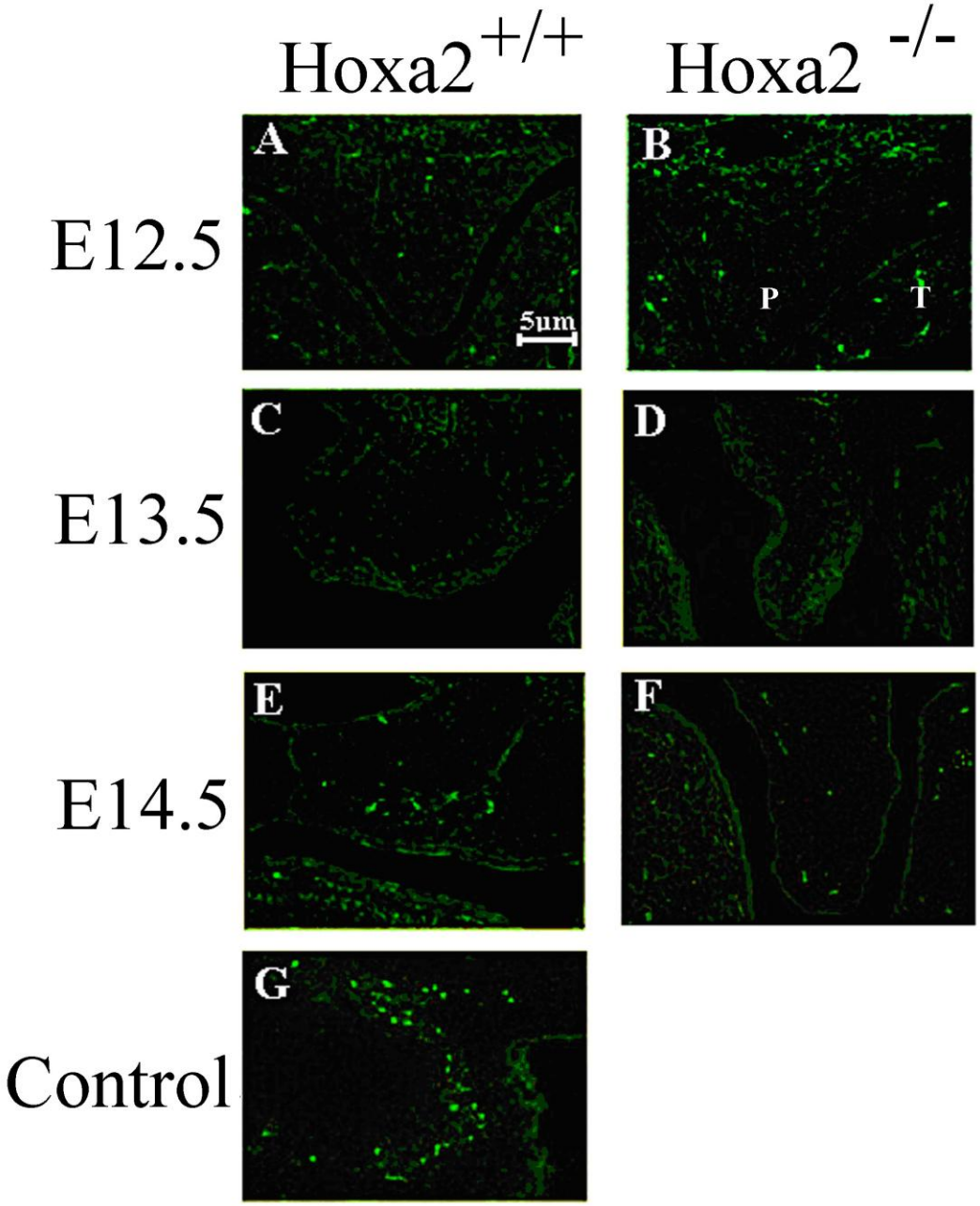
Hoxa2 +/+
Hoxa2 -/-
E12.5
E13.5
E14.5
Control
A
B
C
D
E
F
G
5um
P
T

Figure 15. TUNEL analysis shows Apoptosis was not Altered in *Hoxa*2 null Palates

Wild-type and *Hoxa2* null palates at E12.5 (A,B), E13.5 (C,D) and E14.5 (E,F) (n=3) were analyzed by TUNEL to compare the level of apoptosis. Green stained cells were positive for fragmented DNA and therefore determined to be apoptotic. Loss of Hoxa2 expression did not lead to a detectable change in the level of apoptosis. Representative medial sections are shown. Control section is from an E13.5 hindlimb. P=palatal shelf, T=tongue.

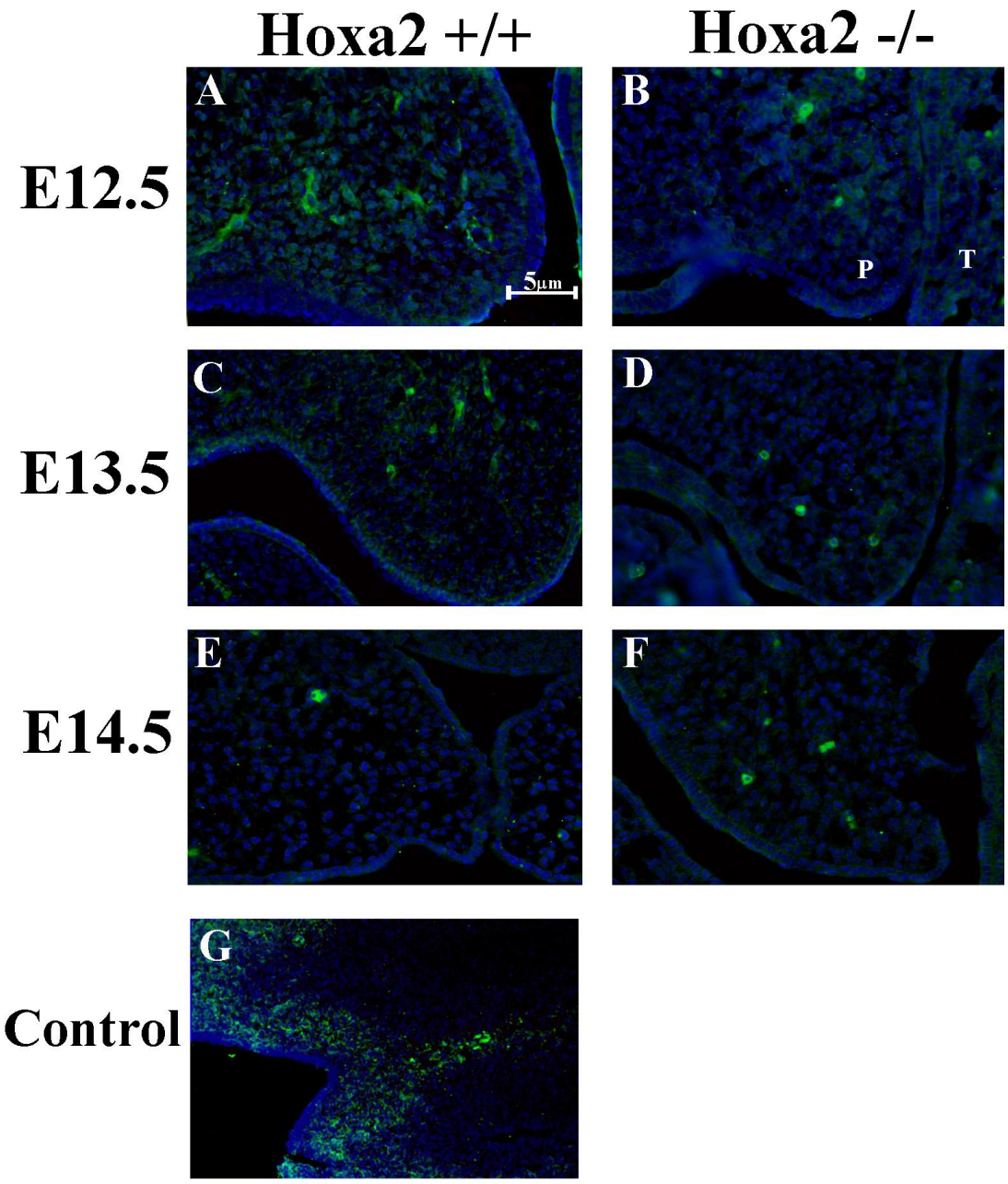
Hoxa2 +/+
Hoxa2 -/-
E12.5
E13.5
E14.5
Control
A
B
C
D
E
F
G
5µm
P
T

Figure 16. Analysis of Activated Caspase 3 shows Apoptosis is not Altered in *Hoxa*2 null Palates

Wild-type and *Hoxa2* null palates at E12.5 (A.B), E13.5 (C,D) and E14.5 (E,F) (n=3) were analyzed by immunohistochemical analysis for activated caspase 3 to compare the level of apoptosis. Green staining is specific for activated caspase 3, while nuclei are stained in blue with Hoechst. Loss of Hoxa2 expression did not lead to a detectable change in the level of apoptosis. Representative medial sections are shown. Control section is from an E13.5 hindlimb. P=palatal shelf, T=tongue.

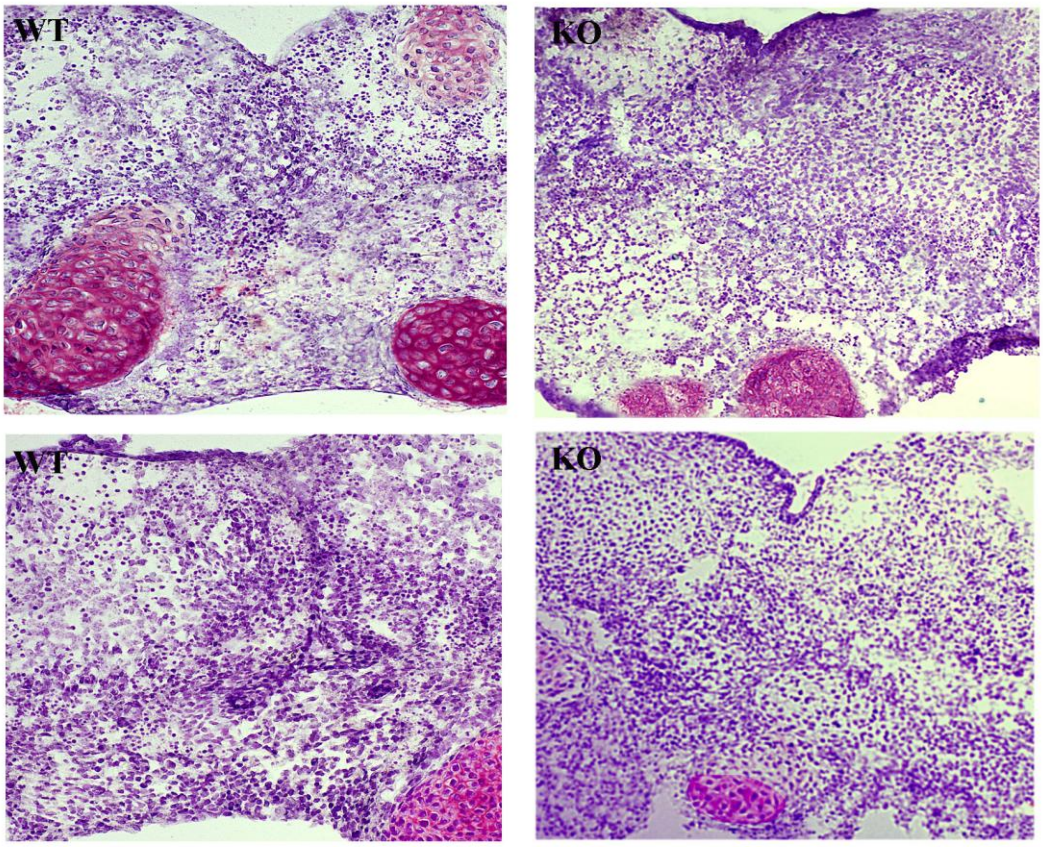

Genotype of the Embryo	Number of Palates Fused	Total Number of Palates Cultured	Percentage of Fused Palates
Wild-type	12	14	87.5 %
Heterozygous	14	15	93.3 %
Hoxa2 null	6	7	87.5%

Figure 17. Absence of the *Hoxa2* gene does not Alter the Ability of Palate Shelves to Fuse.

Palate shelves were dissected from wild-type (WT), heterozygous and *Hoxa2* null (KO) embryos at E14.0 and placed in contact with one another After 72 h in culture the palates were assessed for fusion before being fixed, sectioned and stained with cresyl violet to check for degradation of the epithelial seam.

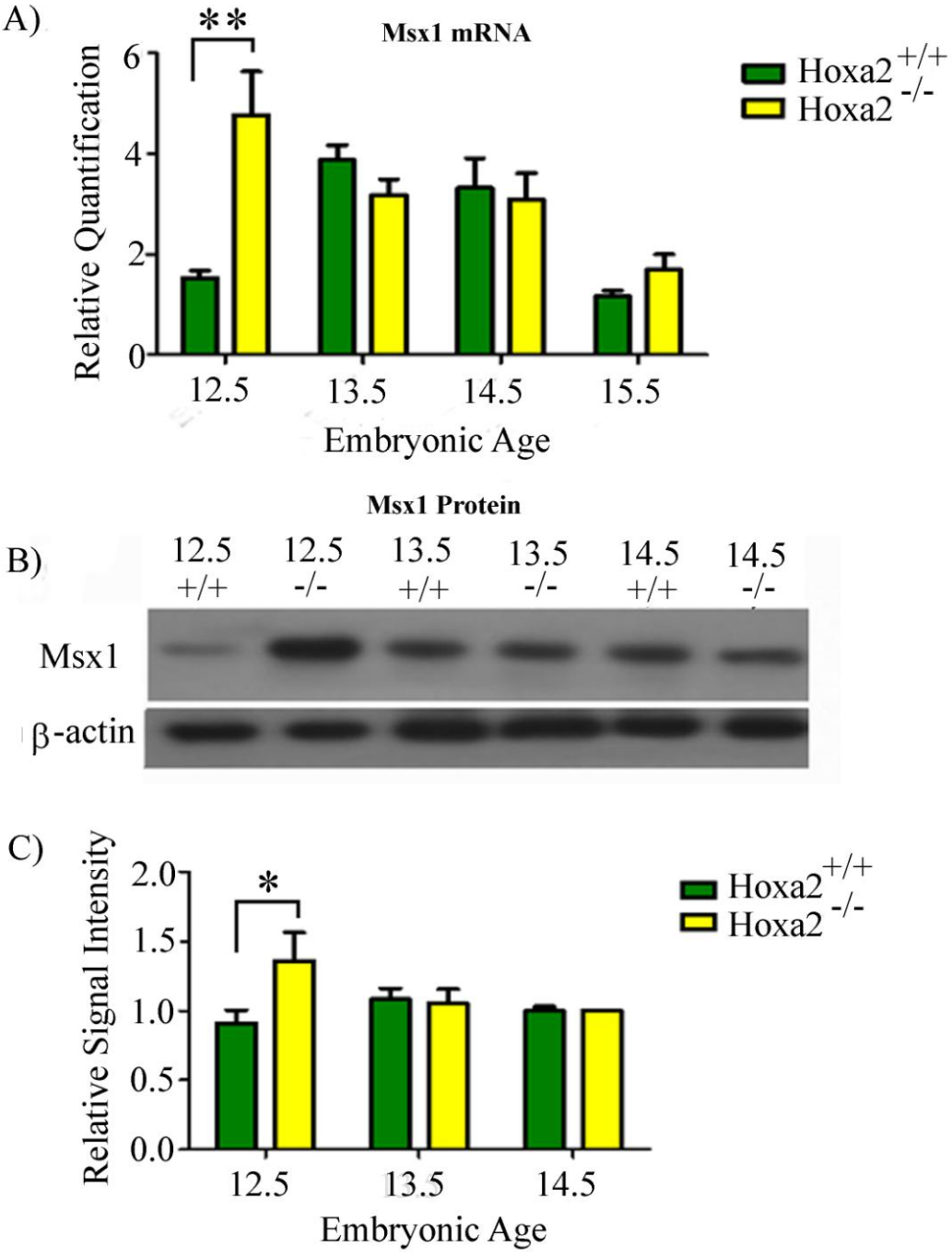
A)
**
Msx1 mRNA
Hoxa2 +/+
Hoxa2 -/-
Relative Quantification
6
4
2
0
12.5
13.5
14.5
15.5
Embryonic Age
Msx1 Protein
B)
12.5 +/+
12.5 -/-
13.5 +/+
13.5 -/-
14.5 +/+
14.5 -/-
Msx1
β-actin
C)
*
Hoxa2 +/+
Hoxa2 -/-
Relative Signal Intensity
2.0
1.5
1.0
0.5
0.0
12.5
13.5
14.5
Embryonic Age

Figure 18. Enhanced Msx1 Expression in *Hoxa2* null Palate Shelves.

Relative quantitative expression of Msx1 throughout murine palatogenesis in $Hoxa2^{+/+}$ and $Hoxa2^{-/-}$ palates. (A) mRNA expression was determined by quantitative real time RT-PCR using Taqman primers and probes. Bars represent mean ± SEM, n=4. (B) Msx1 protein expression was determined by western blot analysis of palatal protein. Beta-actin is used to show equal loading of protein between samples. (C) Densitometry of the western blots was performed to determine a trend in expression levels. Bars represent mean ± SEM, n=3. * $p<0.05$, ** $p<0.01$.

F=7.331). Analysis of the expression of *Msx*1 in the wild-type palate showed differential expression throughout palatogenesis, significantly increasing between E12.5 and E13.5 ($p<0.01$) in wild-type palate shelves and remaining elevated at E14.5 before decreasing at E15.5 ($p<0.001$). Analysis of expression levels in the *Hoxa2* null animals revealed that expression was not significantly different between E12.5, E13.5 and E14.5 but did decrease at E15.5 ($p<0.05$). *Hoxa*2 null embryos display a significant increase in mRNA expression levels at E12.5 ($p<0.01$), but return to normal wild-type levels throughout the remainder of palatogenesis (Fig. 18 A).

Western blot analysis was performed to determine protein expression of Msx1. Wild-type and *Hoxa2* null palate shelves were analyzed at E12.5, E13.5, and E14.5 (Fig. 18 B). Msx1 protein was detected in both wild-type and null palate shelves. Densitometry of the western blots (n=3) confirmed that Msx1 protein is increased in the *Hoxa2* null palates at E12.5 ($p<0.05$). By E13.5, the expression of the Msx1 protein does not appear to be different between wild-type and *Hoxa2* null samples (Fig. 18 C). The protein expression trend matches the mRNA expression profile determined by real time RT-PCR.

5.7 Bmp4 Expression

Bmp4 expression was examined as it is known to be expressed within the palate and is a downstream target of Msx1 (Zhang, et al., 2002). Our results confirm that *Bmp*4 mRNA is present at E12.5, E13.5, E14.5 and E15.5 in the wild-type palate, with no statistical differences in expression levels

throughout development (Fig. 19 A). Two-way ANOVA revealed a significant interaction between genotype and embryonic age ($p=0.0069$, $F=7.331$). Absence of *Hoxa*2 from the palate shelves resulted in a significant increase in the expression level of Bmp4 only at E12.5 ($p< 0.001$)(Fig. 19A). This increase in expression corresponds well with the increase in Msx1 expression at the same stage. Bmp4 protein expression was also examined using western blot analysis. Protein expression increased substantially at E13.5 representing a slight delay following the increase in mRNA at E12.5 (Fig. 19 B). Densitometry revealed that the Bmp4 protein is increased within the *Hoxa2* null palate shelves at E13.5 ($p<0.05$) but appears to return to wild-type levels by E14.5 (Fig. 19 C).

5.8 Barx1 Expression

Hoxa2 is expressed throughout the developing palate and therefore, examining the expression of a posterior specific protein will help determine if there is a role for Hoxa2 in this region of the palate. Barx1 expression has previously been described in the developing palate (Welsh et al., 2007). Expression was detected at E12.5, E13.5, E14.5 and E15.5 within the palate shelves throughout palatogenesis. Two-way ANOVA did not reveal an interaction between genotype and age ($p=0.5731$, $F=0.6803$). Expression in *Hoxa*2 null palate shelves was significantly increased compared to wild-type controls at E13.5. No detectable difference was determined at any other developmental stage (Fig. 20 A). Alteration of Barx1 at E13.5 suggests that

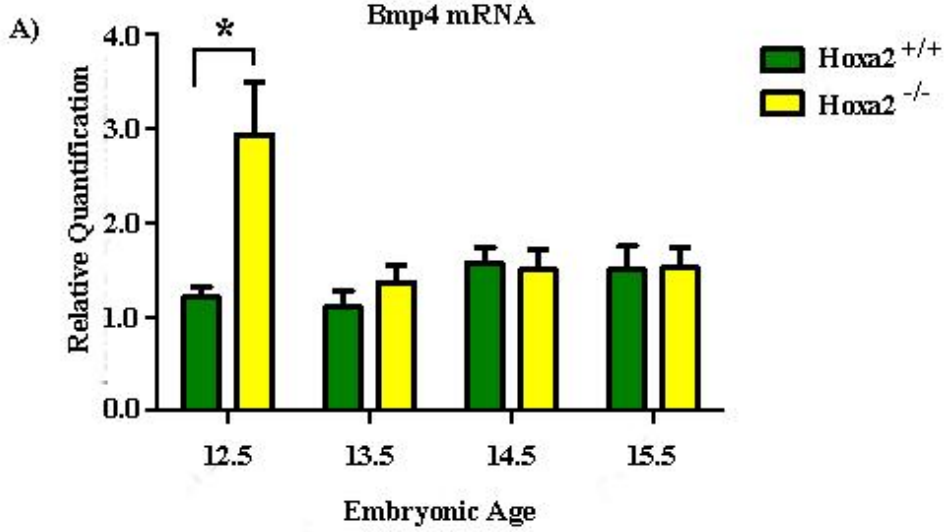
A)
Bmp4 mRNA
Relative Quantification
4.0
3.0
2.0
1.0
0.0
*
Hoxa2 +/+
Hoxa2 -/-
12.5
13.5
14.5
15.5
Embryonic Age

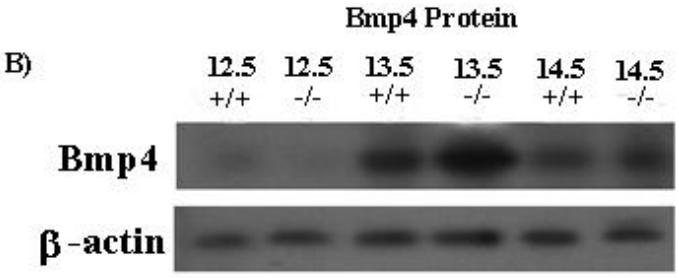
Bmp4 Protein
B)
12.5 +/+
12.5 -/-
13.5 +/+
13.5 -/-
14.5 +/+
14.5 -/-
Bmp4
β-actin

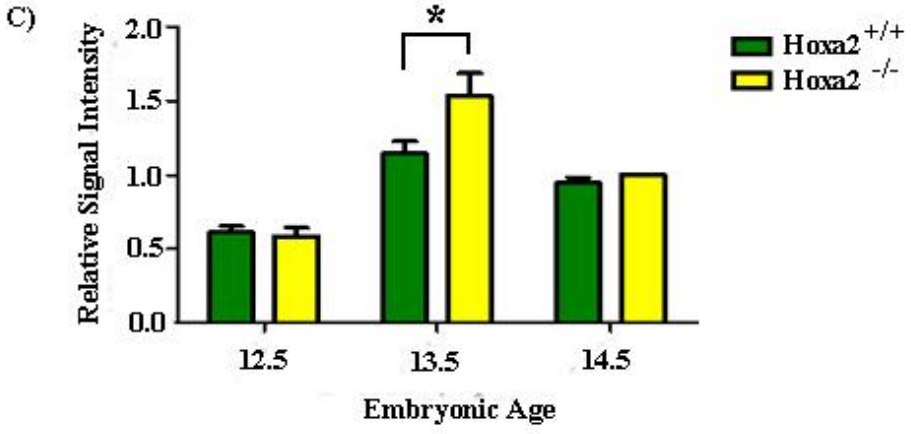
C)
Relative Signal Intensity
2.0
1.5
1.0
0.5
0.0
*
Hoxa2 +/+
Hoxa2 -/-
12.5
13.5
14.5
Embryonic Age

Figure 19. Enhanced Bmp4 Expression in *Hoxa2* null Palate Shelves.

Relative quantitative expression of Bmp4 throughout murine palatogenesis in $Hoxa2^{+/+}$ and $Hoxa2^{-/-}$ palates. (A) mRNA expression was determined by quantitative real time RT-PCR using Taqman primers and probes. Bars represent mean ± SEM, n=4. (B) Bmp4 protein expression was determined by western blot analysis of palatal protein. Beta-actin is used to show equal loading of protein between samples. (C) Densitometry of the western blots was performed to determine a trend in expression levels. Bars represent mean ± SEM, n=3. * $p<0.05$.

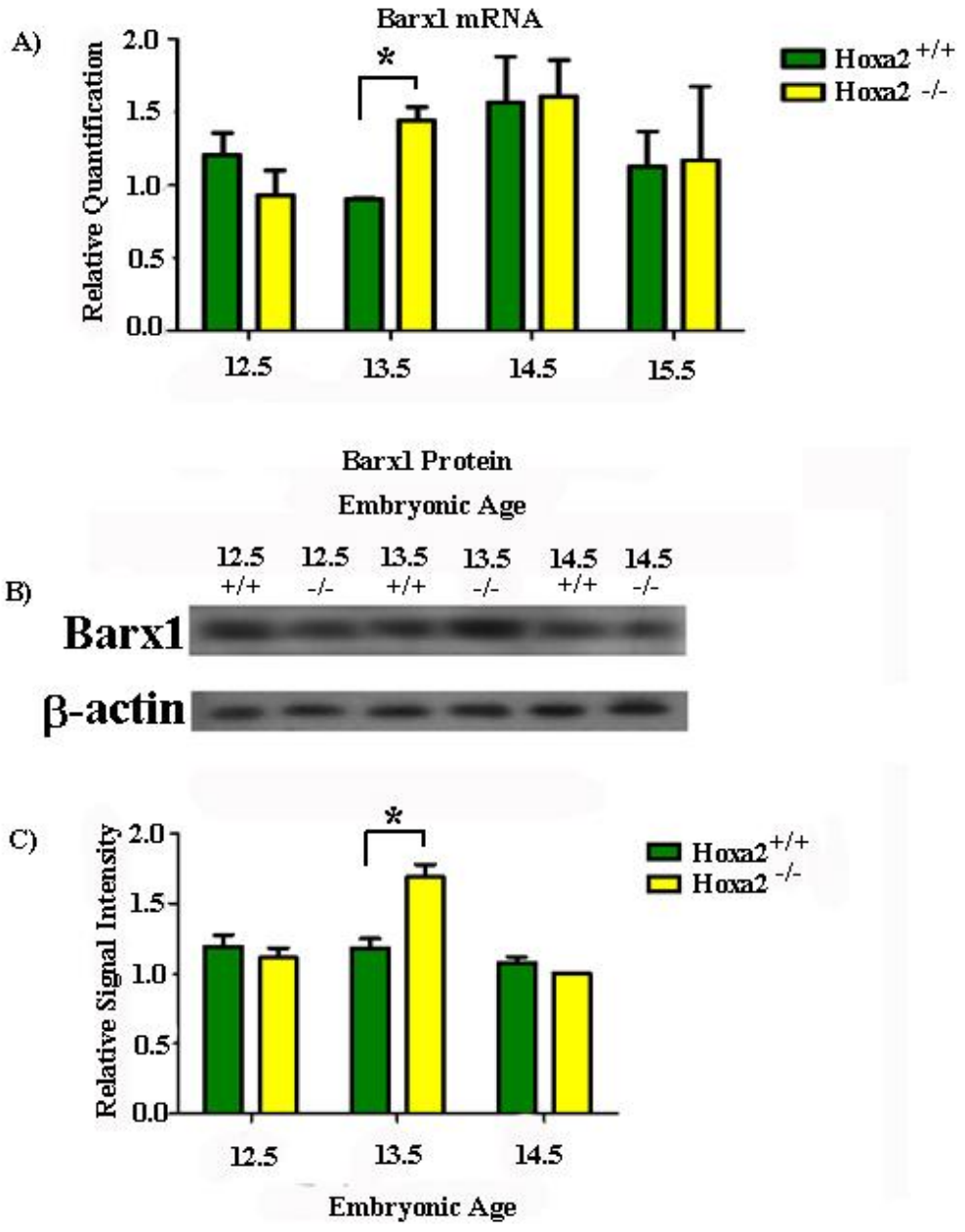
A)
Barxl mRNA
Relative Quantification
2.0
1.5
1.0
0.5
0.0
*
12.5
13.5
14.5
15.5
Hoxa2 +/+
Hoxa2 -/-
Barxl Protein
Embryonic Age
B)
12.5 +/+
12.5 -/-
13.5 +/+
13.5 -/-
14.5 +/+
14.5 -/-
Barx1
β-actin
C)
Relative Signal Intensity
2.0
1.5
1.0
0.5
0.0
*
12.5
13.5
14.5
Embryonic Age
Hoxa2 +/+
Hoxa2 -/-

Figure 20. Enhanced Barx1 Expression in *Hoxa2* null Palate Shelves.

Relative quantitative expression of Barx1 throughout murine palatogenesis in $Hoxa2^{+/+}$ and $Hoxa2^{-/-}$ palates. (A) mRNA expression was determined by quantitative real time RT-PCR using Taqman primers and probes. Bars represent mean ± SEM, n=4. (B) Barx1 protein expression was determined by western blot analysis of palatal protein. Beta-actin is used to show equal loading of protein between samples. (C) Densitometry of the western blots was performed to determine a trend in expression levels. Bars represent mean ± SEM, n=3. * $p<0.05$.

there is a role for Hoxa2 in regulating posterior palate development.

To confirm the increase in Barx1 the levels of the protein were also examined by western blot analysis of wild-type and *Hoxa*2 null palates at E12.5, E13.5 and E14.5 (n=3)(Fig. 20 B). In agreement with the changes in mRNA levels, an increase in the levels of Barx1 protein was observed at E13.5 ($p<0.05$) (Fig 20 C).

5.9 Ptx1 Expression

*Ptx*1 expression has previously been detected by *in situ* hybridization histochemistry in the first branchial arch and its derivatives, including the palate at E15 (Bobola, et al., 2003; Lanctot, et al., 1997). Using quantitative real time RT-PCR *Ptx*1 expression was detected in both wild-type and *Hoxa*2 null palatal shelves at E12.5, E13.5, E14.5 and E15.5 (Fig. 21 A). Two-way ANOVA did not reveal a significant effect of interaction ($p=0.1034$, $F=2.426$). Expression was not significantly altered throughout development. A significant increase in *Ptx*1 mRNA expression was seen in *Hoxa*2 null palatal shelves at E13.5 compared to wild-type ($p<0.05$).

Protein expression of Ptx1 was also detectable in the palate by western blot analysis. A trend of increased expression of Ptx1 protein in the Hoxa2 null palate shelves compared to wild-type palates was seen at E13.5 and E14.5 (Fig. 21 B), however densitometry revealed a significant increase only at E13.5 was significant ($p<0.05$) (Fig. 21 C). These data correspond with the observed

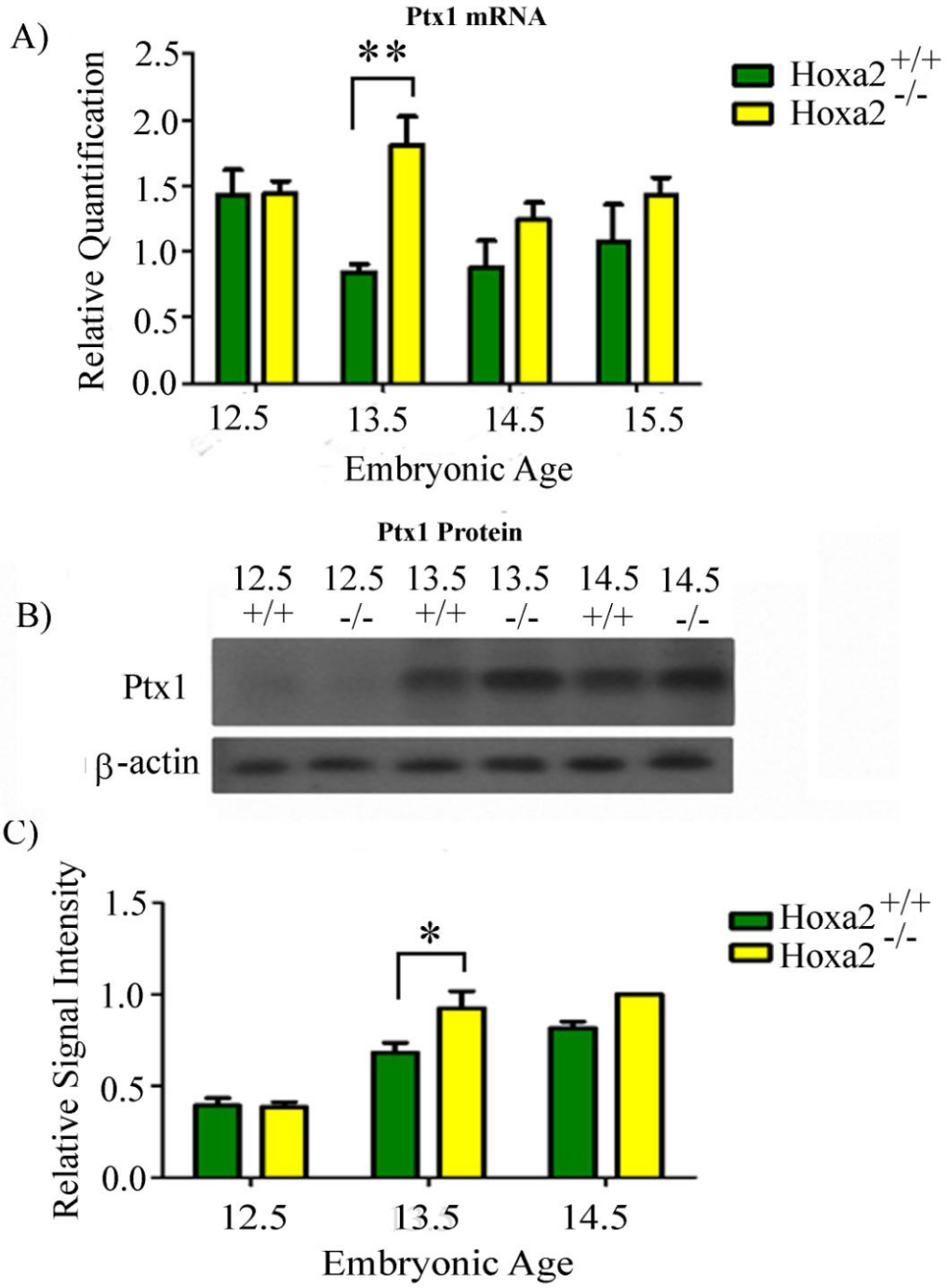
A)
Ptx1 mRNA
Relative Quantification
2.5
2.0
1.5
1.0
0.5
0.0
**
12.5
13.5
14.5
15.5
Embryonic Age
Hoxa2 +/+
Hoxa2 -/-
B)
Ptx1 Protein
12.5 +/+
12.5 -/-
13.5 +/+
13.5 -/-
14.5 +/+
14.5 -/-
Ptx1
β-actin
C)
Relative Signal Intensity
1.5
1.0
0.5
0.0
*
12.5
13.5
14.5
Embryonic Age
Hoxa2 +/+
Hoxa2 -/-

Figure 21. Enhanced Ptx1 Expression in *Hoxa2* null Palate Shelves.

Relative quantitative expression of Ptx1 throughout murine palatogenesis in $Hoxa2^{+/+}$ and $Hoxa2^{-/-}$ palates. (A) mRNA expression was determined by quantitative real time RT-PCR using Taqman primers and probes. Bars represent mean ± SEM, n=4. (B) Ptx1 protein expression was determined by western blot analysis of palatal protein. Beta-actin is used to show equal loading of protein between samples. (C) Densitometry of the western blots was performed to determine a trend in expression levels. Bars represent mean ± SEM, n=3. * $p<0.05$, ** $p<0.01$.

increase of mRNA at E13.5.

5.10 Fgf8 Expression

It is predicted that regulation of Ptx1 expression by Hoxa2 involves Fgf8 and its signalling pathway (Bobola et al., 2003). Quantitative real time RT-PCR was employed to determine whether *Fgf8* was expressed in the palate and if the loss of the *Hoxa2* gene altered its expression. *Fgf8* mRNA expression was detected in palatal shelves from E12.5, E13.5, E14.5 and E15.5 embryos, with the highest level observed at E12.5. After this point, expression decreased dramatically and remained low for the remainder of palatogenesis. Loss of the *Hoxa2* gene did not appear to alter palatal *Fgf8* mRNA expression (Fig. 22 A).

Western blot analysis was used to confirm the presence of Fgf8 protein in the palate, as well as to determine if differences existed in expression between *Hoxa2* null and wild-type palate shelves. Fgf8 protein was detected at E12.5, E13.5 and E14.5 with no observable differences in the null palate samples (Fig. 22 B and C). Interestingly, Fgf8 protein expression was relatively consistent throughout development, which does not correspond with the significantly higher levels of mRNA observed at E12.5 than the other ages. This could be the result of a disconnect between mRNA levels and protein levels. Alternatively the Fgf8 antibosy may be detecting other Fgf family members. It does appear that there is not an alteration of expression in the absence of *Hoxa*2.

Fgf8 protein expression was also examined at E12.5, E13.5, E14.5 and

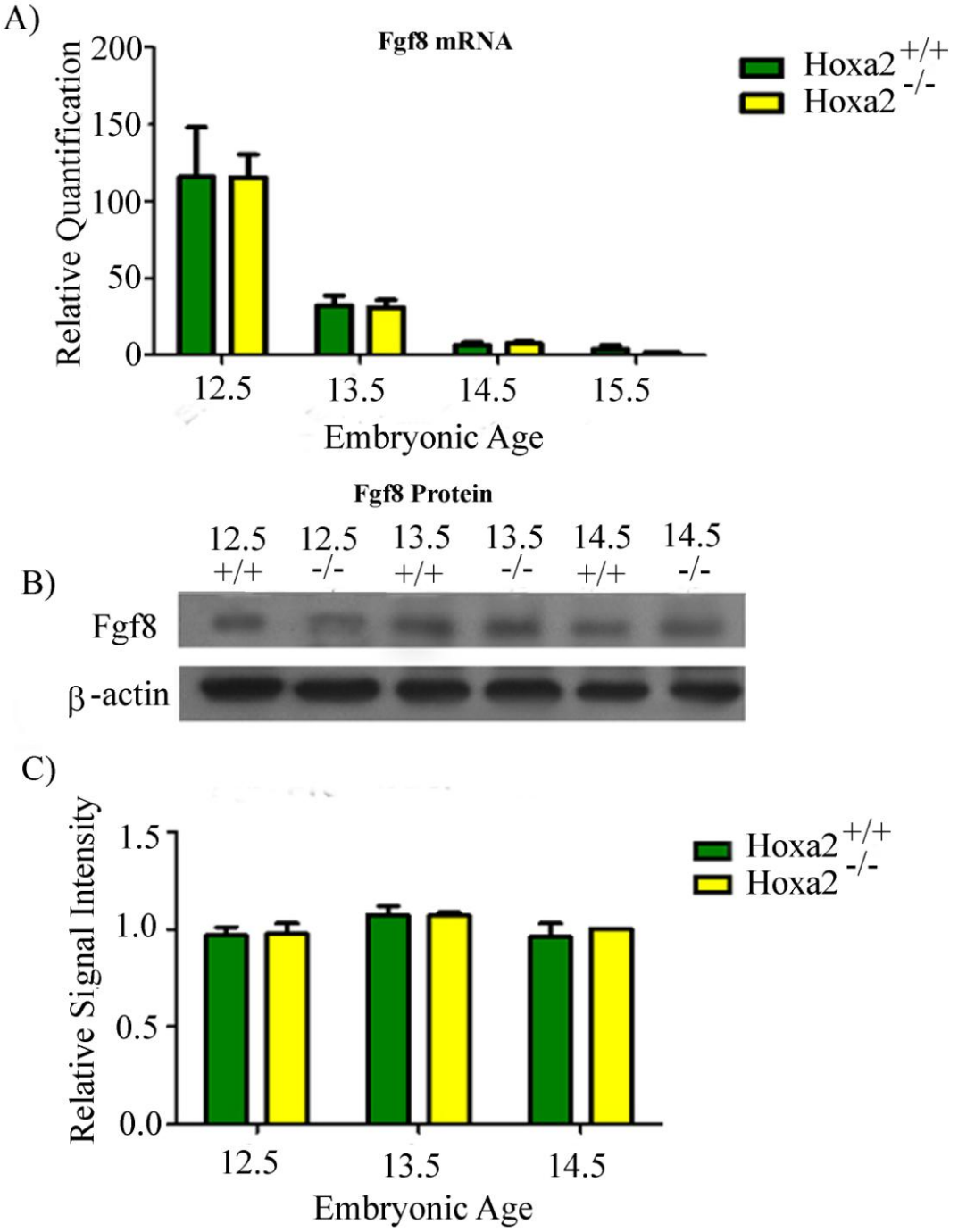
A)
Fgf8 mRNA
Hoxa2 +/+
Hoxa2 -/-
Relative Quantification
200
150
100
50
0
12.5
13.5
14.5
15.5
Embryonic Age
Fgf8 Protein
B)
12.5 +/+
12.5 -/-
13.5 +/+
13.5 -/-
14.5 +/+
14.5 -/-
Fgf8
β-actin
C)
Hoxa2 +/+
Hoxa2 -/-
Relative Signal Intensity
1.5
1.0
0.5
0.0
12.5
13.5
14.5
Embryonic Age

Figure 22. Fgf8 Expression is not Altered in *Hoxa2* null Palate Shelves.

Relative quantitative expression of Fgf8 throughout murine palatogenesis in $Hoxa2^{+/+}$ and $Hoxa2^{-/-}$ palates. (A) mRNA expression was determined by quantitative real time RT-PCR using Taqman primers and probes. Bars represent mean ± SEM, n=4. (B) Fgf8 protein expression was determined by western blot analysis of palatal protein. Beta-actin is used to show equal loading of protein between samples. (C) Densitometry of the western blots was performed to determine a trend in expression levels. Bars represent mean ± SEM, n=3.

E15.5 in the anterior, medial and posterior regions following immunohistochemical analyses. Data suggests that Fgf8 protein is present throughout the developing palate in both the epithelium and mesenchyme. The signal from immunohistochemical analyses was difficult to quantify as Fgf8 is a diffusible protein, however, significant changes were not noticeable between the wild-type and *Hoxa*2 null palates (Fig. 23).

5.11 Lhx8 Expression

Lhx8 is another known downstream target of Fgf8 signalling (Inoue et al., 2006). Lhx8 has previously been shown to be expressed in the palate, and absence of Lhx8 expression has been shown to lead to cleft palate mice (Zhao et al., 1999). To determine whether *Lhx8* mRNA expression in the developing palate was altered in the absence of Hoxa2, quantitative real time RT-PCR was used. Expression of *Lhx8* was detected at all four embryonic stages and Two-way ANOVA revealed differential expression throughout palatogenesis ($p=0.0001$, $F=26.38$) with the highest expression observed early in development, decreasing as palatogenesis proceeds. Loss of the *Hoxa2* gene did not significantly alter the expression of *Lhx8* at any stage of development ($p=0.8006$, $F=0.06525$) (Fig. 24). These data show that although the role of Hoxa2 on Ptx1 expression may occur via Fgf8 not all downstream targets of Fgf8 are altered.

5.12 Six2 Expression

*Six*2 is known to be directly repressed by *Hoxa*2 in the branchial arches

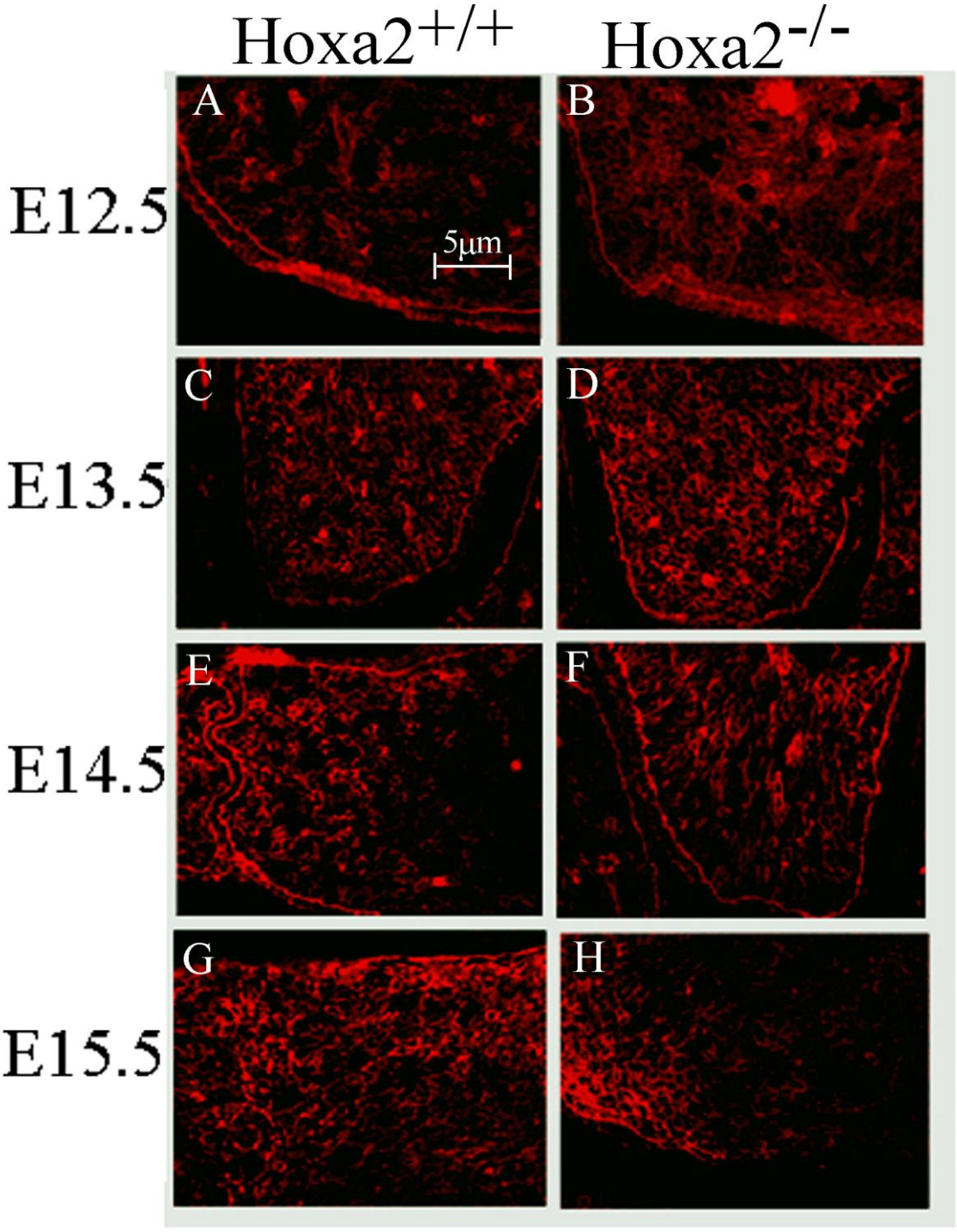
Hoxa2+/+
Hoxa2-/-
E12.5
E13.5
E14.5
E15.5
A
B
C
D
E
F
G
H
5μm

Figure 23. Fgf8 Protein is Expressed Within the Developing Palate.

Immunohistochemical analysis of Fgf8 expression within the developing palate at E12.5 (A,B), E13.5 (C,D), E14.5 (E,F), E15.5 (G,H) of both Hoxa2$^{+/+}$ and Hoxa2$^{-/-}$ embryos. Representative medial sections are shown above.

Lhx8 mRNA

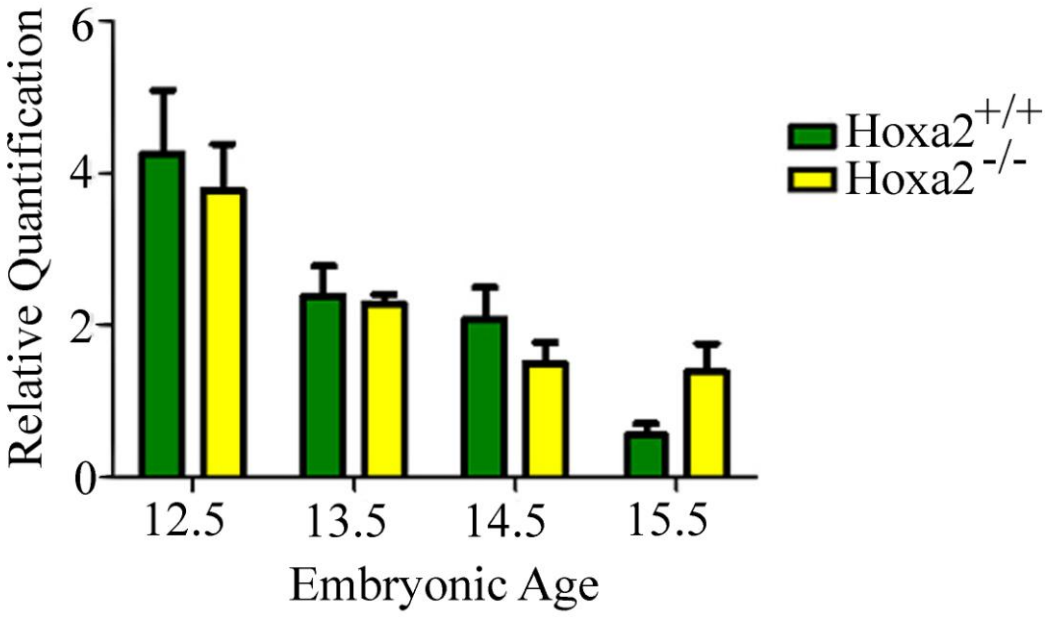
Relative Quantification
6
4
2
0
12.5
13.5
14.5
15.5
Embryonic Age
Hoxa2+/+
Hoxa2-/-

Figure 24. *Lhx8* mRNA Expression is not Altered in the Absence of Hoxa2.

Relative quantitative expression of *Lhx8* throughout murine palatogenesis in $Hoxa2^{+/+}$ (wild-type) and $Hoxa2^{-/-}$ (knock-out) embryos. mRNA levels were determined by quantitative real time RT-PCR using Taqman primers and probes. Bars represent mean ± SEM, n=4.

(Kutejova et al., 2005; Kutejova et al., 2008). Expression within the developing palate has not previously been reported. For the first time, the presence of *Six2* mRNA was shown in palate shelves at E12.5, E13.5, E14.5 and E15.5. A statistical interaction between genotype and embryonic age was detected for the expression of *Six2* mRNA in the palate ($p=0.0103$, $F=4.654$). In wild-type embryos expression was differentially expressed throughout the development of the palate ($p= 0.0079$, $F=6.370$) with levels declining between E12.5 and E15.5 (Fig. 25 A). *Hoxa2* null palate shelves show significantly increased expression of *Six2* mRNA during the early stages of palate development [E12.5 ($p<0.05$), E13.5 ($p<0.01$)] and at E15.5 ($p<0.05$) (Fig. 25 A).

Six2 protein expression was also observed in the developing palate using western blot analysis (Fig. 25 B). Densitometry of the western blots (n=3) revealed that the Six2 protein is more abundant in the palate shelves of *Hoxa2* null embryos at E12.5 ($p<0.01$), E13.5 ($p<0.05$) and E14.5 ($p<0.05$) (Fig. 25 C). Immunohistochemical analyses of wild-type and *Hoxa*2 null palates were examined at all four stages of development in the anterior, medial and posterior (Fig. 26). Protein expression was detected throughout the palate at all developmental stages with an increased signal detected in the *Hoxa2* null palates. The protein data therefore is in agreement with the quantitative real time results, where an apparent increase in Six2 expression levels is observed in the *Hoxa*2 null palate shelves.

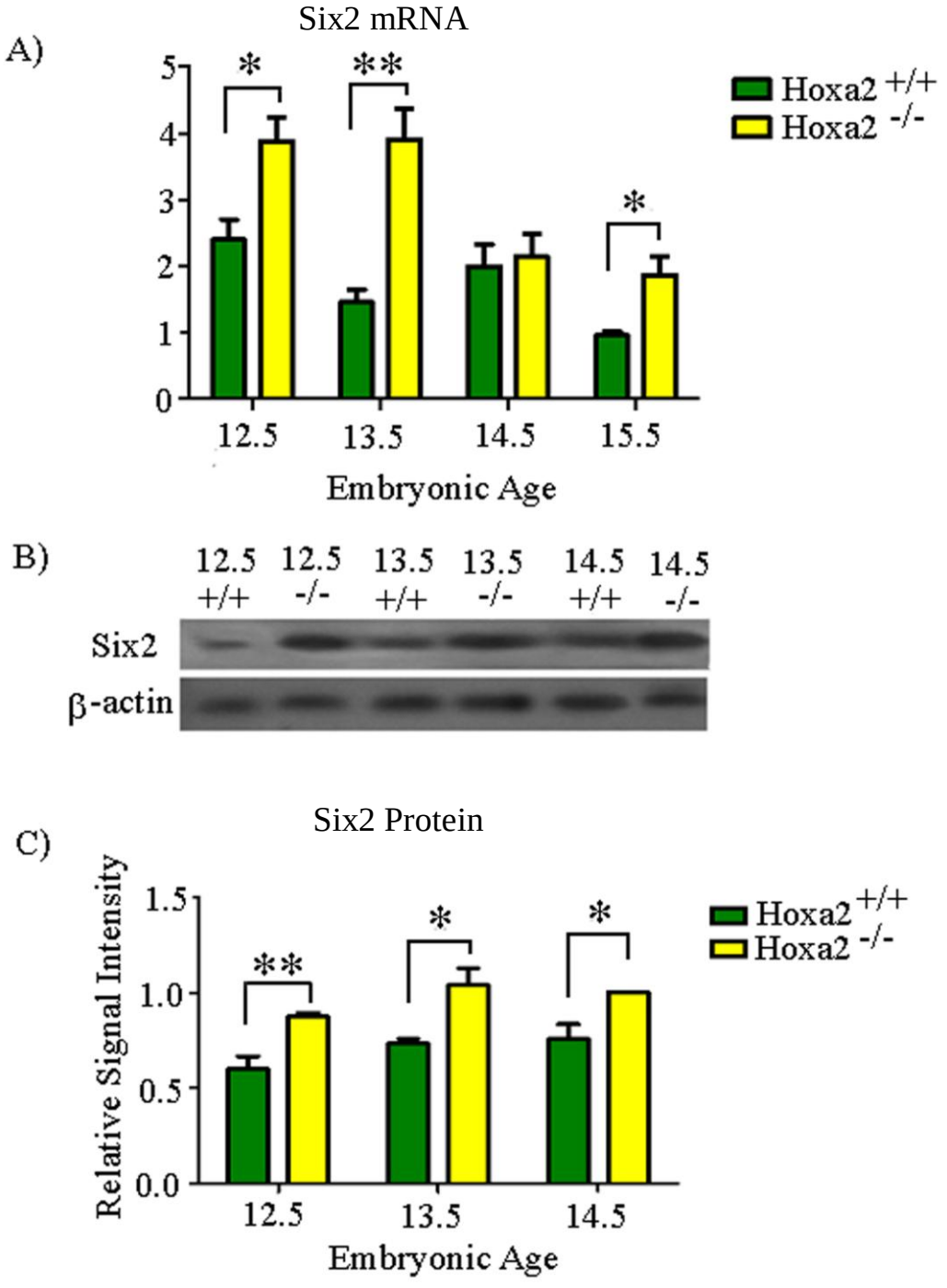
A)
Six2 mRNA
Hoxa2 +/+
Hoxa2 -/-
Embryonic Age
12.5
13.5
14.5
15.5
B)
12.5 +/+
12.5 -/-
13.5 +/+
13.5 -/-
14.5 +/+
14.5 -/-
Six2
β-actin
C)
Six2 Protein
Relative Signal Intensity
Hoxa2 +/+
Hoxa2 -/-
Embryonic Age

Figure 25. Enhanced Six2 Expression in *Hoxa2* null Palate Shelves.

Relative quantitative expression of Six2 throughout murine palatogenesis in $Hoxa2^{+/+}$ and $Hoxa2^{-/-}$ palates. (A) mRNA expression was determined by quantitative real time RT-PCR using Taqman primers and probes. Bars represent mean ± SEM, n=4. (B) Six2 protein expression was determined by western blot analysis of palatal protein. Beta-actin is used to show equal loading of protein between samples. (C) Densitometry of the western blots was performed to determine a trend in expression levels. Bars represent mean ± SEM, n=3. * $p<0.05$, ** $p<0.01$.

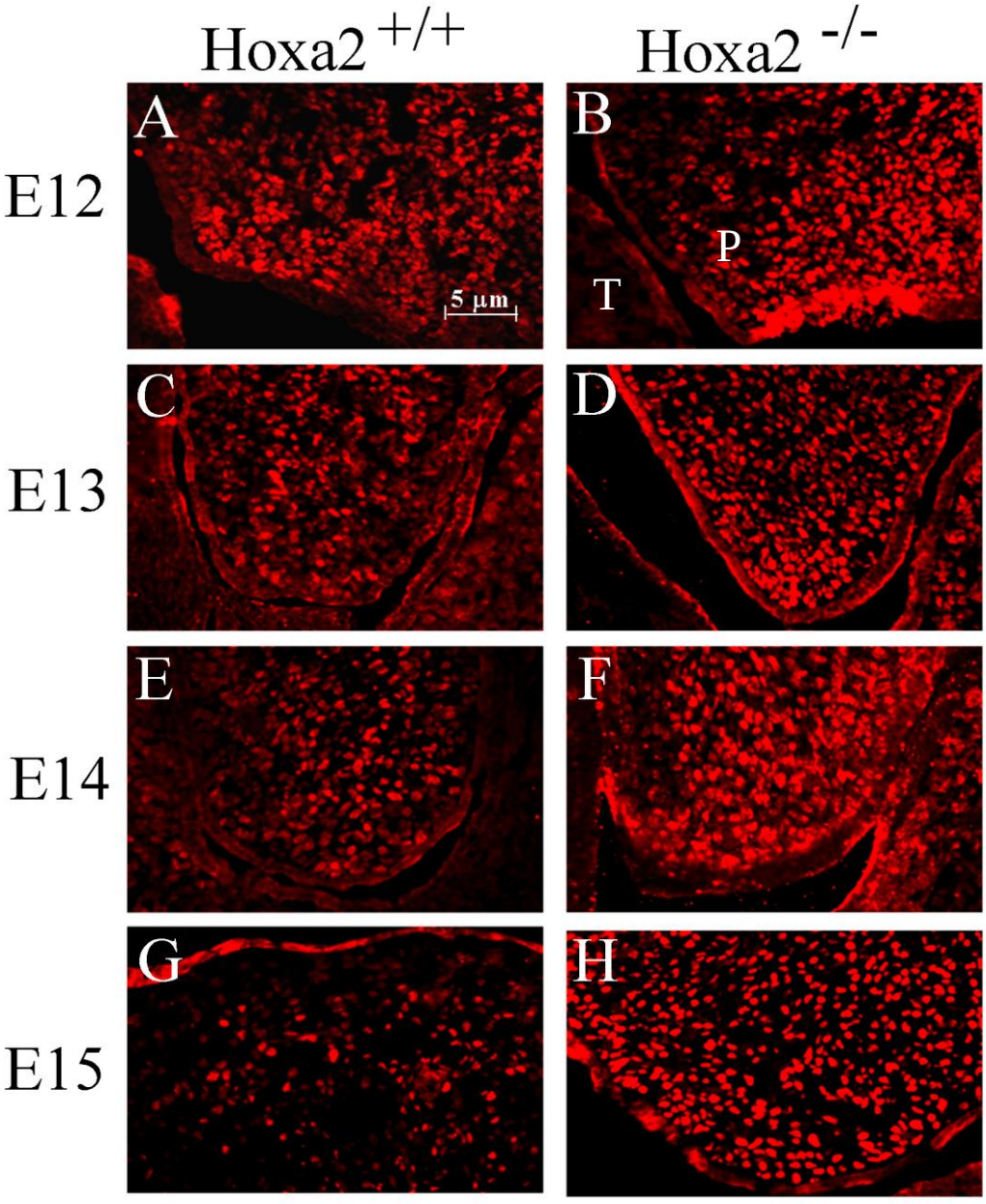
Hoxa2 +/+
Hoxa2 -/-
E12
E13
E14
E15
A
B
C
D
E
F
G
H
P
T
5 µm

Figure 26. Immunohistochemical Analysis of Six2 Expression

Immunohistochemical staining for Six2(red) on coronal sections from mouse palatal shelves at E12 (A,B), E13 (C,D), E14 (E,F) and E15 (G,H). Hoxa2$^{-/-}$ palates show an increase in Six2 staining. Representative medial sections are shown above. P=palatal shelf, T=tongue.

5.13 Tbx1 Expression

Expression of the *Tbx1* gene is known to be crucial for normal palatogenesis (Jerome and Papaioannou, 2001). The expression of *Tbx1* mRNA was examined in the palate of wild-type and *Hoxa*2 null embryos. A statistical interaction on the expression of *Tbx1* was shown between genotype and embryonic age ($p=0.0012$, $F=8.654$). *Tbx1* mRNA was detected at all four developmental stages, showing differential expression throughout development ($p=0.0001$, $F=22.18$), with levels increasing as palate development proceeds. Unlike other downstream targets of Hoxa2 in the palate, which are repressed only at the early stages of palate development, *Tbx1* expression remains unchanged in early development and is only significantly increased at E15.5 ($p<0.001$) (Fig. 27). These data demonstrate that *Hoxa2* also plays a role at later stages of development although at present it is not clear what this role is.

5.14 Lef1 Expression

*Lef*1 expression was detected in the developing palate shelves of wild-type mice at E12.5, E13.5, E14.5 and E15.5. A statistical interaction between genotype and embryonic age on the expression level of *Lef1* mRNA was detected by two way ANOVA ($p<0.0001$, $F=26.38$). Expression was variable throughout palatogenesis in the wild-type embryo between E12.5 and E13.5 ($p<0.01$), followed by a significant decrease in expression by E15.5 ($p<0.01$).

Tbx1 mRNA Expression

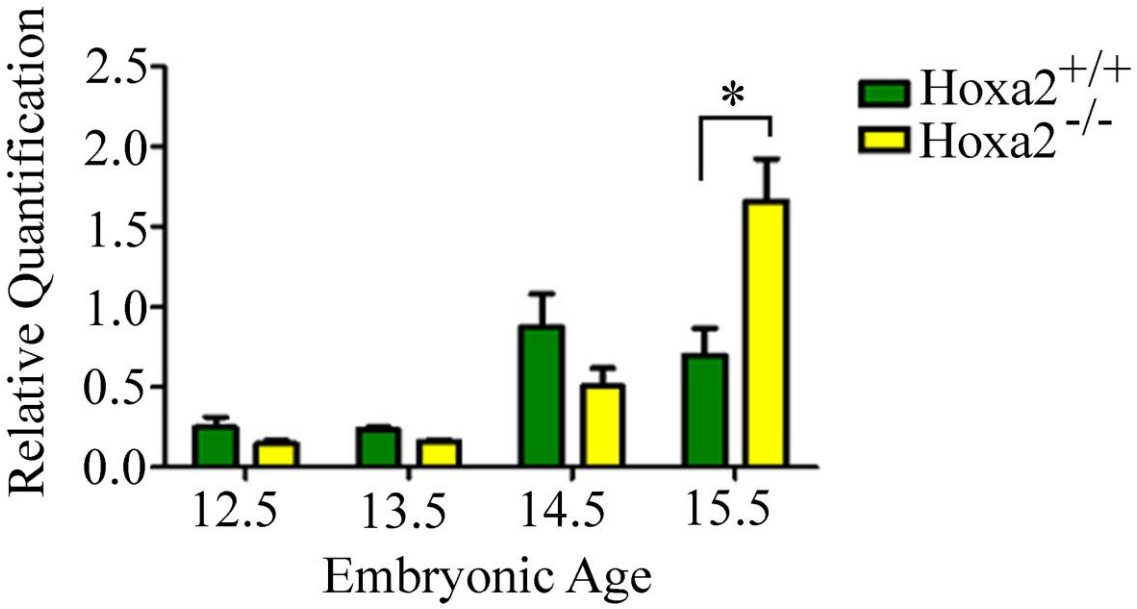

Figure 27. Enhanced *Tbx1* Expression in Hoxa2 null Palate Shelves.

Relative quantitative expression of *Tbx1* throughout murine palatogenesis in $Hoxa2^{+/+}$ (wild-type) and $Hoxa2^{-/-}$ (knock-out) embryos. mRNA levels were determined by quantitative real time RT-PCR using Taqman primers and probes. Bars represent mean ± SEM, n=4. * $p<0.05$.

*Hoxa*2 null embryos show a significant increase in the expression levels of *Lef*1 at E12.5 ($p<0.001$). Expression decreased rapidly and returns to wild-type levels by E13.5 with little change at E14.5 and E15.5 (Fig. 28).

5.15 Htra3 Expression

Quantitative real time RT-PCR analysis revealed novel *Htra*3 expression in the palatal shelves at E12.5, E13.5, E14.5 and E15.5. Expression levels in wild-type embryos increased as palate development proceeds ($p=0.007$, $F=8..099$), with low levels observed at E12.5 and a peak in expression by E15.5 ($p<0.05$). *Hoxa2* null palatal shelves also displayed *Htra*3 expression at all of the above stages. The expression profile in these mutants was not significantly different from the wild-type ($p=0.6102$) (Fig. 29 A).

Htra3 protein expression was detected in the palate using western blot analysis at E12.5, E13.5 and E14.5. Protein expression appeared to be relatively constant throughout palate development. No change was observed in expression between *Hoxa2* null palate shelf samples and wild-type controls (Fig. 29 B and C).

*Htra*3 expression was also detected using immunohistochemistry, showing increasing expression within the palate as development proceeds. Expression appears to be strongest in the medial region of the palate (Fig. 30).

Lef1 mRNA Expression

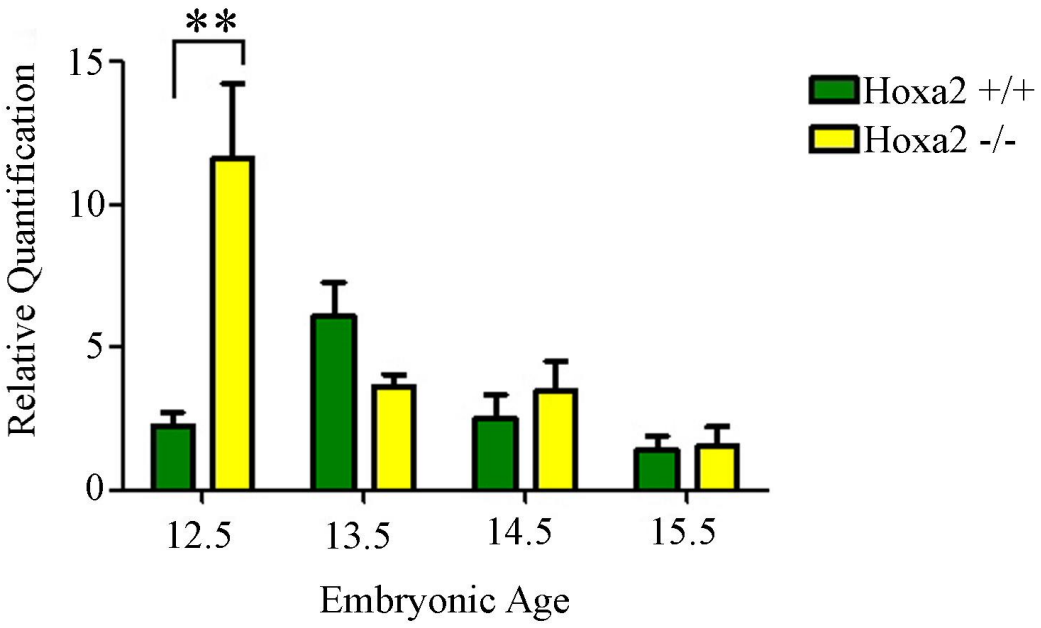

Figure 28. Enhanced *Lef1* Expression in Hoxa2 null Palate Shelves.

Relative quantitative expression of *Lef1* throughout murine palatogenesis in $Hoxa2^{+/+}$ (wild-type) and $Hoxa2^{-/-}$ (knock-out) embryos. mRNA levels were determined by quantitative real time RT-PCR using Taqman primers and probes. Bars represent mean ± SEM, n=4. ** $p<0.01$.

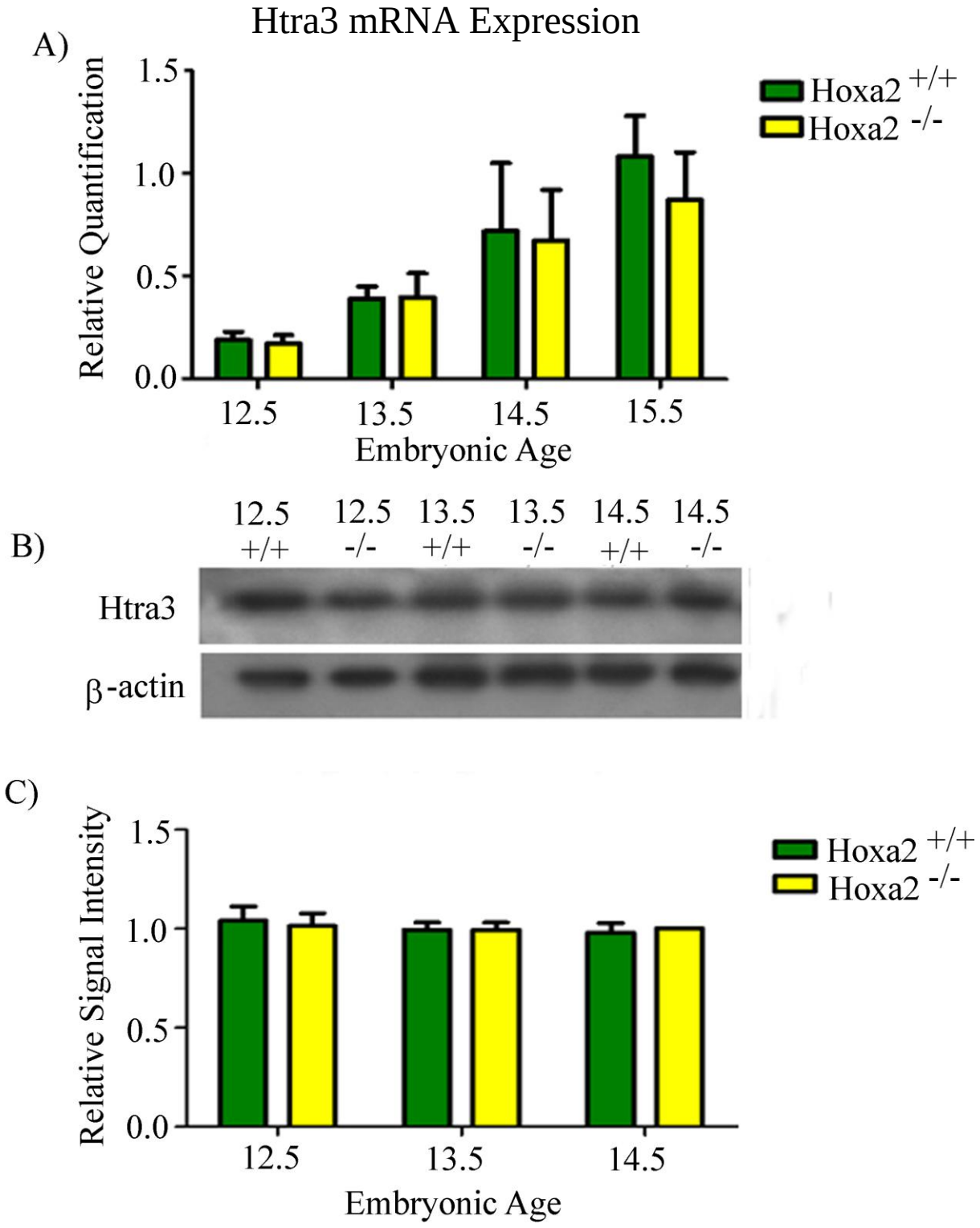
Htra3 mRNA Expression
A)
Relative Quantification
1.5
1.0
0.5
0.0
12.5
13.5
14.5
15.5
Embryonic Age
Hoxa2 +/+
Hoxa2 -/-
B)
12.5 +/+
12.5 -/-
13.5 +/+
13.5 -/-
14.5 +/+
14.5 -/-
Htra3
β-actin
C)
Relative Signal Intensity
1.5
1.0
0.5
0.0
12.5
13.5
14.5
Embryonic Age
Hoxa2 +/+
Hoxa2 -/-

Figure 29. Expression of Htra3 is not Altered in *Hoxa2* null Palate Shelves.

Relative quantitative expression of Htra3 throughout murine palatogenesis in $Hoxa2^{+/+}$ and $Hoxa2^{-/-}$ palates. (A) mRNA expression was determined by quantitative real time RT-PCR using Taqman primers and probes. Bars represent mean ± SEM, n=4. (B) Htra3 protein expression was determined by western blot analysis of palatal protein. Beta-actin is used to show equal loading of protein between samples. (C) Densitometry of the western blots was performed to determine a trend in expression levels. Bars represent mean ± SEM, n=3.

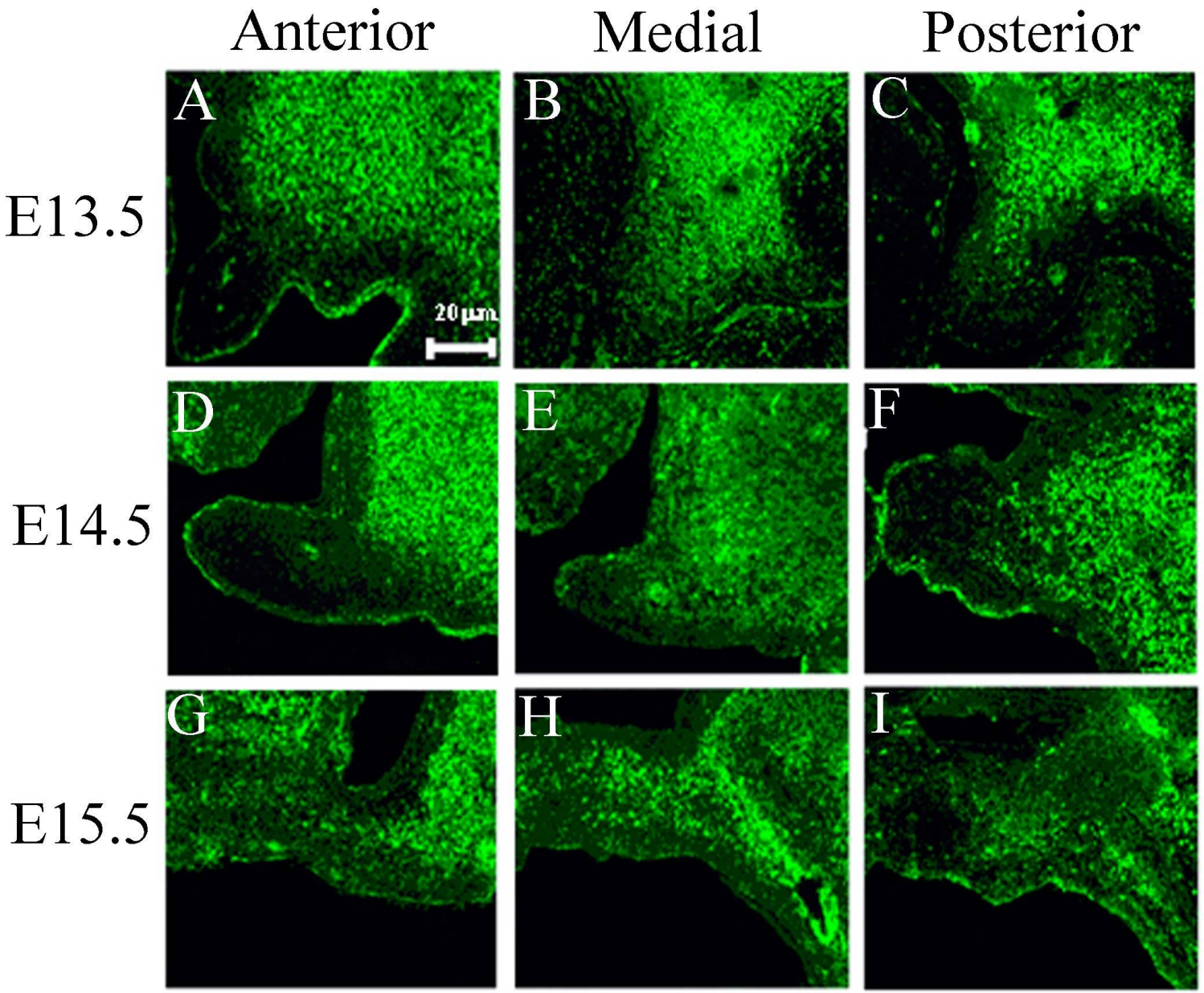
Anterior
Medial
Posterior
E13.5
E14.5
E15.5
A
B
C
D
E
F
G
H
I
20 µm

Figure 30. Immunohistochemical Analysis of Htra3 Protein Expression in the Palate

Immunohistochemical analysis of the Htra3 (green) protein expression in the anterior, medial and posterior regions of the palate at E13.5 (A,B,C), E14.5 (D,E,F) and E15.5 (G,H,I). Htra3 expression appears most intense in the medial regions of the palate with increasing expression as development proceeds.

6. Discussion

6.1 Hoxa2 is Expressed in the Secondary Palate

The tissue that forms the secondary palate develops as outgrowths of the maxillary prominences, which are known to be derivatives of the first branchial arch. The CNCC that migrate into the first branchial arch have been shown to originate from r1 and r2. The CNCC from the first two rhombomeres have been shown to be devoid of *Hox* gene expression at this stage. In contrast, the cells that migrate to form the second branchial arch originate from r4 and are known to express *Hoxa2*. Before the onset of CNCC migration from the rhombomeres, the expression domain of *Hoxa2* expands to the r1/2 boundary (Prince and Lumsden, 1994; Rijli et al., 1993). Hence, the cells that are migrating in the first branchial arch which will eventually populate the secondary palate are null of *Hox* gene expression during their migration, but were previously capable of Hoxa2 expression.

The presence of a cleft palate in approximately 80% of *Hoxa*2 null mice has been postulated to be a secondary defect to abnormal tongue development (Barrow and Capecchi, 1999). This theory is generally accepted due to the absence of *Hoxa*2 expression in the first branchial arch, from which the secondary palate is derived. The muscles of the tongue attach to the hyoid bone, a derivative of the second branchial arch, which does normally express *Hoxa2*. It was therefore previously suggested, that the secondary palate is also void of *Hoxa2* expression and therefore a loss of expression in the knockout

could not lead to alterations in the development of the palate proper. Recent data however suggests *Hoxa*2 is expressed within the developing palate (Nazarali *et al*., 2000). Furthermore, whole organ culture data suggest an increased incidence of cleft palate in *Hoxa*2 null palates grown in the absence of the tongue (Zhang, 2003). Together, these data suggest a more direct role for *Hoxa*2 in regulating palatogenesis.

To further support a direct role for *Hoxa*2 in the palate, a more thorough and detailed analysis of Hoxa2 expression within the palate was required. Expression of *Hoxa*2 was analyzed at both the mRNA and protein levels. *Hoxa2* mRNA was detected in the palate at E12.5, E13.5, E14.5 and E15.5 using quantitative real time RT-PCR (Fig.9 A). Levels of the *Hoxa2* mRNA were significantly higher at E12.5 and E13.5 than later in development with peak expression occurring at E13.5. These data would suggest that there may be an important role in the early growth of the palate shelves. Expression is detected until E15.5 and therefore a role in fusion is possible as well. In addition, Hoxa2 protein expression was also detected in the secondary palate using both western blot and immunohistochemical analysis (Fig. 10). The protein levels were also highest in the palate at the early stages of development (E12.5 and E13.5) which agreed with the real-time RT-PCR results and confirmed the previously reported expression profile of Hoxa2 within the palate (Nazarali et al., 2000).

Immunohistochemical analysis allowed for the determination of the

location of expression within the palate in addition to confirming the expression levels seen by real-time RT-PCR and western blot analysis. Low levels of Hoxa2 protein was observed in both the mesenchyme and the epithelium of the palate at E12.5 after which the levels in both increase significantly. At E14.5 Hoxa2 is detected most intensely in the midline epithelial seam. By E15.5 there is only minimal Hoxa2 expression throughout the palate (Fig. 11). Schematic representation of the expression profile of the Hoxa2 protein can be seen in figure 31. In all cases the highest expression was observed during the early stages of palate development with a significant peak in expression at E13.5. Expression predominantly during the early stages of palatogenesis suggests that the role of Hoxa2 is likely to be in the growth and development of the palate shelves. The expression profile described above closely matches the expression profile that had been previously reported (Nazarali et al., 2000).

These data confirm that despite an absence of *Hoxa*2 expression within the migrating first branchial arch, it is expressed within its derivative the secondary palate. This implies that an absence of expression in the migrating cells that populate the branchial arches does not ensure that expression of genes is not turned on later in development once the first arch migrating neural crest cells differentiate into its later derived structures such as the secondary palate. Expression of Hoxa2 within the palate during its crucial stages of development suggests that there is likely to be a direct role for *Hoxa2* in

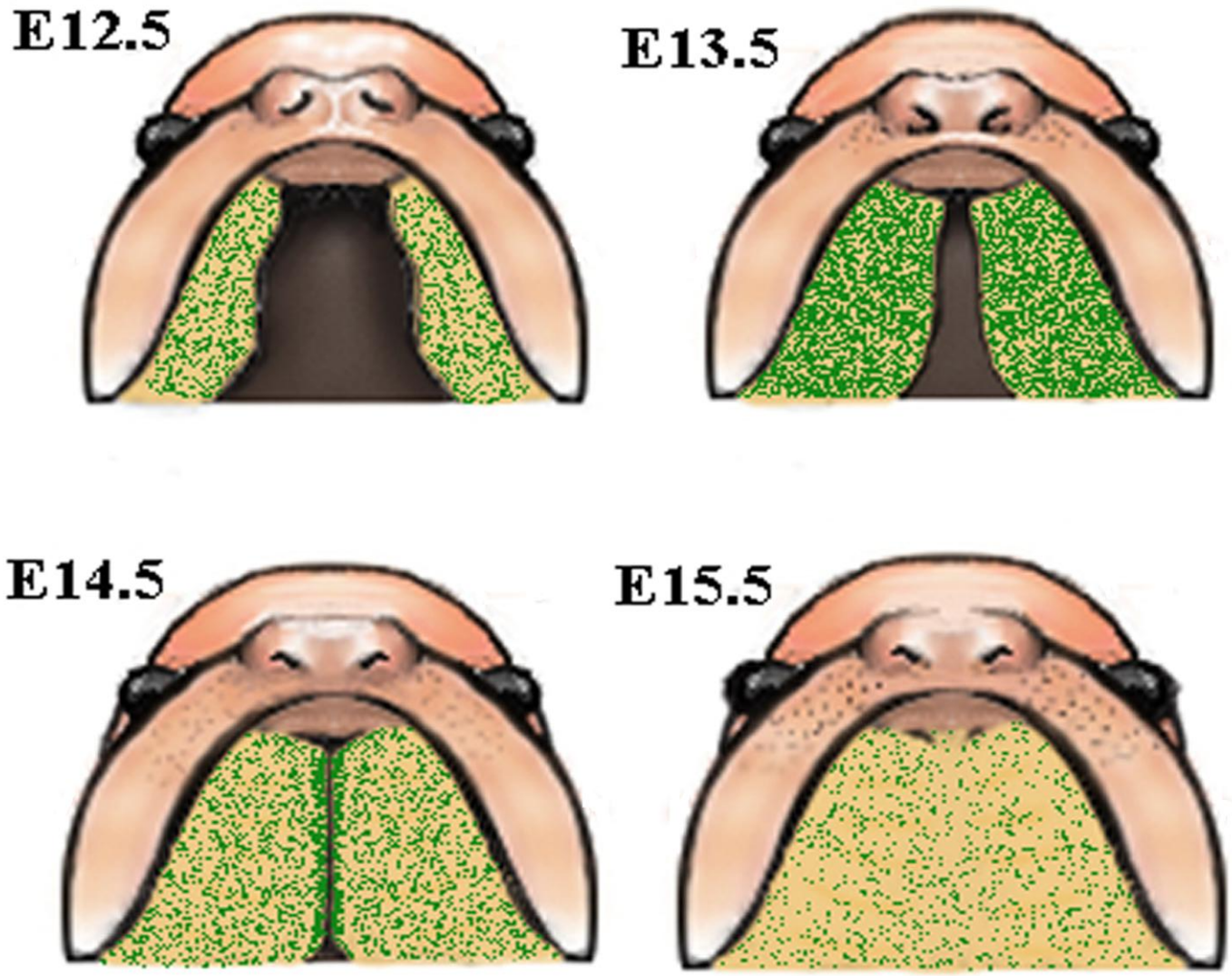
E12.5
E13.5
E14.5
E15.5

Figure 31. Schematic Representation of Hoxa2 Protein Expression

Green dots indicate areas that are expressing the Hoxa2 protein. Expression is seen in both the epithelium and mesenchyme throughout the palate at all ages. Highest levels of expression are seen at E13.5 and along the epithelial seam at E14.5.

regulating the development of the palate, and that the high incidence of cleft palate seen in *Hoxa2* null embryos may in fact be due to a primary defect in palate development.

6.2 Altered Palate Growth in Hoxa2 null Embryos

The expression of Hoxa2 within the developing palate strongly suggested a direct role for the gene in regulating proper palate development. In order to confirm this, various cell processes and stages of palate development were examined and comparisons made between wild-type and *Hoxa2* null embryos. The major processes involved in palate development include proper timing of the growth, elevation and fusion of the palate shelves. Each of these stages was examined in the Hoxa2 null palates and compared to wild-type controls.

The growth of the palate shelves occurs throughout palatogenesis beginning at E11.5 when the shelves bud from the maxillary prominences and continues as they grow vertically, and after they reorient to their final horizontal position. It is essential that the growth of the palates be tightly regulated in order to ensure that they are large enough to contact one another once they are oriented above the tongue, but that they remain small enough that they are capable of flipping up when the tongue flattens. If the timing of the growth and development of the palate is not coordinated with that of the tongue, then the tongue can act as a physical barrier and lead to a cleft palate.

To determine if *Hoxa*2 has an effect on the growth of the palate shelves, wild-type and *Hoxa*2 null palates were analyzed for both proliferation and

apoptosis rates. TUNEL analysis was used to specifically label fragmented chromosomal DNA which is a hallmark of apoptosis. Results of this analysis revealed that apoptosis was not altered in *Hoxa*2 null palate shelves at E12.5, E13.5 or E14.5 compared to wild-type animals (Fig. 15). These findings were confirmed by staining wild-type and *Hoxa2* null palates with an antibody specific for the activated form of the caspase 3 enzyme (Fig. 16). Using both techniques demonstrated that only a low level of programmed cell death was observed within the palate at any stage of its development and a difference between the rates of apoptosis was not evident at any point in development.

Alternatively, cell proliferation rates do vary in *Hoxa*2 null palates (Fig. 14). BrdU incorporation was used to label dividing cells, followed by immunohistochemical analysis. Proliferation rates were then calculated by the percentage of cells that were BrdU positive cells per μm^2. Counts were only done in the palatal mesenchyme as accurate counts of the total number of cells in the epithelium were not possible due to the dense cell population. The anterior, medial and posterior regions of the palates were examined at E12.5, E13.5, E14.5 and E15.5. Overall the general trend suggested an increase in the rate of proliferation in the *Hoxa*2 null palate shelves. Initially, it would seem that an increase in proliferation is unlikely to lead to a cleft palate. This phenomena has, however, been previously reported in mice lacking the Fgf antagonist *Spry2* (Welsh *et al*., 2007). Interestingly, the cleft palate penetrance in these animals is 83% which is very similar to that seen in *Hoxa*2 null mice

(81%).

In many cases, alterations in proliferation are only observed in either the anterior or posterior regions of the palate. *Hoxa2* null palates display an overall increase in cell proliferation throughout the developing palate. The Hoxa2 protein is expressed throughout the palate as well, so this result is not surprising. Distinct pathways are known to regulate growth of the anterior and posterior palate, and therefore these results suggest that Hoxa2 is likely to be involved in the regulation of a variety of pathways that control proliferation in the palate.

6.3 Palatal Shelves Fail to Elevate in *Hoxa2* null Embryos

To determine if an increase in palate growth due to increased cell proliferation led to problems with proper elevation of the palate shelves, histology was performed on wild-type and *Hoxa2* palate sections. The major difference in development appears to occur at E14.5. In the wild-type embryos the palate shelves have elevated and are positioned horizontally above the tongue. *Hoxa2* null palate shelves fail to elevate at E14.5 and even by E15.5 when wild-type palates have fused the null palate shelves remain oriented in a vertical direction (Fig. 12). This observation, along with the data from the cell proliferation studies, provides a clearer understanding of the defects in palate development in *Hoxa2* null animals. These combined data suggest that one of the possible mechanisms of cleft in null embryos is the increase in proliferation in the palate leads to a loss of the coordinated development normally occurring

between the palate and other craniofacial structures such as the tongue and mandible.

Mechanisms of palate shelf elevation were not directly investigated, as they are poorly described in the literature. It is largely accepted that palate shelf elevation is the result of both intrinsic forces within the palate shelves, and proper coordination of growth between the palate shelves and other craniofacial structures. The extracellular matrix has been demonstrated to progressively accumulate hyaluronan, which is capable of retaining a large quantity of water and is predicted to provide the changes in rigidity required for the rapid elevation of the palate shelves (Brinkley and Morris-Wiman, 1984; Brinkley and Morris-Wiman, 1987; Ferguson, 1978; Larsson et al., 1959; Pratt et al., 1973; Singh et al., 1994; Singh et al., 1997). Changes in rigidity have also been attributed to variations in blood flow to the palate shelves (Amin et al., 1994), and increased cell proliferation and change in morphology in specific regions of the mesenchyme elevation (Babiarz et al., 1979; Brinkley, 1980; Brinkley and Bookstein, 1986; Bulleit and Zimmerman, 1985; Greene and Pratt, 1976; Greene and Pratt, 1976; Innes, 1978).

The only target that has been identified to play a role in elevation is the neurotransmitter γ-aminobutyric acid (GABA). Agonists of GABA have been shown to result in cleft palate through inhibition of palate shelf elevation, whereas antagonists have been shown to stimulate elevation (Miller and Becker, 1975; Wee and Zimmerman, 1983). Glutamic acid decarboxylase 67

(Gad 67) is involved in the synthesis of GABA, and both have been shown to be expressed within the developing palate (Asada et al., 1997; Hagiwara et al., 2003; Wee et al., 1986). It is possible that the loss of the *Hoxa2* gene does lead to defects in the intrinsic mechanisms involved in palate shelf elevation, but this will require further studies.

6.4 Physical Barrier of the Tongue Appears to be Secondary to Altered Palate Growth

Previous research in our lab investigated the ability of the palates to fuse in the absence of the tongue. Organ cultures were performed where the lower mandible was removed including the tongue and the palate was cultured and then examined for fusion. These experiments showed that in the absence of the *Hoxa*2 gene the ability of the palate shelves to fuse was significantly decreased (Wang, 2006; Zhang, 2003). This, in combination with the new increased proliferation data, shows that the loss of the *Hoxa*2 gene does in fact lead to problems in the development of the palate proper which ultimately leads to the formation of a cleft palate. Although the fusion rate in these *Hoxa2* null cultured palates were decreased relative to the wild-type fusion rates (44.4% vs 90.0% respectively), they were not as low as the reported 17-19% seen *in vivo* (Barrow and Capecchi, 1999; Rijli et al., 1993; Wang, 2006; Zhang, 2003). The finding that the palate shelves do not appear to be capable of re-orientation above the tongue in most cases could help to explain these differences.

The interaction between the tongue and palate shelves clearly only

explains a portion of the reported cleft palates in *Hoxa2* null mice due to the high incidence of cleft even in the absence of the tongue. An increase in cleft palate due to altered proliferation has previously been reported for *Spry2* null animals (Welsh et al., 2007). These mutant embryos did not have defects in their ability to elevate above the tongue, but still displayed a cleft palate that was suggested to be the direct result of increased cell proliferation. Therefore, it is likely that the alteration in proliferation in *Spry2* null mice leads to changes in the normal development of the palate that prevents palatal fusion even if they are capable of elevation.

6.5 Hoxa2 Null Palates are Capable of Fusion

The ability of the palate shelves to fuse with one another was also investigated. Palate shelves were placed in direct contact with one another and allowed to fuse for 72 h. This technique investigated whether the palate shelves had the intrinsic ability to fuse together, without the necessity of having to grow together and contact one another. The *Hoxa*2 null, heterozygous and wild-type palate shelves were all equally capable of fusion (Fig. 17). Previous culture experiments removed any interference that the tongue may have caused, but did not eliminate any problems that resulted from altered palate shelf growth (Wang, 2006; Zhang, 2003). These new findings clearly demonstrate that there are defects with palate development in the *Hoxa*2 null palates, but that they occur prior to fusion, and that the process of fusion is not altered.

6.6 Hoxa2 acts as a Transcriptional Repressor in the Palate

The Hoxa2 protein acts as a transcription factor, and therefore any effects that the protein has on the development of the palate is through regulating the expression of other genes. In order to confirm that there is in fact a role for Hoxa2 within the palate proper, it was essential to determine downstream targets within the developing palate and characterize any changes to their expression profile that occurs in the absence of the Hoxa2 protein.

The Hoxa2 protein has previously been reported to be able to both activate and repress the expression of other genes during craniofacial development (Bobola et al., 2003; Kutejova et al., 2005; Santagati et al., 2005). The only direct downstream target of Hoxa2 that has been reported is *Six2* which is repressed by Hoxa2 (Kutejova et al., 2005; Kutejova et al., 2008).

The expression of numerous targets was investigated within the palates of wild-type and *Hoxa*2 null palates using both quantitative real time RT-PCR and western blot analysis to determine if the absence of *Hoxa*2 resulted in altered expression. A number of downstream targets of Hoxa2 in the palate were identified all of which appear to be repressed by Hoxa2. *Msx1*, *Bmp4*, *Barx1*, *Six2*, *Ptx1*, *Lef1* and *Tbx1* all display increased expression levels in *Hoxa*2 null palate shelves. It appears that Hoxa2 is most active as a repressor at the early stages of palate development (E12.5 and E13.5), as for the majority of genes the only alterations in expression were seen at this stage. *Six2*

expression was an exception to this phenomenon and continued to be elevated throughout palatogenesis in the Hoxa2 null palates (Fig. 25). The expression of *Tbx1* was also an exception with an increase in expression in the null palates only observed at E15.5 (Fig. 27). These findings suggest that although the primary role of Hoxa2 may be in regulating the expression of genes early in palate development, there may also be a role for Hoxa2 at the later stages of development.

6.7 Altered Expression of Downstream Targets Agrees with Increased Proliferation in *Hoxa2* null Palates

Regulation of proliferation rates within the palate have been attributed to a variety of genes in the past. As discussed in section 3.4.1 (pg 22) distinct pathways have been shown to regulate growth of the palate in the anterior and posterior regions of the palate. The Hoxa2 protein is expressed throughout the entire palate shelf including the epithelium and the mesenchyme (Fig. 11). These data, combined with the observed increase in proliferation throughout the palate of *Hoxa*2 null embryos (Fig. 14), led me to investigate what role Hoxa2 may play in regulating the expression of both anterior and posterior specific genes.

Cell proliferation (Santagati et al., 2005) in the anterior mesenchyme is regulated by *Msx*1 and its downstream targets (Zhang, et al., 2002). In addition, within the branchial arches *Hoxa*2 is involved in regulating the expression of *Msx*1 (Santagati et al., 2005). Msx1 levels at both the mRNA

($p<0.01$) and protein levels ($p<0.05$) are increased at the early stages of palatogenesis (E12.5) in *Hoxa*2 null embryos (Fig. 18). Bmp4 is a known downstream target of Msx1 and an essential component in the Msx1 signalling pathway that regulates proliferation in the anterior palate (Zhang et al., 2002). The expression of Bmp4 was also increased in the Hoxa2 null palate shelves (Fig. 19). At E12.5, a significant increase was shown at the mRNA level ($p<0.05$) while protein levels did not increase until E13.5 ($p<0.05$) indicating a delay in translation of the mRNA message into protein (Fig. 19). Msx1 and Bmp4 have been described to work within a feedback loop (Zhang et al., 2002), which may explain why the levels of both mRNA and protein return to wild-type levels relatively quickly. Together, the increase in Msx1 and Bmp4 provide a mechanism by which Hoxa2 may be regulating the level of proliferation in the anterior region of the palate. Increased and ectopic expression of *Msx*1 has previously been described to lead to increased proliferation throughout the palate (Welsh et al., 2007). Therefore, the increase in Msx1 and Bmp4 expression could in fact also account for the altered proliferation levels seen in the medial and posterior palate, either directly, or by altering the expression of other genes which leads to increased proliferation.

Alterations in the expression of the predominantly posteriorly expressed *Barx1* gene have also been suggested to be responsible for changes in proliferation rates within the posterior palate (Welsh et al., 2007). Significantly increased levels of Barx1 mRNA ($p<0.05$) and protein ($p<0.05$) were observed

in the palate shelves of *Hoxa*2 null embryos at E13.5 (Fig. 20). It is unclear which pathway links Barx1 to proliferation, but an increase in Barx1 protein is predicted to lead to increases in posterior cell proliferation (Welsh *et al*, 2007). However, why expression levels return to normal is unclear but could be the results of a feedback loop as is the case for Msx1.

6.8 Novel Pathway in the Developing Palate involving New Downstream Targets of Hoxa2

*Hoxa*2 has been demonstrated to repress *Ptx*1 expression in the second branchial arch, likely through an indirect mechanism (Bobola *et al*., 2003). *Ptx1* is expressed within the palate at E15 (Lanctot et al., 1997). Our findings show that *Ptx*1 is expressed throughout palate development (E12.5-E15.5) and as in the branchial arches, it is repressed by *Hoxa*2, with a significant increase ($p<0.05$) in both mRNA and protein expression evident at E13.5 in the *Hoxa*2 null embryos (Fig. 21). Interestingly, in the branchial arches Ptx1 is completely absent from the second branchial arch in the wild-type, but is ectopically expressed in the absence of Hoxa2 (Bobola et al., 2003). This finding would suggest a much stronger repression of Ptx1 in the branchial arches than is observed in the developing palate.

The mechanism by which *Hoxa*2 represses *Ptx*1 expression in the branchial arches remains largely unclear. It has been suggested that epithelial Fgf8 expression is an absolute requirement (Bobola, et al., 2003). *Fgf*8 expression has not been described in the murine palate. However, a recent

genetic linkage study in humans did show *Fgf*8 mutations lead to cleft palate (Riley *et al*., 2007). Fgf8 protein expression was observed in the developing palate between E12.5 and E15.5 at the mRNA and protein levels. No differences in the expression levels of either the mRNA or protein were observed in the *Hoxa*2 null palate shelves (Fig. 22). Immunohistochemical analysis revealed that contrary to its epithelial specific expression in the first branchial arch, Fgf8 protein is present in both the epithelium and the mesenchyme of the developing palate (Fig. 23). In the hindlimb, it has been suggested that while Ptx1 is not likely linked to the expression of growth factors such as Fgfs it may provide the cell with the ability to respond to these signals and therefore be involved in the regulation of growth and patterning of embryonic structures (Marcil et al., 2003).

A role may exist for *Hoxa2* downstream of Fgf8, which allows for its repression of Ptx1. This could be through either the regulation of transducers or repressors of the Fgf8 signal. Lhx8 is another known downstream target of Fgf8 which has previously been linked to cleft secondary palate (Inoue et al., 2006; Zhao et al., 1999). The expression of *Lhx8* mRNA remains unaltered in the absence of Hoxa2 in the palate (Fig. 24). These data would suggest that, although a role may exist for Hoxa2 downstream of Fgf8, not all of the Fgf8 downstream targets are affected. It has been well documented that numerous members of the Fgf signalling family are present and important in the development of the secondary palate (Alappat et al., 2005; Eblaghie et al.,

2004; Goodnough et al., 2007; Lee et al., 2008; Rice et al., 2004; Riley et al., 2007; Thomason et al., 2008) and therefore these contrary results may be due to redundancy between Fgf signals in regulating certain downstream targets.

Ptx1 expression has been studied within the developing mandible and teeth. Its expression has been shown to be tightly regulated by both activating and repressing mechanisms. Ectopic Fgf8 signals in the mandible have been shown to induce and maintain the expression of Ptx1 (St. Amand et al., 2000). This mechanism appears to be similar to that in the branchial arches and may be conserved in the palate as discussed above. In contrast, ectopic expression of Bmp4 represses Ptx1 in the mandible (St. Amand et al., 2000). In the palate, loss of *Hoxa2* expression leads to an increase in Bmp4 at E12.5 (Fig. 19) and Ptx1 (Fig. 21) at E13.5. It would appear that this would be opposite to the observed repression in the mandible. Multiple mechanisms could result in these contrary results including, alterations in the expressions in the anterior and posterior regions of the palate. Bmp4 has been reported to have an anterior specific expression profile and therefore, it is possible that as only total expression was investigated Ptx1 may be repressed in the anterior region but increased in the posterior. Alternatively, different factors may be involved in the pathway that transduces the Bmp4 signal within the palate than in the mandible. To determine if there is a relation between Ptx1 and Bmp4 will require further investigation.

Hoxa2 has been shown to be downregulated in the branchial arches in

the presence of exogenous Fgf (Trainor et al., 2002). The possibility therefore exists, that a feedback loop occurs between Hoxa2 and members of the Fgf family in order to regulate the proper growth and development of craniofacial structures including the secondary palate.

*Hoxa*2 null palate shelves show a significant increase ($p<0.05$) in *Lef*1 mRNA expression at E12.5 (Fig. 28). To date the only role that has been described for Lef1 in the developing palate is at the stage of fusion. The role of *Lef*1 in palate shelf fusion has been extensively researched (Nawshad *et al*, 2007; Nawshad and Hay, 2003). A recent study showed that *Lef*1 directly represses the expression of epithelial specific E-Cadherin while promoting the expression of mesenchymal markers vimentin and fibronectin (Nawshad et al., 2007). This mechanism clearly helps explain the role *Lef*1 plays in eliciting the *Tgf*-β3 dependent degradation of the midline epithelial seam. Although the only previously described role for *Lef*1 in the palate has been at the fusion stage (Nawshad and Hay, 2003; Nawshad et al., 2007), its expression throughout development as well as the significant increase early in development in the *Hoxa*2 null mutants suggests a role earlier in palate development. In tooth development, *Lef*1 has been shown to be critical for proper development by acting as a survival factor (Sasaki et al., 2005). Additionally, *Lef*1 expression has been linked to the expression of Fgf (Eblaghie et al., 2004; Kratochwil et al., 2002; Sasaki et al., 2005) and of Bmp4 (Kratochwil et al., 1996), both of which are known to be important for proper palate development. Taken together, this

suggests that there may be a role for *Lef*1 in early palatogenesis although its exact function remains unclear.

Lef1 has been shown to be involved in regulating the cell cycle throughout development through the regulation of genes such as *cyclin D1* and *c-myc* (Reya and Clevers, 2005; Shtutman et al., 1999). The binding of Lef1 to the *cyclin D1* promoter has been shown to induce its expression and ultimately to the progression of the cell through the cell cycle (Shtutman et al., 1999; St Amand et al., 2000). The increase in Lef1 expression could therefore also help to explain the increase in proliferation observed in *Hoxa*2 null palate shelves.

Although *Lef*1 has not previously been shown to be a downstream target of *Hoxa*2, it has been recently reported that there is a direct link between *Ptx*2 and *Lef*1 in the developing embryo (Amen et al., 2007; Vadlamudi et al., 2005). *Ptx*2 and *Ptx*1 are members of the Ptx subfamily of paired-like homeodomain genes and share a high level of sequence homology and have been shown to demonstrate similar DNA-binding specificities *in vitro* (Tremblay et al., 2000). This suggests that the increase in *Lef*1 and *Ptx*1 expression in *Hoxa*2 null embryos may be linked. Both Lef1 and members of the Ptx family are known to act downstream of the Wnt canonical pathway, which has been shown to be important in cell survival and proliferation (Amen et al., 2007). Lef1 has two known isoforms, the full length isoform is dependent on β-catenin while the N-terminally truncated form is not. Ptx2 appears to differentially regulate the expression of each *Lef1* isoform, and it may through this mechanism be capable

of regulating growth and migration (Amen et al., 2007).

Ptx1 has also been linked to a number of other genes expressed within the developing palate. *Ptx1* null embryos show a significant decrease in the expression of *Barx1* in the mandible (Mitsiadis and Drouin, 2008). In *Hoxa2* null palates, there is a significant increase in the expression of both Ptx1 (Fig. 21) and Barx1 (Fig. 20) at E13.5. These data suggest that there may also be a link between Ptx1 and Barx1 expression in the palate. This would once again link Ptx1 to a known proliferative pathway in the palate.

Tbx1 expression was shown to be significantly increased at E15.5 in the palates of *Hoxa2* null embryos (Fig. 27). This increase in expression may also be linked to the observed increase in Ptx1 expression earlier in palatogenesis. In the dental epithelium, loss of the *Ptx1* gene resulted in a subsequent decrease in the levels of *Tbx1* (Mitsiadis and Drouin, 2008).

The isolation and characterization of Ptx1, Barx1, Lef1 and Tbx1 as downstream targets of Hoxa2 in the palate represents a new and interesting pathway within the developing palate, which may be important in regulating the normal growth of the palate. Hoxa2 appears to repress all 4 of these gene targets. Its repression of Ptx1 is unlikely to be direct based on the regulation in the branchial arches (Bobola et al., 2003)/ It is more likely to occur through, or involve, the expression of Fgf8. Barx1, Lef1 and Tbx1 could all be downstream of Ptx1, and provide a second pathway through which *Hoxa2* maintains normal proliferation in the palate.

6.9 Novel *Six*2 Expression

Six2 is expressed in the mesenchyme of the nasal prominences of E11.5 mice (Brodbeck et al., 2004; Fogelgren et al., 2008; Ohto et al., 1998; Oliver et al., 1995). *Brachyrrhine* mice, which have been linked to decreased Six2 expression throughout the developing embryo, were described to have an absence of the primary and secondary palates (McBratney et al., 2003; Singh et al., 1998). Contrary to this finding, *Six2* knockout mice did not display any craniofacial defects (Self et al., 2006). These contrary results make it difficult to determine the exact role of Six2 in regulating the development of the murine face.

*Hoxa*2 has previously been shown to act directly on the *Six*2 promoter to totally repress its expression in the second branchial arch (Kutejova et al., 2005; Kutejova et al., 2008; Santagati et al., 2005). Overexpression of *Six*2 in the second branchial arch of wild-type mice results in a phenotype similar to *Hoxa*2 null mutants (Kutejova et al., 2005). *Six*2 expression was detected for the first time within the developing palate. mRNA expression was detected using real time RT-PCR (Fig. 25 A). In the wild-type mouse palate, *Six*2 mRNA expression is relatively constant throughout palatogenesis, although appearing to peak at E12.5 and decrease slightly at E15.5. As observed in the branchial arches, *Hoxa*2 appears to act as a repressor of *Six*2 expression at early stages of palatogenesis, with a significant increase ($p<0.05$) observed at both E12.5 and E13.5 in null mutants. The presence of Six2 protein was also confirmed

within the developing palate. The upregulation in *Six*2 expression in *Hoxa*2 null mice was also observed at the protein level in immunohistochemical analysis of the palate (Fig. 26) and western blot (Fig. 25 B and C).

Detection of Six2 expression within the developing palate provides an interesting new target that requires further investigation. A link between Six2 and cell proliferation within a subset of CNCC has been reported (Ma and Lozanoff, 1999). It is therefore possible that the observed increase in Six2 expression is directly related to the increase in the level of proliferation within the palate. Little data has been reported on possible downstream targets of Six2, especially in craniofacial development. In the kidney, it was shown that Six2 was capable of activating the expression of both glial-cell-line-derived neurotropic factor (*Gdnf*) and its own expression (Brodbeck et al., 2004).

The Six family of transcription factors have been shown to work in conjunction with the Eya family of proteins, to regulate the expression of genes (Purcell et al., 2005; Zou et al., 2004). *Eya1* null embryos have been reported to display a cleft secondary palate (Alkuraya et al., 2006; Xu et al., 1999). Also of interest, is the finding that Eya1 is upstream of the *Tbx1* gene in the developing mouse ear (Friedman et al., 2005). The potential interactions between Six2, Eya1 and Tbx1 provide another downstream pathway of *Hoxa*2 that is important in the developing palate. Further analysis of these targets, as well as identification of other potential components of this pathway, could provide new insights into the players involved in the regulation of palatogenesis.

6.10 Novel *Htra*3 Expression

*Htra*3 expression, which has not previously been described in the developing palate, was detected at the mRNA and protein levels for the first time by means of real time RT-PCR, western blot and immunohistochemical analysis. In the wild-type mouse palate, *Htra*3 mRNA is expressed between E12.5 and E15.5 with levels steadily increasing throughout palatogenesis (Fig. 29). Western blot analysis showed that Htra3 protein is expressed throughout palate development, although levels appear to remain constant between E12.5 and E14.5. This constant level of protein expression suggests that although the level of mRNA is increasing within the palate, there does not appear to be an overall increase in amount of protein within the palate.

Immunohistochemical analysis revealed that Htra3 is expressed throughout the palate (Fig. 30). Expression of Htra3 protein is the highest in the medial regions in the palate at E13.5, E14.5 and E15.5. At E13.5 and E14.5 the majority of Htra3 expression appears to be located in the proximal areas of the palate with little to no expression in the mesenchyme of the shelves, although expression is visible in the epithelium. At E15.5, expression increases to include the mesenchyme as well as the epithelim. This increase in the area of expression occurs at the same point in which the palate shelves are fusing together.

*Htra*3 is known to bind to and inactivate numerous members of the *Tgf*-β

family including: *Tgf*-β1, *Tgf*-β2, *Bmp*4 and *Bmp*2 (Tocharus, et al., 2004). Both *Bmp*4 and *Bmp*2 have been shown to be crucial in the regulation of cell proliferation within the palate (Zhang, et al., 2002). Limiting the expression of Htra3 to the proximal regions of the palate at E12.5 and E13.5 may ensure that Bmp2 and Bmp4 are not degraded, allowing them to function in promoting cell proliferation. The increase in the domain of *Htra*3 at E14.5 may play a role in the degradation of these proteins at later stages of palatogenesis when proliferation levels decline and palate shelves fuse. In addition, *Tgf*-β1 has been shown to act to promote cell survival in the palate epithelium, inhibiting the ability of *Tgf*-β3 to degrade the midline epithelial seam (Martinez-Alvarez, et al., 2004). *Htra*3 may act to degrade *Tgf*-β1 in the epithelium late in palatogenesis allowing for *Tgf*-β3 to induce fusion. Due to the large number of potential *Htra*3 targets known to be expressed in the developing palate, and its increased expression throughout palatogenesis, the role of *Htra*3 in the palate is an interesting area of study and may provide further insight into the regulation of palate development.

*Hoxa*2 has been shown to bind to the genomic sequence of *Htra*3 *in vivo*; in *Hoxa*2 null embryos *Htra*3 shows an increase in expression throughout the spinal cord and hindbrain (Akin, 2004). In contrast, within the palate shelves *Htra*3 expression does not seem to change in the absence of *Hoxa*2 (Fig 29). The difference in the ability of *Hoxa*2 to regulate the expression of Htra3 is likely to be due to the different subset of co-factors that are expressed in the spinal

cord and palate.

6.11 Conclusion

Hoxa2 mRNA and protein is present in the palate between E12.5 and E15.5 (Fig. 9, 10 and 11). The confirmation of Hoxa2 within the developing palate shows that although Hoxa2 is not expressed in the migrating CNCC of the first branchial arch, it is activated in the cells arising from this arch at later stages of development. This is contradictory to the current theory that all of the derivatives of the first branchial arch are devoid of *Hox* expression. The Hoxa2 protein is most highly expressed in the palate at E13.5, an age when there is significant growth in the palate shelves. High levels of expression are also seen in the midline epithelial seam as the palates fuse with one another (Fig. 11).

The growth of palate shelves is altered in *Hoxa*2 null embryos. An increase in the rate of proliferation is observed in the palates of null embryos, without an apparent increase in the level of apoptosis (Fig. 14, 15 and 16). Problems also exist in the ability of the palate shelves to reorient from their initial vertical position, to the horizontal position above the tongue (Fig. 12). This was previously hypothesized to be the direct result of altered tongue musculature. Increased cell proliferation provides an alternate mechanism for the inability of the palate shelves to reorient. Organ culture experiments clearly demonstrated that the palate shelves of wild-type and *Hoxa*2 null embryos are equally capable of undergoing fusion when placed in contact (Fig. 17). Together, these data suggest that defects in the development of *Hoxa*2 null

palates are primarily the result of altered growth of the palate shelves.

The direct role of Hoxa2 appears to be as a transcriptional repressor within the developing palate. *Msx1*, *Bmp4*, *Barx1*, *Ptx1*, *Six2*, *Lef1* and *Tbx1* all have increased expression in the *Hoxa2* null palate shelves compared to wild-type controls. Msx1, Bmp4 and Barx1 expression have previously been shown to be part of a common pathway that regulates cell proliferation within the development. Increase in the expression of these genes is in agreement with the increase in proliferation. Additionally, Ptx1, Lef1, Tbx1 and Barx1 may be linked together in a common pathway involving Hoxa2, which could also lead to the observed increase in proliferation.

Three novel targets were also identified within the developing palate (Six2, Fgf8 and Htra3). Six2 was shown to be downstream of Hoxa2 within the palate, while Fgf8 and Htra3 expression was not altered by the loss of Hoxa2.

A schematic representation of the signalling pathways known to function within the palate along with the predicted role of Hoxa2 and its newly identified targets can be seen in Figure 32.

Together these data all point towards a direct role for Hoxa2 in regulating the development of the secondary palate, particularly in maintaining normal cell proliferation rates.

6.12 Future Directions

A complete understanding of the role of Hoxa2 and its downstream targets within the developing palate will require additional experiments. How

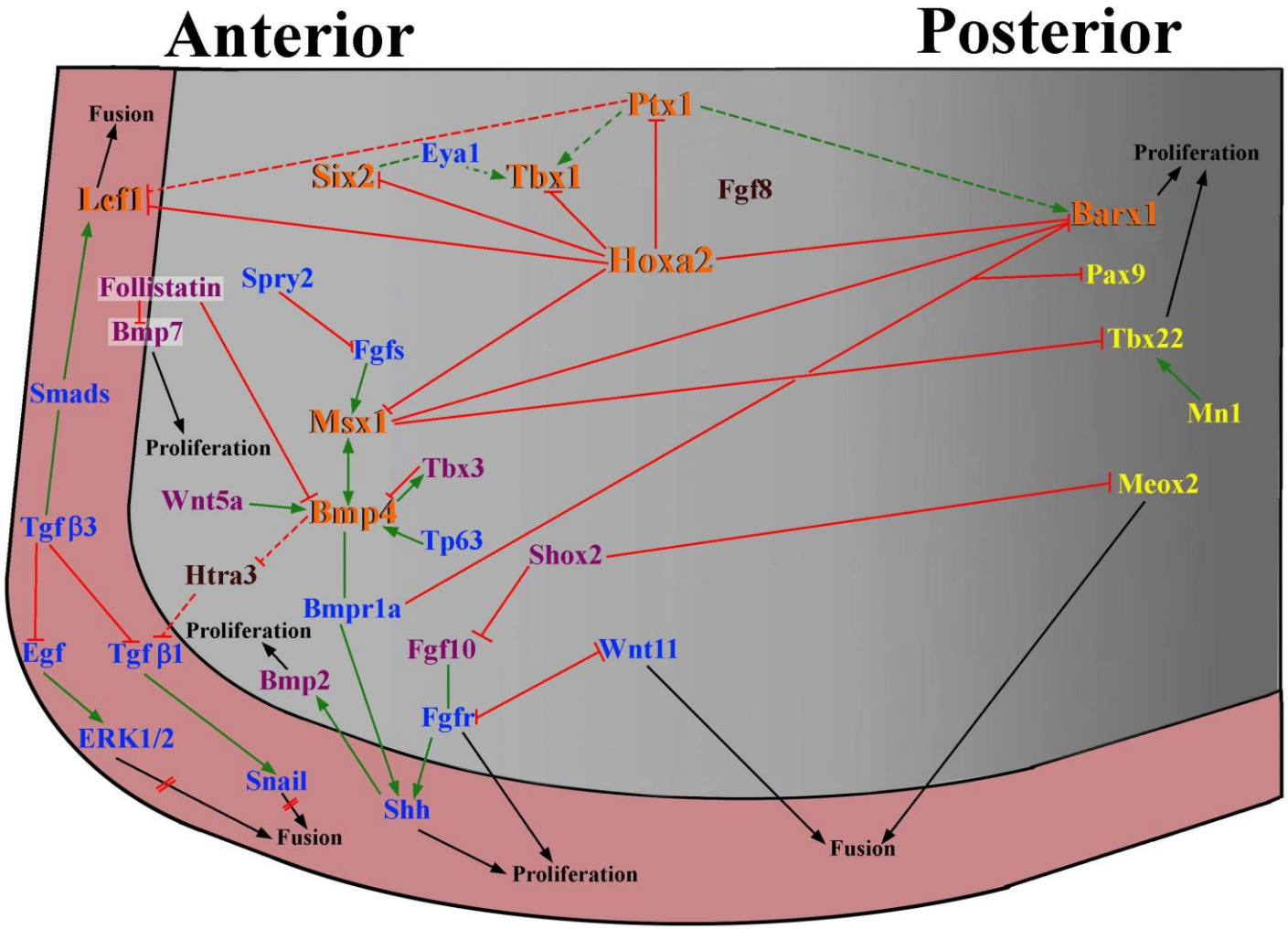
Anterior
Posterior
Fusion
Lef1
Ptx1
Eya1
Six2
Tbx1
Fgf8
Barx1
Proliferation
Hoxa2
Pax9
Follistatin
Spry2
Bmp7
Fgfs
Tbx22
Smads
Msx1
Mn1
Proliferation
Tbx3
Wnt5a
Bmp4
Meox2
Tgfβ3
Tp63
Shox2
Htra3
Bmpr1a
Proliferation
Egf
Tgfβ1
Fgf10
Wnt11
Bmp2
Fgfr
ERK1/2
Snail
Shh
Fusion
Fusion
Proliferation

Figure 32. Overview of the signalling pathways involved in regulating palatogenesis, highlighting the role of Hoxa2

Schematic representation of the major signalling pathways known to be involved in regulating murine palatogenesis. Hoxa2 downstream targets are highlighted in orange, two novel targets unrelated to Hoxa2 are denoted in brown. Green arrows denote activation of one factor on the other. Red lines denote repression of one factor on another. Black lines represent the effects of that factor on the denoted process (proliferation or fusion), if crossed by red lines the process is inhibited by the factor. Dotted lines represent predicted interactions. The pink area representing the epithelium, grey represents the mesenchyme. Factors are shown in their relative anteroposterior region of expression with factors with an exclusively anterior expression pattern in purple, posterior expression indicated in yellow. Expression patterns that are not region specific or are confirmed are shown in blue.

the loss of *Hoxa2* affects the spatial expression of its downstream targets remains to be investigated. Due to the importance of proper anteroposterior expression of genes within the palate, it is possible that the effect of Hoxa2 on gene expression resides in regulating their expression domains in addition to their total expression level. To gain a complete overview of the area of the palate that genes are expressed within, a whole mount system would need to be developed. Whole palate *in situ* analysis has previously been reported by other groups (Li and Ding, 2007; Liu *et al*., 2005; Welsh *et al*., 2007). This technique is limited by the fact that it only evaluates the expression of mRNA, and therefore it may be desirable to attempt to optimize a whole mount immunohistochemical analysis system to visualize the areas of protein expression, although this technique has not been reported in the palate to date.

Determination of whether any of the newly identified targets are directly repressed by Hoxa2 is required for a better understanding of its role in regulating palate development. The most likely candidates for direct regulation are *Msx1* and *Six2*. It is possible that *Barx1*, *Bmp4*, *Lef1* and *Tbx1* are also directly repressed by Hoxa2. To determine if these targets are directly downstream of Hoxa2 it is necessary to show whether Hoxa2 is capable of recognizing and binding to the promoter or coding region of the DNA encoding for each target. Chromatin Immunoprecipitation (ChIP) could be used to determine the ability of Hoxa2 to bind to the genomic sequences of these genes. This could be performed *in vivo*, nuclei samples would be isolated from

the palate and the DNA and protein cross-linked. A Hoxa2 specific antibody would then be used to isolate the Hoxa2 protein and any bound DNA. Following a reversal of the crosslinking, PCR analysis can be performed to determine if the DNA that was bound by Hoxa2 falls in the promoter or coding regions of the gene targets being examined.

ChIP analysis will provide valuable insight into what targets are potentially directly downstream of Hoxa2. Further examination would be required to confirm that a direct regulation is occurring. Electrophoretic mobility shit assays (EMSA) would allow the direct examination of Hoxa2 protein binding to target sites. In addition, it would be desirable to confirm that Hoxa2 is capable of repressing downstream genes by binding to any isolated target sequences *in vivo*. This can be achieved by cloning the isolated binding sequences into a vector upstream of a reporter gene such as luciferase. This vector can be cloned into a cell line along with a Hoxa2 expression vector. If the effect of Hoxa2 is direct, the level of activity of the reporter gene should be altered in the presence of Hoxa2 expression. Taken together, these data would allow for the identification of targets that are directly downstream of Hoxa2 within the developing palate.

Further investigation into the potential of a Hoxa2-Ptx1 pathway in the palate which involves Barx1, Lef1 and Tbx1 is also required. It has been suggested that in the branchial arches Fgf8 is responsible for mediating the signal between Hoxa2 and *Ptx1* (Bobola *et al*., 2003). In order to investigate if

this link is occurring within the palate, an Fgf8 antagonist could be incorporated into organ cultures. If the increase in Ptx1 expression in the *Hoxa*2 null palate shelves requires Fgf8, then blocking its activity should prevent the increased Ptx1 expression seen in these null embryos. If this is the case, then examination of how growth and fusion are altered by preventing this increase in Ptx1 could also provide insight into its role in regulating palate development. Barx1, Lef1 and Tbx1 are all potentially involved in the pathway with Ptx1 and therefore examining their expression patterns would also provide a more complete picture of how these genes interact.

To confirm the two novel pathways that have been suggested here will require further analysis. Addition of siRNA specific for any of the genes shown to be upregulated by Hoxa2 would provide valuable information. Knocking down the increased expression of these genes individually followed by characterization of growth and fusion of the palates as well as expression of the other targets identified would provide a more complete picture of the role of these downstream targets and how they are interconnected. It is possible that knocking down increased expression of one or more of the downstream targets will be capable of rescuing the observed cleft palate in *Hoxa*2 null embryos.

Eya1 expression would also be an interesting target to investigate within the palate. Determination of whether *Eya1* expression is altered in *Hoxa2* null palates could also provide an interesting link between Hoxa2 and palatogenesis.

The novel expression of Htra3 within the palate provides an exciting new target that could potentially play an important role in regulating palatogenesis. Htra3 is capable of binding to and inactivating members of the TGF-β family (Tocharus *et al*., 2004). Due to important roles that members of the TGF-β family play in palate development, it would be interesting to determine how their expression and activity is altered by Htra3. Ideally, an Htra3 knockout mouse line would be developed, but this would be costly and time-consuming. Knocking down Htra3 expression in culture, using a siRNA construct, would be an easier starting point. Additionally, increasing Htra3 expression in culture, potentially by retroviral infection, could aid in elucidating any potential role it may play in the developing palate. Following the up or downregulation of Htra3 palate cultures could be examined for growth, fusion and expression levels of TGF-β family members. Htra3 is an extracellular protein, capable of degrading extracellular matrix proteoglycans, including decorin and biglycan (Tocharus *et al*., 2004). Examination of the composition of the extracellular matrix when the levels of Htra3 are altered would also be required.

7.0 References

Adler, R. and Canto-Soler, V. (2007). Molecular Mechanisms of Optic Vesicle Development:Complexities, Ambiguities and Controversies. *Dev. Biol.* 305, 1-13.

Akin, Z. N. (2004). Identification of *Hoxa*2 Target genes*, Ph.D. Thesis*, University of Saskatchewan.

Akin, Z. N. and Nazarali, A. J. (2005). *Hox* Genes and their Candidate Downstream Targets in the Developing Central Nervous System. *Cell. Mol. Neurobiol.* 25, 697-741.

Alappat, S., Zhang, Z. and Chen, Y. P. (2003). Msx Homeobox Gene Family and Craniofacial Development. *Cell Res.* 13, 429-442.

Alappat, S. R., Zhang, Z., Suzuki, K., Zhang, X., Liu, H., Jiang, R., Yamada, G. and Chen, Y. (2005). The Cellular and Molecular Etiology of the Cleft Secondary Palate in Fgf10 Mutant Mice. *Dev. Biol.* 277, 102-113.

Alkuraya, F. S., Saadi, I., Lund, J. J., Turbe-Doan, A., Morton, C. C. and Maas, R. L. (2006). *SUMO1* Haploinsufficiency Leads to Cleft Lip and Palate. *Science* 313, 1751.

Amen, M., Liu, X., Vadlamudi, U., Elizondo, G., Diamond, E., Engelhardt, J. F. and Amendt, B. A. (2007). PITX2 and Beta-Catenin Interactions Regulate Lef-1 Isoform Expression. *Mol. Cell. Biol.* 27, 7560-7573.

Amin, N., Ohashi, Y., Chiba, J., Yoshida, S. and Takano, Y. (1994). Alterations in Vascular Pattern of the Developing Palate in Normal and Spontaneous Cleft Lip and Palate. *Cleft Palate Craniofac. J.* 31, 332-344.

Andreou, A. M., Pauws, E., Jones, M. C., Singh, M. K., Bussen, M., Doudney, K., Moore, G. E., Kispert, A., Brosens, J. J. and Stanier, P. (2007). TBX22 Missense Mutations found in Patients with X-Linked Cleft Palate Affect DNA Binding, Sumoylation, and Transcriptional Repression. *Am. J. Hum. Genet.* 81, 700-712.

Applied Biosystems. (2004). Amplification Efficiency of Taqman Gene Expression Assays. Application Note 127AP05-02,.

Asada, H., Kawamura, Y., Maruyama, K., Kume, H., Ding, R. G., Kanbara, N., Kuzzume, H., Sanbo, M., Yagi, T. and Obata, K. (1997). Cleft Palate and Decreased Brain Gamma-Aminobutyric Acid in Mice Lacking the 67-kDa Isoform of Glutamic Aci Decarboxylase. *Proc. Natl. Acad. Sci. U. S. A.* 94, 6496-6499.

Babiarz, B. S., Wee, E. L. and Zimmerman, E. F. (1979). Palate Morphogenesis. III. Changes in Cell Shape and Orientation during Shelf Elevation. *Teratology* 20, 249-278.

Balkaschina, E. I. (1929). Ein Fall Der Erbhomeosis Bei *Drosophila Melanogaster*. *Wilhelm Roux' Arch. Entwichlungsmech Org.* 115, 448-463.

Barlow, A. J., Bogardi, J. P., Ladher, R. and Francis-West, P. H. (1999). Expression of Chick Barx-1 and its Differential Regulation by FGF-8 and BMP in the Maxillary Primordial. *Dev. Dyn.* 214, 291-302.

Barrow, J. R. and Capecchi, M. R. (1999). Compensatory Defects Associated with Mutations in *Hoxa*1 Restore Normal Palatogenesis to *Hoxa*2 Mutants. *Development* 126, 5011-5026.

Bei, M. and Maas, R. (1998). FGFs and BMP4 Induce both Msx1-Independent and Msx1-Dependent Signaling Pathways in Early Tooth Development. *Development* 125, 4325-4333.

Berkovitz, B. K. B., Holland, G. R. and Moxham, B. J. (2002). *Oral Anatomy, Histology and Embryology.* Edinburgh: Mosby.

Bobola, N., Carapuco, M., Ohnemus, S., Kanzler, B., Leibbrandt, A., Neubuser, A., Drouin, J. and Mallo, M. (2003). Mesenchymal Patterning by *Hoxa*2 Requires Blocking Fgf-Dependent Activation of *Ptx1.* . *Development* 130, 3403-3414.

Bridges, C. B. and Dobzhansky, T. (1933). The Mutant 'Proboscipedia' in *Drosophila Melanogaster*- a Case of Hereditary Homeosis. *Wilhelm Roux's Arch. Dev. Biol.* 127, 575-590.

Bridges, C. B. and Morgan, T. H. (1923). *The Third-Chromosome Group of Mutant Characters of Drosophila Melanogaster*, pp. 1-251. Baltimore, MD: Carnegie Institution of Washington Press.

Brinkley, L. L. (1980). In Vitro Studies of Palatal Shelf Elevation. In *Current Research Trends in Prenatal Craniofacial Development* (ed. R. M. Pratt and R. L. Christiansen), pp. 203-220.

Brinkley, L. L. and Bookstein, F. L. (1986). Cell Distribution during Mouse Secondary Palate Closure II. Mesenchymal Cells. *J. Embryol. Exp. Morphol.* 96, 111-130.

Brinkley, L. L. and Morris-Wiman, J. (1984). Role of Extracellular Matrices in Palatal Shelf Closure. *Curr. Top. Dev. Biol.* 19, 17-36.

Brinkley, L. L. and Morris-Wiman, J. (1987). Computer-Assisted Analysis of Hyaluronate Distribution during Morphogenesis of the Mouse Secondary Palate. *Development* 100, 629-636.

Brodbeck, S., Besenbeck, B. and Englert, C. (2004). The Transcription Factor Six2 Activates Expression of the Gdnf Gene as Well as its Own Promoter. *Mech. Develop.* 121, 1211-1222.

Bronner-Fraser, M. (1993). Neural Crest Cell Migration in the Developing Embryo. *Trends Cell Biol* 3, 392-397.

Brunet, A., Roux, D., Lenormand, P., Dowd, S., Keyse, S. and Pouyssegur, J. (1999). Nuclear Translocation of p42/p44 Mitogen-Activated Protein Kinase is Required for Growth Factor-Induced Gene Expression and Cell Cycle Entry. *EMBO J.* 18, 664-674.

Brunet, C. L., Sharpe, P. M. and Ferguson, M. W. (1995). Inhibition of TGF-Beta 3 (but Not TGF-Beta 1 Or TGF-Beta 2) Activity Prevents Normal Mouse Embryonic Palate Fusion. *Int. J. Dev. Biol.* 39, 345-355.

Bulleit, R. F. and Zimmerman, E. F. (1985). The Influence of the Epithelium on Palate Shelf Reorientation. *J. Embryol. Exp. Morphol.* 88, 265-279.

Burglin, T. R. (1997). Analysis of TALE Superclass Homeobox Genes (MEIS, PBC, KNOX, Iroquois, TGIF) Reveals a Novel Domain Conserved between Plants and Animals. *Nucleic Acid Res.* 25, 4173-4180.

Carette, M. J. and Ferguson, M. W. (1992). The Fate of Medial Edge Epithelial Cells during Palatal Fusion in Vitro: An Analysis by DiI Labelling and Confocal Microscopy. *Development* 114, 379-388.

Carette, M. J., Lane, E. B. and Ferguson, M. W. (1991). Differentiation of Mouse Embryonic Palatal Epithelium in Culture: Selective Cytokeratin Expression Distinguishes between Oral, Medial Edge and Nasal Epithelial Cells. *Differentiation* 47, 149-161.

Chai, Y., Bringas, P., Shuler, C., Devaney, E., Grosschedl, R. and Slavkin, H. C. (1998). A Mouse Mandibular Culture Model Permits the Study of Neural Crest Cell Migration and Tooth Development. *Int. J. Dev. Biol.* 42, 87-94.

Chai, Y. and Maxson, R. E. (2006). Recent Advances in Craniofacial Morphogenesis. *Dev. Dyn.* 235, 2353-2375.

Chong S.S., Cheah, F.S.H. and Jabs, E.W. Genes implicated in lip and palate development. In *Cleft Lip and Palate: From Origin to Treatment* (ed. D. F. Wyszynski), New York, New York USA: Oxford University Press.

Christensen, K., Juel, K., Herskind, A. M. and Murray, J. C. (2004). Long Term Follow Up Study of Survival Associated with Cleft Lip and Palate at Birth. *B. M. J.* 328, 1405-1408.

Christensen, K. and Mortensen, P. B. (2002). Facial Clefting and Psychiatric Diseases: A Follow-Up of the Danish 1936-1987 Facial Cleft Cohort. *Cleft Palate Craniofac. J.* 39, 392-396.

Cohen, S. R., Chen, L., Trotman, C. A. and Burdi, A. R. (1993). Soft Palate Myogenesis: A Developmental Field Paradigm. *Cleft Palate Craniofac. J.* 30, 441-446.

Colvin, J. S., Feldman, B., Nadeau, J. H., Goldfarb, M. and Ornitz, D. M. (1999). Genomic Organization and Embryonic Expression of the Mouse Fibroblast Growth Factor 9 Gene. *Dev. Dyn.* 216, 72-88.

Colvin, J. S., White, A. C., Pratt, S. J. and Ornitz, D. M. (2001). Lung Hypoplasia and Neonatal Death in Fgf9-Null Mice Identify this Gene as an Essential Regulator of Lung Mesenchyme. *Development* 128, 2095-2106.

Cuervo, R., Valencia, C., Chandraratna, R. A. S. and Covarrubias, L. (2002). Programmed Cell Death is Required for Palate Shelf Fusion and is Regulated by Retinoic Acid. *Dev. Biol.* 245, 145-156.

Cui, X., Shiomi, N., Chen, J., Saito, T., Yamamoto, T., Ito, Y., Bringas, P., Chai, Y. and Shuler, C. F. (2005). Overexpression of Smad2 in *Tgf*-β3-Null Mutant Mice Rescues Cleft Palate. *Dev. Biol.* 278, 193-202.

Cui, X. M. and Shuler, C. F. (2000). The TGF-Beta Type III Receptor is Localized to the Medial Edge Epithelium during Palatal Fusion. *Int. J. Dev. Biol.* 44, 397-402.

Davenport, T. G., Jerome-Majewska, L. A. and Papaioannou, V. E. (2003). Mammary Gland, Limb and Yolk Sac Defects in Mice Lacking Tbx3, the Gene Mutated in Human Ulnar Mammary Syndrome. *Development* 130, 2263-2273.

De Angelis, V. and Nalbandian, J. (1968). Ultrastructure of Mouse and Rat Palatal Processes Prior to and during Secondary Palate Formation. *Arch. Oral Biol.* 13, 601-608.

Diewert, V. M. (1978). A Quantitative Coronal Plane Evaluation of Craniofacial Growth and Spatial Relations during Secondary Palate Development in the Rat. *Arch. Oral Biol.* 23, 607-629.

Diewert, V. M. (1980). Differential Changes in Cartilage Cell Proliferation and Cell Density in the Rat Craniofacial Complex during Secondary Palate Development. *Anat. Rec.* 198, 219-228.

Diewert, V. M. (1983). A Morphometric Analysis of Craniofacial Growth and Changes in Spatial Relations during Secondary Palatal Development in Human Embryos and Fetuses. *Am. J. Anat.* 167, 495-522.

Dressler, G. R. and Gruss, P. (1989). Anterior Boundaries of Hox Gene Expression in Mesoderm-Derived Structures Correlate with the Linear Gene Order Along the Chromosome. *Differentiation* 41, 193-201.

Duboule, D. and Morata, G. (1994). Colinearity and Functional Hierarchy among Genes of the Homeotic Complexes. *Trends. Genet.* 10, 358-364.

Eblaghie, M. C., Song, S., Kim, J., Akita, K., Tickle, C. and Jung, H. (2004). Interactions between FGF and Wnt Signals and Tbx3 Gene Expression in Mammary Gland Initiation in Mouse Embryos. *J. Anat.* 205, 1-13.

Farbman, A. I. (1968). Electron Microscope Study of Palate Fusion in Mouse Embryos. *Dev. Biol.* 18, 93-116.

Ferguson, C. A., Tucker, A. S. and Sharpe, P. T. (2000). Temporospatial Cell Interactions Regulating Mandibular and Maxillary Arch Patterning. *Development* 127, 403-412.

Ferguson, M. W. (1978). Palatal Shelf Elevation in the Wistar Rat Fetus. *J. Anat.* 125, 555-577.

Ferguson, M. W. (1987). Palate Development: Mechanisms and Malformations. *Irish J. Med. Sci.* 156, 309-315.

Ferguson, M. W. (1988). Palate Development. *Development* 103, 41-60.

Fitchett, J. E. and Hay, E. D. (1989). Medial Edge Epithelium Transforms to Mesenchyme After Embryonic Palate Shelves Fuse. *Dev. Biol.* 131, 455-474.

Fitzpatrick, D. R., Denhez, F., Kondaiah, P. and Akhurst, R. J. (1990). Differential Expression of TGF Beta Isoforms in Murine Palatogenesis. *Dev. Biol.* 109, 585-595.

Fogelgren, B., Kuroyama, M. C., McBratney-Owen, B., Spence, A. A., Malahn, L. E., Anawati, M. K., Cabatbat, C., Alarcon, V. B., Marikawa, Y. and Lozanoff, S. (2008). Misexpression of Six2 is Associated with Heritable Frontonasal Dysplasia and Renal Hypoplasia in 3H1 Br Mice. *Dev. Dyn.* 237, 1767-1779.

Fogelgren, B., Yang, S., Sharp, I. C., Huckstep, O. J., Ma, W., Somponpun, S. J., Carlson, E. C., Uyehara, C. F. T. and Lozanoff, S. (2009). Deficiency in Six2 during Prenatal Development is Associated with Reduced Nephron Number, Chronic Renal Failure, and Hypertension in Br/+ Adult Mice. *Am. J. Physiol. Renal Physiol.* 296, 1166-1178.

Formstecher, E., Ramos, J. W., Fauquet, M., Calderwood, D. A., Hsieh, J. C., Canton, B., Nguyen, X. T., Barnier, J. V., Camonis, J., Ginsberg, M. H. et al. (2001). PEA-15 Mediates Cytoplasmic Sequestration of ERK MAP Kinase. *Dev. Cell* 1, 239-250.

Francis-West, P. H., Ladher, R., Barlow, A. J. and Graveson, A. (1998). Signalling Interactions during Facial Development. *Mech. Develop.* 75, 3-28.

Fraser, S., Keynes, R. and Lumsden, A. (1990). Segmentation in the Chick Embryo Hindbrain is Defined by Cell Lineage Restriction. *Nature* 344, 431-435.

Friedman, R. A., Makmura, L., Biesiada, E., Wang, X. and Keithley, E. M. (2005). Eya1 Acts Upstream of Tbx1, Neurogenin 1, Neuro D and the Neurotrophin BDNF and NT-3 during Inner Ear Development. *Mech. Develop.* 122, 625-634.

Gaare, J. D. and Langman, J. (1977). Fusion of Nasal Swellings in the Mouse Embryo: Regression of the Nasal Fin. *Am. J. Anat.* 150, 477-499.

Gammill, L. S. and Bronner-Fraser, M. (2003). Neural Crest Specification: Migrating into Genomics. *Nat. Rev. Neurosci.* 4, 795-805.

Gaunt, S. J., Krumlauf, R. and Duboule, D. (1989). Mouse Homeo-Genes within a Subfamily, Hox-1.4, -2.6, and -5.1, Display Similar Anteroposterior Domains of Expression in the Embryo, but show Stage- and Tissue-Dependent Differences in their Regulation. *Development* 107, 131-141.

Gaunt, S. J. and Strachan, L. (1996). Temporal Colinearity in Expression of Anterior Hox Genes in Developing Chick Embryos. *Dev. Dyn.* 207, 270-280.

Gehring, W. J., Muller, M., Affolter, M., Percival-Smith, A., Billeter, M., Qian, Y. Q., Otting, G. and Wuthrich, K. (1990). The Structure of the Homeodomain and its Functional Implications. *Trends Genet.* 6, 323-329.

Gendron-Maguire, M., Mallo, M., Zhang, M. and Gridley, T. (1993). *Hoxa-2* Mutant Mice Exhibit Homeotic Transformation of Skeletal Elements Derived from Cranial Neural Crest. *Cell* 75, 1317-1331.

Gilbert, S. F. (2003). *Developmental Biology*, pp. 838. Sunderland, MA, USA: Sinauer Associates Inc.

Goodnough, L. H., Brugmann, S. A., Hu, D. and Helms, J. A. (2007). Stage-Dependent Craniofacial Defects Resulting from Sprouty2 Overexpression. *Dev. Dyn.* 236, 1918-1928.

Gorlin, R. J., Cohen, M. M. J. and Hennekam, R. C. M. (2001). *Syndromes of the Head and Neck*, pp. 850-853. New York, New York, USA: Oxford University Press.

Graba, Y., Aragnol, D. and Pradel, J. (1997). *Drosophila* Hox Complex Downstream Targets and the Function of Homeotic Genes. *BioEssays* 19, 379-388.

Graham, A., Heyman, I. and Lumsden, A. (1993). Even-Numbered Rhombomeres Control the Apoptotic Elimination of Neural Crest Cells from Odd-Numbered Rhombomeres in the Chick Hindbrain. *Development* 119, 223-245.

Graham, A., Papalopulu, N. and Krumlauf, R. (1989). The Murine and *Drosophila* homeobox Gene Complexes have Common Features of Organization and Expression. *Cell* 57, 367-378.

Grammatopoulos, G. A., Bell, E., Toole, L., Lumsden, A. and Tucker, A. S. (2000). Homeotic Transformation of Branchial Arch Identity After *Hoxa*2 Overexpression. *Development* 127, 5355-5365.

Graves, L. M., Guy, H. I., Kozlowski, P., Huang, M., Lazarowski, E., Pope, R. M., Collins, M. A., Dahlstrand, E. N., Earp, H. S. and Evans, D. R. (2000). Regulation of Carbamoyl Phosphate Synthetase by MAP Kinase. *Nature* 403, 328-332.

Greene, R. M. and Kochhar, D. M. (1974). Surface Coat on the Epithelium of Developing Palatine Shelves in the Mouse as Revealed by Electron Microscopy. *J. Embryol. Exp. Morphol.* 31, 683-692.

Greene, R. M. and Pratt, R. M. (1976). Developmental Aspects of Secondary Palate Formation. *J. Embryol. Exp. Morphol.* 36, 225-245.

Greene, R. M. and Pratt, R. M. (1977). Inhibition by Diazo-Oxo-Norleucine (DON) of Rat Palatal Glycoproteins Synthesis and Epithelial Cell Adhesion in Vitro. *Exp. Cell Res.* 105, 27-37.

Griffith, C. M. and Hay, E. D. (1992). Epithelial-Mesenchymal Transformation during Palatal Fusion: Carboxyfluorescein Traces Cells at Light and Electron Microscopic Levels. *Development* 116, 1087-1099.

Gritli-Linde, A. (2007). Molecular Control of Secondary Palate Development. *Dev. Biol.* 301, 309-326.

Gritli-Linde, A. (2008). The Etiopathogenesis of Cleft Lip and Cleft Palate: Usefulness and Caveats of Mouse Models. In *Current Topics in Developmental Biology*, pp. 37-120: Elsevier Inc.

Gupta, V. and Bei, M. (2006). Modification of Msx1 by SUMO-1. *Biochem. Biophys. res. Commun.* 345, 74-77.

Guthrie, S. and Lumsden, A. (1991). Formation and Regeneration of Rhombomere Boundaries in the Developing Chick Hindbrain. *Development* 112, 221-229.

Guthrie, S., Prince, V. and Lumsden, A. (1993). Selective Dispersal of Avian Rhombomere Cells in Orthotopic and Heterotopic Grafts. *Development* 118, 527-538.

Hackel, P. O., Zwick, E., Prenzel, N. and Ullrich, A. (1999). Epidermal Growth Factors: Critical Mediators of Multiple Receptor Pathways. *Curr. Opin. Cell Biol.* 11, 184-189.

Hagiwara, N. l., Katarova, Z., Siracusa, L. D. and Brilliant, M. H. (2003). Nonneuronal Expression of the GABAa-beta3 Subunit Gene is Required for Normal Palate Development in Mice. *Dev. Biol.* 254, 93-101.

Hao, Z., Yeung, J., Wolf, L., Doucette, R. and Nazarali, A. (1999). Differential Expression of Hoxa-2 Protein Along the Dorsal-Ventral Axis of the Developing and Adult Mouse Spinal Cord. *Dev. Dyn.* 216, 201-217.

He, F., Xiong, W., Yu, X., Espinoza-Lewis, R., Liu, C., Gu, S., Nishita, M., Suzuki, K., Yamada, G., Minami, Y. et al. (2008). Wnt5a Regulates Directional Cell Migration and Cell Proliferation Via Ror2-Mediated Noncanonical Pathway in Mammalian Palate Development. *Development* 135, 3871-3879.

Helms, J. A., Cordero, D. and Tapadia, M. D. (2005). New Insights into Craniofacial Morphogenesis. *Development* 132, 851-861.

Herr, A., Meunier, D., Müller, I., Rump, A., Fundele, R., Ropers, H. H. and Nuber, U. A. (2003). Expression of Mouse Tbx22 Supports its Role in Palatogenesis and Glossogenesis. *Dev. Dyn.* 266, 579-586.

Hinrichsen, K. (1985). The Early Development of Morphology and Patterns of the Face in the Human Embryo. *Adv. Anat. Embryol. Cell. Biol.* 98, 1-79.

Houzelstein, D., Cohen, A., Buckingham, M. E. and Robert, B. (1997). Insertional Mutation of the Mouse *Msx1* Homeobox Gene by an nlacZ Reporter Gene. *Mech. Develop.* 65, 123-133.

Huang, X., Goudy, S. L., Ketova, T., Litingtung, Y. and Chiang, C. (2008). *Gli3*-Deficient Mice Exhibit Cleft Palate Associated with Abnormal Tongue Development. *Dev. Dyn.* 237, 3079-3087.

Humphrey, T. (1969). The Relation between Human Fetal Mouth Opening Reflexes and Closure of the Palate. *Am. J. Anat.* 125, 317-344.

Hunter, M. P. and Prince, V. E. (2002). Zebrafish Hox Paralogue Group 2 Genes Function Redundantly as Selector Genes to Pattern the Second Pharyngeal Arch. *Dev. Biol.* 247, 367-389.

Innes, P. B. (1978). The Ultrastructure of the Mesenchymal Element of the Palatal Shelves of the Fetal Mouse. *J. Embryol. Exp. Morphol.* 43, 185-194.

Inoue, M., Kawakami, M., Tatsumi, K., Manabe, T., Makinodan, M., Matsuyoshi, H., Kirita, T. and Wanaka, A. (2006). Expression and Regulation of the LIM Homeodomain Gene L3/Lhx8 Suggests a Role in Upper Lip Development of the Chick Embryo. *Anat. Embryol.* 211, 247-253.

Izpisua-Belmonte, J. C., Tickle, C., Dolle, P., Wolpert, L. and Duboule, D. (1991). Expression of the Homeobox Hox-4 Genes and the Specification of Position in Chick Wing Development. *Nature* 350, 585-589.

Jerome, L. A. and Papaioannou, V. E. (2001). DiGeorge Syndrome Phenotype in Mice Mutant for the T-Box Gene, Tbx1. *Nat. Genet.* 27, 286-291.

Jiang, R., Bush, J. O. and Lidral, A. (2006). Development of the Upper Lip: Morphogenetic and Molecular Mechanisms. *Dev. Dyn.* 235, 1152-1166.

Jin, J. Z. and Ding, J. (2006). Analysis of Meox-2 Mutant Mice Reveals a Novel Postfusion-Based Cleft Palate. *Dev. Dyn.* 235, 539-546.

Kaartinen, V., Cui, X., Heisterkamp, N., Groffen, J. and Shuler, C. F. (1997). Transforming Growth Factor- Beta 3 Regulates Transdifferentiation of Medial Edge Epithelium during Palatal Fusion and Associated Degradation of the Basement Membrane. *Dev. Dyn.* 209, 255-260.

Kaartinen, V., Voncken, J. W., Shuler, C. F., Warburton, D., Bu, D., Heisterkamp, N. and Groffen, J. (1995). Abnormal Lung Development and Cleft Palate in Mice Lacking Tgf-Beta 3 Indicates Defects of Epithelial-Mesenchymal Interactions. *Nat. Genet.* 11, 415-421.

Kalionis, B. and O'Farrell, P. H. (1993). A Universal Target Sequence is Bound in Vitro by Diverse Homeodomains. *Mech. Develop.* 43, 57-70.

Kaufman, M. H. (1992). *The Atlas of Mouse Development.*. New York: Academic press.

Kaufman, T. C., Seeger, M. A. and Olsen, G. (1990). Molecular and Genetic Organization of the Antennapedia Gene Complex of *Drosophila Melanogaster*. *Adv. Genet.* 27, 309-362.

Khokhlatchev, A. V., Canagarajah, B., Wilsbacher, J., Robinson, M., Atkinson, M., Goldsmith, E. and Cobb, M. H. (1998). Phosphorylation of the MAP Kinase ERK2 Promotes its Homodimerization and Nuclear Translocation. *Cell* 93, 605-615.

Kissinger, C. R., Liu, B. S., Martin-Blanco, E., Kornberg, T. B. and Pabo, C. O. (1990). Crystal Structure of Engrailed Homeodomain-DNA Complex at 2.8 A Resolution: A Framework for Understanding Homeodomain-DNA Interactions. *Cell* 63, 579-590.

Kjaer, I. (1992). Human Prenatal Palate Shelf Elevation Related to Craniofacial Skeletal Maturation. *Eur. J. Orthod* 14, 26-30.

Kratochwil, K., Dull, M., Farinas, I., Galceran, J. and Grosschedl, R. (1996). LEF1 Expression is Activated by BMP-4 and Regulates Inductive Tissue Interactions in Tooth and Hair Development. *Genes Dev.* 10, 1382-1394.

Kratochwil, K., Galceran, J., Tontsch, S., Roth, W. and Grosschedl, R. (2002). FGF4, a Direct Target of LEF1 and Wnt Signaling, can Rescue the Arrest of Tooth Organogenesis in *Lef*1$^{-/-}$ Mice. *Genes Dev.* 16, 3173-3185.

Kutejova, E., Engist, B., Self, M., Oliver, G., Kirilenko, P. and Bobola, N. (2008) Six2 Functions Redundantly Immediately Downstream of Hoxa2. *Development* 135, 1463-1470.

Kutejova, E., Engist, B., Mallo, M., Kanzler, B. and Bobola, N. (2005). *Hoxa*2 Downregulates *Six*2 in the Neural Crest-Derived Mesenchyme. *Development* 132, 469-478.

Lanctot, C., Lamolet, B. and Drouin, J. (1997). The Bicoid-Related Homeoprotein Ptx1 Defines the most Anterior Domain of the Embryo and Differentiates Posterior from Anterior Lateral Mesoderm. *Development* 124, 2807-2817.

Larsson, K. S., Bostrom, H. and Carlsoo, S. (1959). Studies on the Closure of the Secondary Palate. *Exp. Cell Res.* 16, 379-383.

Laughton, A. (1991). DNA Binding Specificity of Homeodomains. *Biochemistry* 30, 11357-11367.

Le Douarin, N. M., Creuzet, S., Couly, G. and Dupin, E. (2004). Neural Crest Cell Plasticity and its Limits. *Development* 131, 4637-4650.

Le Douarin, N. M. and Kalcheim, C. (1999). *The Neural Crest*. Cambridge: Cambridge University Press.

Lee, J., Kim, J., Cho, K., Lee, M., Cho, S., Kwak, S., Cai, J. and Jung, H. (2008). Wnt11/Fgfr1b Cross-Talk Modulates the Fate of Cells in Palate Development. *Dev. Biol.* 314, 341-350.

Lee, J., Kim, J., Cho, K., Lee, M., Cho, S., Zhang, Y., Byun, S., Yi, C. and Jung, H. (2007). Modulation of Cell Proliferation during Palatogenesis by the Interplay between *Tbx3* and *Bmp4.*. *Cell Tissue Res.* 327, 285-292.

Levi, G., Mantero, S., Barbieri, O., Cantatore, D., Paleari, L., Beverdam, A., Genova, F., Robert, B. and Merlo, G. R. (2006). *Msx1* and *Dlx5* Act Independently in Development of Craniofacial Skeleton, but Converge on the Regulation of Bmp Signaling in Palate Formation. *Mech. Develop.* 123, 3-16.

Lewis, E. B. (1978). A Gene Complex Controlling Segmentation in Drosophila. *Nature* 276, 565-570.

Li, Q. and Ding, J. (2007). Gene Expression Analysis Reveals that Formation of the Mouse Anterior Palate Involves Recruitment of Cells from the Posterior Side. *Int. J. Dev. Biol.* 51, 167-172.

Li, S., Crenshaw, E. B., III, R., E.J., Simmons, D. M., Swanson, L. W. and Rosenfeld, M. G. (1990). Dwarf Locus Mutants Lacking Three Pituitary Cell Types Result from Mutations in the POU-Domain Gene *Pit-1*. *Nature* 347, 528-533.

Lidral, A. C., Romitti, P. A., Basart, A. M., Doetschman, T., Leysens, N. J., Daack-Hirsh, S., Semina, E. V., Johnson, L. R., Machida, J., Burds, A. et al. (1998). Association of MSX1 and TGFB3 with Nonsyndromic Clefting in Humans. *Am. J. Hum. Genet.* 63, 557-568.

Like, B. and Massague, J. (1986). The Antiproliferative Effect of Type Beta Transforming Growth Factor Occurs at a Level Distal from Receptors for Growth-Activating Factors. *J. Biol. Chem.* 261, 13426-13429.

Litingtung, Y., Dahn, R. D., Li, Y., Fallon, J. F. and Chiang, C. (2002). Shh and Gli3 are Dispensable for Limb Skeleton Formation but Regulate Digit Number and Identity. *Nature* 418, 979-983.

Liu, W., Lan, Y., Pauws, E., Meester-Smoor, M. A., Stanier, P., Zwarthoff, E. C. and Jiang, R. (2008). The Mn1 Transcription Factor Acts Upstreeam of Tbx22 and Preferentially Regulates Posterior Palate Growth in Mice. *Development* 135, 3959-3968.

Liu, W., Sun, X., Braut, A., Mishina, Y., Behringer, R. R., Mina, M. and Martin, J. F. (2005). Distinct Functions for Bmp Signaling in Lip and Palate Fusion in Mice. *Development* 132, 1453-1461.

Lozanoff, S. (1993). Midfacial Retrusion in Adult Brachyrrhine Mice. *Acta Anat. (Basel)* 147, 125-132.

Lozanoff, S., Johnston, J., Ma, W. and Jourdan-LeSaux, C. (2001). Immunohistochemical Localization of Pax2 and Associated Proteins in the Developing Kidney of Mice with Renal Hypoplasia. *J. Histochem. Cytochem.* 49, 1081-097.

Lumsden, A. and Keynes, R. (1989). Segmental Patterns of Neuronal Development in the Chick Hindbrain. *Nature* 337, 424-428.

Lumsden, A. and Krumlauf, R. (1996). Patterning the Vertebrate Neuraxis. *Science* 274, 1109-1115.

Ma, W. and Lozanoff, S. (1996). Morphological Deficiency in the Prenatal Anterior Cranial Base of Midfacially Retrognathic Mice. *J. Anat.* 188, 547-555.

Ma, W. and Lozanoff, S. (1999). Spatial and Temporal Distribution of Cellular Proliferation in the Cranial Base of Normal and Midfacially Retrusive Mice. *Clin. Anat.* 12, 315-325.

Maconochie, M., Krishnamurthy, R., Nonchev, S., Meier, P., Manzanares, M., Mitchell, P. J. and Krumlauf, R. (1999). Regulation of Hoxa2 in Cranial Neural Crest Cells Involves Members of the AP-2 Family. *Development* 126, 1483-1494.

Manley, N. R. and Capecchi, M. R. (1998). Hox Group 3 Paralogs Regulate the Development and Migration of the Thymus, Thyroid and Parathyroid Glands. *Dev. Biol.* 195, 1-15.

Marcano, A. C., Doudney, K., Braybrook, C., Squires, R., Patton, M. A., Lees, M. M., Richieri-Costa, A., Lidral, A. C., Murray, J. C., Moore, G. E., Stanier, P. (2004). TBX22 Mutations are a Frequent Cause of Cleft Palate. *J. Med. Genet.* 41, 68-74.

Marcil, A., Dumontier, E., Chamberland, M., Camper, S. A. and Drouin, J. (2003). Pitx1 and Pitx2 are Required for Development of Hindlimb Buds. *Development* 130, 45-55.

Marcucio, R. S., Cordero, D. R., Hu, D. and Helms, J. A. (2005). Molecular Interactions Coordinating the Development of the Forebrain and Face. *Dev. Biol.* 284, 48-61.

Marshall, M. S. (1995). Ras Target Proteins in Eukaryotic Cells. *FASEB J.* 9, 1311-1318.

Martinez-Alvarez, C., Blanco, M. J., Perez, R., Rabadan, M. A., Aparicio, M., Resel, E., Maritnez, T. and Nieto, M. A. (2004). Snail Family Members and Cell Survival in Physiological and Pathological Cleft Palates. *Dev. Biol.* 265, 207-218.

Martinez-Alvarez, C., Tudela, C., Perez-Miquelsanz, J., O'Kane, S., Puerta, J. and Ferguson, M. W. (2000). Medial Edge Epithelial Cell Fate during Palatal Fusion. *Dev. Biol.* 220, 343-357.

Massague, J. (1990). The Transforming Growth Factor-Beta Family. *Annu. Rev. Cell Biol.* 6, 597-641.

McBratney, B. M., Margaryan, E., Ma, W., Urban, Z. and Lozanoff, S. (2003). Frontonasal Dysplasia in 3H1 Br/Br Mice. *Anat. Rec. A. Discov. Mol. Cell. Evol. Biol.* 271, 291-302.

Miller, R. P. and Becker, B. A. (1975). Teratogenicity of Oral Diazepam and Diphenylhydantoin in Mice. *Toxicol. Appl. Pharmacol.* 32, 53-61.

Mitsiadis, T. A. and Drouin, J. (2008). Deletion of the Pitx1 Genomic Locus Affects Mandibular Tooth Morphogenesis and Expression of the Barx1 and Tbx1 Genes. *Dev. Biol.* 313, 887-896.

Morgan, P. R. and Pratt, R. M. (1977). Ultrastructure of the Expected Fusion Zone in Rat Fetuses with Diazo-Oxo-Norleucine (DON) Induced Cleft Palate. *Teratology* 15, 281-290.

Nakajima, A., Ito, Y., Asano, M., Maeno, M., Iwata, K., Mitsui, N., Shimizu, N., Cui, X. M. and Shuler, C. F. (2007). Functional Role of Transforming Growth Factor-Beta Type III Receptor during Palatal Fusion. *Dev. Dyn.* 236, 791-801.

Nawshad, A. and Hay, E. D. (2003). TGF{Beta}3 Signaling Activates Transcription of the LEF1 Gene to Induce Epithelial Mesenchymal Transformation during Mouse Palate Development. *J. Cell. Biol.* 163, 1291-1301.

Nawshad, A., LaGamba, D. and Hay, E. D. (2004). Transforming Growth Factor β (TGFβ) Signalling in Palatal Growth, Apoptosis and Epithelial Mesenchymal Transformation (EMT). *Ar. Oral Biol.* 49, 675-689.

Nawshad, A., Medici, D., Liu, C. C. and Hay, E. D. (2007). TGFbeta3 Inhibits E-Cadherin Gene Expression in Palate Medial-Edge Epithelial Cells through a Smad2-Smad4-LEF1 Transcription Complex. *J. Cell Sci.* 120, 1646-1653.

Nazarali, A., Kim, Y. and Nirenberg, M. (1992). *Hox-1.11* and *Hox-4.9* Homeobox Genes. *Proc. Natl. Acad. Sci. U. S. A.* 89, 2883-2887.

Nazarali, A., Puthucode, R., Leung, V., Wolf, L., Hoa, Z. and Yeung, J. (2000). Temporal and Spatial Expression of *Hoxa-2* during Murine Palatogenesis. *Cell. Mol. Neurobiol.* 20, 269-290.

Niswander, L. (2003). Pattern Formation: Old Models Out on a Limb. *Nat Rev. Genet.* 4, 133-143.

Noden, D. M. (1983). The Role of the Neural Crest in Patterning of Avian Cranial Skeletal, Connective and Muscle Tissues. *Dev. Biol.* 96, 144-165.

Noden, D. M. (1988). Interactions and Fates of Avian Craniofacial Mesenchyme. *Development* 103 Suppl., 121-140.

Noden, D. M. and Trainor, P. A. (2005). Relations and Interactions between Cranial Mesoderm and Neural Crest Populations. *J. Anat.* 207, 575-601.

Nonchev, S., Vesque, C., Maconochie, M., Seitanidou, T., Ariza-McNaughton, L., Frain, M., Marchall, H., Sham, M. H., Krumlauf, R. and Charnay, P. (1996). Segmental Expression of Hoxa-2 in the Hindbrain is Directly Regulated by Krox-20. *Development* 122, 543-554.

Nopoulos, P., Langbehn, D. R., Canady, J., Magnotta, V. and Richman, L. (2007). Abnormal Brain Structure in Children with Isolated Clefts of the Lip Or Palate. *Arch. Pediatr. Adolesc. Med.* 161, 753-758.

Ohbayashi, N. and Eto, K. (1986). Relative Contributions of the Facial Processes to Facial Development: A Microsurgical Assay. *J. Craniofac. Genet. Dev. Biol. Suppl.* 2, 41-44.

Ohto, H., Takizawa, T., Saito, T., Kobayashi, M., Ikeda, K. and Kawakami, K. (1998). Tissue and Developmental Distribution of Six Family Gene Products. *Int. J. Dev. Biol.* 42, 141-148.

Oliver, G., Mailhos, A., Wehr, R., Copeland, N. G., Jenkins, N. A. and Gruss, P. (1995). Six3, a Murine Homologue of the Sine Oculis Gene, Demarcates the most Anterior Border of the Developing Neural Plate and is Expressed during Eye Development. *Development* 121, 4045-4055.

O'Rahilly, R. (1967). The Early Development of the Nasal Pit in Staged Human Embryos. *Anat. Rec.* 157, 380.

Osumi-Yamashita, N., Noji, S., Nohno, T., Koyama, E., Doi, H., Eto, K. and Taniguchi, S. (1990). Expression of Retinoic Acid Receptor Genes in Neural Crest-Derived Cells during Mouse Facial Development. *FEBS Lett.* 264, 71-74.

Pasqualetti, M., Ori, M., Nardi, I. and Rijli, F. M. (2000). Ectopic *Hoxa*2 Induction After Neural Crest Migration Results in Homeosis of Jaw Elements in *Xenopus*. *Development* 127, 5367-5378.

Pearson, G., Robinson, F., Beers Gibson, T., Xu, B. E., Karandikar, M., Berman, K. and Cobb, M. H. (2001). Mitogen-Activated Protein (MAP) Kinase Pathways: Regulation and Physiological Functions. *Endocr. Rev.* 22, 153-183.

Pelton, R. W., Hogan, B. L., Miller, D. A. and Moses, H. L. (1990). Differential Expression of Genes Encoding TGFs Beta 1, Beta 2, and Beta 3 during Murine Palate Formation. *Dev. Biol.* 141, 456-460.

Pourtois, M. (1966). Onset of the Acquired Potentiality for Fusion in the Palatal Shelves of Rats. *J. Embryol. Exp. Morphol.* 16, 171-182.

Pratt, R. M., Goggins, J. F., Wilk, A. L. and King, C. T. G. (1973). Acid Mucopolysaccharide Synthesis in the Secondary Palate of the Developing Rat at the Time of Rotation and Fusion. *Dev. Biol.* 32, 230-237.

Pratt, R. M. and Hassell, J. R. (1975). Appearance and Distribution of Carbohydrate Rich Macromolecules on the Epithelial Surface of the Rat Palatal Shelf. *Dev. Biol.* 45, 192-198.

Prince, V. and Lumsden, A. (1994). *Hoxa-2* Expression in Normal and Transposed Rhombomeres: Independent Regulation in the Neural Tube and Neural Crest. *Development* 120, 911-923.

Proetzel, G., Pawlowski, S. A., Wiles, M. V., Yin, M., Boivin, G. P., Howles, P. N., Ding, J., Ferguson, M. W. J. and Doetschman, T. (1995). Transforming Growth Factor-Beta 3 is Required for Secondary Palate Fusion. *Nat. Genet.* 11, 409-414.

Purcell, P., Oliver, G., Mardon, G., Donner, A. L. and Maas, R. L. (2005). Pax6-Dependence of Six3, Eya1 and Dach1 Expression during Lens and Nasal Placode Induction. *Gene Expr. Patterns* 6, 110-118.

Reya, T. and Clevers, H. (2005). Wnt Signalling in Stem Cells and Cancer. *Nature* 434, 843-850.

Rice, R., Connor, E. and Rice, D. P. (2006). Expression Patterns of Hedgehog Signalling Pathway Members during Mouse Palate Development. *Gene Expr. Patterns* 6, 206-212.

Rice, R., Spencer-Dene, B., Connor, E. C., Gritli-Linde, A., McMahon, A. P., Dickson, C., Thesleff, I. and Rice, D. P. (2004). Disruption of *Fgf*10/*Fgfr2b*-Coordinated Epithelial-Mesenchymal Interactions Causes Cleft Palate. *J. Clin. Invest.* 113, 1692-1700.

Rijli, F. M., Mark, M., Lakkaraju, S., Dierich, A., Dolle, P. and Chambon, P. (1993). A Homeotic Transformation is Generated in the Rostral Branchial Region of the Head by Disruption of *Hoxa-2* which Acts as a Selector Gene. *Cell* 75, 1333-1349.

Riley, B. M., Mansilla, M. A., Ma, J., Daack-Hirsch, S., Maher, B. S., Raffensperger, L. M., Russo, E. T., Viera, A. R., Dode, C., Mohammadi, M. et al. (2007). Impaired FGF Signaling Contributes to Cleft Lip and Palate. *Proc. Natl. Acad. Sci. U. S. A.* 104, 4512-4517.

Rossel, M. and Capecchi, M. R. (1999). Mice Mutant for both Hoxa1 and Hoxb1 show Extensive Remodeling of the Hindbrain and Defects in Craniofacial Development. *Development* 126, 5027-5040.

Santagati, F., Minoux, M., Ren, S. and Rijli, F. (2005). Temporal Requirement of *Hoxa*2 in Cranial Neural Crest Skeletal Morphogenesis. *Development* 132, 4927-4936.

Santagati, F. and Rijli, F. (2003). Cranial Neural Crest and the Building of the Vertebrate Head. *Nat. Rev. Neurosci.* 4, 806-818.

Sasaki, T., Ito, Y. X., X., Han, J., Bringas, P., Maeda, T., Slavkin, H., Grosschedl, R. and Chai, Y. (2005). LEF1 is a Critical Epithelial Survival Factor during Tooth Morphogenesis. *Dev. Biol.* 278, 130-143.

Satokata, I. and Maas, R. (1994). *Msx-1* Deficient Mice Exhibit Cleft Palate and Abnormalities of Craniofacial and Tooth Development. *Nat. Genet.* 6, 348-356.

Saunders, J. W. J. (1966). Death in Embryonic Systems. *Science* 154, 604-612.

Scott, M. P., Weiner, A. J., Hazelrigg, T. I., Polisky, B. A., Pirrotta, V., Scalenghe, F. and Kaufman, T. C. (1983). The Molecular Organization of the Antennapedia Locus of Drosophila. *Cell* 35, 763-776.

Self, M., Lagutin, O. V., Bowling, B., Hendrix, J., Cai, Y., Dressler, G. R. and Oliver, G. (2006). Six2 is Required for Suppression of Nephrogenesis and Progenitor Renewal in the Developing Kidney. *EMBO J.* 25, 5214-5228.

Selleck, M. A., Scherson, T. Y. and Bronner-Fraser, M. (1993). Origins of Neural Crest Cell Diversity. *Dev. Biol.* 159, 1-11.

Serbedzija, G. N., Bronner-Fraser, M. and Fraser, S. E. (1992). Vital Dye Analysis of Cranial Neural Crest Cell Migration in the Mouse Embryo. *Development* 116, 297-307.

Shiomi, N., Cui, X. M., Yamamoto, T., Saito, T. and Shuler, C. F. (2006). Inhibition of SMAD2 Expression Prevents Murine Palatal Fusion. *Dev. Dyn.* 235, 1785-1793.

Shtutman, M., Zhurinsky, J., Simcha, I., Albanese, C., D'Amico, M., Pestell, R. and Ben-Ze'ev, A. (1999). The Cyclin D1 Gene is a Target of the Beta-catenin/LEF1 Pathway. *Proc. Natl. Acad. Sci. U. S. A.* 96, 5522-5527.

Shuler, C. F. (1995). Programmed Cell Death and Cell Transformation in Craniofacial Development. *Crit. Rev. Oral Biol. Med.* 6, 202-217.

Shuler, C. F., Halpern, D. E., Guo, Y. and Sank, A. C. (1992). Medial Edge Epithelium Fate Traced by Cell Lineage Analysis during Epithelial-Mesenchymal Transformation *in Vivo*. *Dev. Biol.* 154, 318-330.

Sildu, A. M., Nijo, B., Solow, B. and Kjaer, I. (1994). Prenatal Sagittal Growth of the Osseous Components of the Human Palate. *J. Craniofac. Genet. Devel. Biol.* 14, 252-256.

Singh, G. D., Johnston, J., Ma, W. and Lozanoff, S. (1998). Cleft Palate Formation in Fetal Br Mice with Midfacial Retrusion: Tenascin, Fibronectin, Laminin, and Type IV Collagen Immunolocalization. *Cleft Palate Craniofac. J.* 35, 65-76.

Singh, G. D., Moxham, B. J., Langley, M. S. and Embery, G. (1997). Glycosaminoglycan Biosynthesis during 5-Fluoro-2-Deoxyuridine-Induced Palatal Clefts in Rats. *Arch. Oral Biol.* 42, 355-363.

Singh, G. D., Moxham, B. J., Langley, M. S., Waddington, R. J. and Embery, G. (1994). Changes in the Composition of Glycosaminoglycans during Normal Palatogenesis in the Rat. *Arch. Oral Biol.* 39, 401-407.

Souchon, R. (1975). Surface Coat of the Palatal Shelf Epithelium during Palatogenesis in Mouse Embryos. *Anat. Embryol.* 147, 133-142.

Sperber, G. H. (2002a). Craniofacial Embryogenesis: Normal Developmental Mechanisms. In *Understanding Craniofacial Anomalies: The Etiopathogenesis of Craniosynostoses and Facial Clefting* (ed. M. P. Mooney and M. I. Siegel), pp. 31-60. New York: Wiley-Liss.

Sperber, G. H. (2002b). Formation of the Primary Palate. In *Cleft Lip and Palate: From Origin to Treatment.* (ed. D. F. Wyszynski), pp. 5-13. New York: Oxford University Press.

Sperber, G. H., Chong, S. S., Cheah, F. S. H. and Jabs, E. W. (2002). Basic Embryology of Cleft Lip and Palate. In *Cleft Lip and Palate: From Origin to Treatment* (ed. D. F. Wyszynski), pp. 5-40. New York, New York USA: Oxford University Press.

Sperber, G. H. and Sperber, S. M. (2009). Embryology of Orofacial Clefting. In *Comprehensive Cleft Care* (ed. J. E. Losee and R. E. Kirschner), pp. 3-20. China: McGraw-Hill.

St Amand, T. R., Zhang, Y., Semina, E. V., Zhoa, X., Hu, Y., Nguyen, L., Murray, J. C. and Chen, Y. (2000). Antagonistic Signals between BMP4 and FGF8 Define the Expression of Pitx1 and Pitx2 in Mouse Tooth-Forming Anlage. *Dev. Biol.* 217, 323-332.

Sun, D., Vanderburg, C. R., Odierana, G. S. and Hay, E. D. (1998). TGFbeta3 Promotes Transformation of Chicken Palate Medial Edge Epithelium to Mesenchyme *in Vitro*. *Development* 125, 95-105.

Tan, D. P., Ferrante, J., Nazarali, A., Shao, X., Kozak, C. A., Guo, V. and Nirenberg, M. (1992). Murine *Hoxa-1.11* Homeobox Gene Structure and Expression. *Proc. Natl. Acad. Sci. U. S. A.* 89, 6280-6284.

Thomason, H. A., Dixon, M. J. and Dixon, J. (2008). Facial Clefting in *Tp63* Deficient Mice Results from Altered Bmp4, Fgf8 and Shh Signaling. *Dev. Biol.* 321, 273-282.

Tocharus, J., Tsuchiya, A., Kajikawa, M., Ueta, Y., Oka, C. and Kawaich, M. (2004). Developmentally Regulated Expression of Mouse Htra3 and its Role as an Inhibitor of TGF-Beta Signaling. *Dev. Growth Differ.* 46, 257-274.

Tohgo, A., Pierce, K. L., Choy, E. W., Lefkowitz, R. J. and Luttrell, L. M. (2002). Beta-Arrestin Scaffolding of the ERK Cascade Enhances Cytosolic ERK Activity but Inhibits ERK-Mediated Transcription Following Angiotensin AT1a Receptor Stimulation. *J. Biol. Chem.* 277, 9429-9436.

Trainor, P. A., Ariza-McNaughton, L. and Krumlauf, R. (2002). Role of Isthmus and FGFs in Resolving the Paradox of Neural Crest Plasticity and Prepatterning. *Science* 295, 1288-1291.

Trainor, P. A. and Krumlauf, R. (2001). Hox Genes, Neural Crest Cells and Branchial Arch Patterning. *Curr. Opin. Cell Biol.* 13, 698-705.

Trasler, D. G. (1968). Pathogenesis of Cleft Lip and its Relation to Embryonic Face Shape in A-J and C57BL Mice. *Teratology* 1, 33-49.

Tremblay, J. J., Goodyer, C. G. and Drouin, J. (2000). Transcriptional Properties of *Ptx*1 and *Ptx*2. *Neuroendocrinology* 71, 277-286.

Tsukzaki, T., Chiang, T. A., Davison, A. F., Attisano, L. and Wrana, J. L. (1998). SARA, a FYVE Domain Protein that Recruits Smad2 to the TGFbeta Receptor. *Cell* 95, 779-791.

Tumpel, S., Cambronero, F., Ferretti, E., Blasi, F., Wiedemann, L. M. and Krumlauf, R. (2007). Expression of Hoxa2 in Rhombomere 4 is Regulated by a Conserved Cross-Regulatory Mechanism Dependent upon Hoxb1. *Dev. Biol.* 302, 646-660.

Tumpel, S., Sanz-Ezquerro, J. J., Isaac, A., Eblaghie, M. C., Dobson, J. and Tickle, C. (2002). Regulation of Tbx3 Expression by Anteroposterior Signalling in Vertebrate Limb Development. *Dev. Biol.* 250, 251-262.

Vadlamudi, U., Espinoza, H., Ganga, M., Martin, D., Liu, X., Engelhardt, J. and Amendt, B. (2005). PITX2, β-Catenin and LEF-1 Interact to Synergistically Regulate the LEF-1 Promoter. *J. Cell Sci.* 118, 1129-1137.

Van den Boogaard, M. J. H., Dorland, M., Beemer, F. A. and van Amstel, H. K. P. (2000). *MSX1* Mutation is Associated with Orofacial Clefting and Tooth Agenesis in Humans. *Nat. Genet.* 24, 342-343.

Vastardis, H., Karimbux, N., Guthua, S. W., Seidman, J. G. and Seidman, C. E. (1996). A Human *MSX1* Homeodomain Missense Mutation Causes Selective Tooth Agenesis. *Nat. Genet.* 13, 417-421.

Verzi, M. P., Agarwal, P., Brown, C., McCulley, D. J., Schwarz, J. J. and Black, B. L. (2007). The Transcription Factor MEF2C is Required for Craniofacial Development. *Dev. Cell* 12, 645-652.

Wang, B., Fallon, J. F. and Beachy, P. A. (2000). Hedgehog-Regulated Processing of Gli3 Produces an anterior/posterior Repressor Gradiant in the Developing Vertebrate Limb. *Cell* 100, 423-434.

Wang, X. (2006). Investigation of *Hoxa*2 Gene Function in Palate Development using a Retroviral Expression System. *M.Sc. Thesis*, University of Saskatchewan.

Wee, E. L., Norman, E. J. and Zimmerman, E. F. (1986). Presence of Gamma-Aminobutyric Acid in Embryonic Palates of AJ and SWV Mouse Strains. *J. Craniofac. Genet. Dev. Biol.* 6, 53-61.

Wee, E. L. and Zimmerman, E. F. (1983). Involvement of GABA in Palate Morphogenesis and its Relation to Diazepam Teratogenesis in Two Mouse Strains. *Teratology* 28, 15-22.

Welsh, I. C., Hagge-Greenberg, A. and O'Brien, T. P. (2007). A Dosage-Dependent Role for *Spry2* in Growth and Patterning during Palate Development. *Mech. Develop.* 124, 746-761.

Wolf, L. V., Yeung, J. M., Doucette, J. R. and Nazarali, A. J. (2001). Coordinated Expression of Hoxa2, Hoxd1 and Pax6 in the Developing Diencephalon. *Neuroreport* 12, 329-333.

Wood, H. B. and Episkopou, V. (1999). Comparative Expression of the Mouse Sox1, Sox2 and Sox3 Genes from Pre-Gastrulation to Early Somite Stages. *Mech. Develop.* 86, 197-201.

Xu, P., Adams, J., Peters, H., Brown, C., Heaney, S. and Maas, R. (1999). Eya1-Deficient Mice Lack Ears and Kidneys and show Abnormal Apoptosis of Organ Primordia. *Nat. Genet.* 23, 113-117.

Xu, X., Han, J., Ito, Y., Bringas, P. J., Urata, M. M. and Chai, Y. (2006). Cell Autonomous Requirement for Tgfbr2 in the Disappearance of Medial Edge Epithelium during Palatal Fusion. *Dev. Biol.* 297, 238-248.

Yamamoto, T., Cui, X. and Shuler, C. F. (2003). Role of ERK1/2 Signaling during EGF-Induced Inhibition of Palatal Fusion. *Dev. Biol.* 260, 512-521.

Yoon, H., Chung, I. S., Seol, E. Y., Park, B. Y. and Park, H. W. (2000). Development of the Lip and Palate in Staged Human Embryos and Early Fetuses. *Yonsei Med. J.* 41, 477-484.

Yu, L., Gu, S., Alappat, S., Song, Y., Yan, M., Zhang, X., Zhang, G., Jiang, Y., Zhang, Z., Zhang, Y. et al. (2005). *Shox*2-Deficient Mice Exhibit a Rare Type of Incomplete Clefting of the Secondary Palate. *Development* 132, 4397-4406-4406.

Zhang, W. (2003). Temporal and Spatial Expression of Hoxa2 Gene in the Developing Mouse Palate and the Effect of Valproic Acid on Hoxa2 Expression during Murine Palatogenesis. *M.Sc. Thesis,* University of Saskatchewan.

Zhang, Z., Song, Y., Zhao, X., Zhang, X., Fermin, C. and Chen, Y. (2002). Rescue of Cleft Palate in *Msx1*-Deficient Mice by Transgenic *Bmp4* Reveals a Network of BMP and SHH Signaling in the Regulation of Mammalian Palatogenesis. *Development* 129, 4135-4146-4146.

Zhao, Y., Guo, Y., Tomac, A. C., Taylor, N. R., Grinberg, A., Lee, E. J., Huang, S. and Westphal, H. (1999). Isolated Cleft Palate in Mice with a Targeted Mutation of the LIM Homeobox Gene *Lhx*8.. *Proc. Natl. Acad. Sci. U.S.A.* 96, 15002-15006.

Zhong, Y., Butts, T. and Holland, P. W. H. (2008). HomeoDB: A Database of Homeobox Gene Diversity. *Evol. Dev.* 10, 516-518.

Zou, D., Silvius, D., Fritzsch, B. and Xu, P. X. (2004). Eya1 and Six1 are Essential for Early Steps of Sensory Neurogenesis in Mammalian Cranial Placodes. *Development* 131, 5561-5572.

Apppendix- Accepted Manuscript

Developmental Dynamics

DEVELOPMENTAL DYNAMICS 238:2364–2373, 2009

RESEARCH ARTICLE

Hoxa2 Plays a Direct Role in Murine Palate Development

Tara M. Smith,[1†] Xia Wang,[1†] Wei Zhang,[1] William Kulyk,[2] and Adil J. Nazarali[1*]

The cleft palate exhibited by *Hoxa2* null murine embryos has been described as being secondary to abnormalities of tongue musculature, and *Hoxa2* was presumed to not play a direct role in palate development. However, we detected *Hoxa2* expression in the developing palate at both the mRNA and protein levels between embryonic day (E) 12.5 and E15.5. Organ cultures of $Hoxa2^{-/-}$ palates maintained in the absence of the tongue showed decreased fusion rates than either $Hoxa2^{+/-}$ or $Hoxa2^{+/+}$ palate cultures. Knocking down *Hoxa2* expression with antisense retroviral constructs resulted in decreased fusion rates than corresponding controls. An overall increase in cell proliferation was observed in *Hoxa2* null palates providing a potential mechanism by which *Hoxa2* may be affecting palate development. *Hoxa2* also repressed the expression of its downstream targets *Msx1*, *Bmp4*, *Barx1*, and *Ptx1* within the palate. These results demonstrate the cleft palate phenotype of *Hoxa2* null embryos is not solely due to abnormal tongue musculature, and indicate a direct role of *Hoxa2* in regulating murine palatogenesis. *Developmental Dynamics 238:2364–2373, 2009.* © 2009 Wiley-Liss, Inc.

Key words: secondary palate; *Hox* genes; cleft palate; downstream targets; *Hoxa2*; *Msx1*; *Ptx1*; *Bmp4*; *Barx1*

Accepted 14 June 2009

INTRODUCTION

The formation and fusion of the secondary palate in vertebrates is a complex and tightly regulated process. In the mouse, the secondary palate initially develops as two bilateral projections of the maxillary prominences at embryonic day (E) 11.5. The palatal shelves initially grow vertically downward on either side of the tongue. Then, at E14, the tongue flattens and allows the palate shelves to elevate and assume a horizontal position above the tongue. The elevated palate shelves then grow medially toward one another and contact to form the midline epithelial seam (MES). The MES subsequently undergoes a rapid degradation to form a mesenchymal confluence across the secondary palate, at which point palatogenesis is considered complete (Ferguson, 1988).

Hoxa2 is a member of a highly conserved family of transcription factors that share a 60 amino acid region known as the homeodomain. The homeodomain is comprised of a helix-turn-helix motif that is capable of recognizing and binding to DNA, and influencing transcription of downstream target genes (Akin and Nazarali, 2005). The *Hoxa2* gene encodes for encodes a 41-kDa protein (Nazarali et al., 1992; Tan et al., 1992) that acts as the selector gene for second branchial arch patterning (Gendron-Maguire et al., 1993; Rijli et al., 1993; Grammatopoulos et al., 2000; Pasqualetti et al., 2000).

Deletion of the *Hoxa2* gene in mice leads to an altered specification of neural crest cells, resulting in numerous craniofacial abnormalities (Gendron-Maguire et al., 1993; Grammatopoulos et al., 2000; Santagati et al., 2005). One of these abnormalities is a cleft secondary palate, which occurs in 81% of $Hoxa2^{-/-}$ embryos (Gendron-Maguire et al., 1993; Rijli et al., 1993; Barrow and Capecchi, 1999). A mutation in the *HOXA2* gene in humans

Additional Supporting information may be found in the online version of this article.

[1]Laboratory of Molecular Biology, College of Pharmacy and Nutrition, University of Saskatchewan, Saskatoon, Saskatchewan, Canada
[2]Department of Anatomy and Cell Biology, College of Medicine, University of Saskatchewan, Saskatoon, Saskatchewan, Canada

Grant sponsor: Natural Sciences and Engineering Research Council of Canada.

†T.M. Smith and X. Wang contributed equally to this work.

*Correspondence to: Adil J. Nazarali, Laboratory of Molecular Biology, College of Pharmacy and Nutrition, 116 Thorvaldson Building, 110 Science Place, University of Saskatchewan, Saskatoon SK, S7N 5C9. E-mail: aj.nazarali@usask.ca

DOI 10.1002/dvdy.22040
Published online 3 August 2009 in Wiley InterScience (www.interscience.wiley.com).

leads to similar abnormalities including a partial cleft secondary palate (Alasti et al., 2008). Because *Hoxa2* is expressed in the second and third branchial arches, but not in the first branchial arch (Prince and Lumsden, 1994) from which the palatal shelves later emerge, it was originally presumed that *Hoxa2* could not play a direct role in murine palate development. Barrow and Capecchi (1999) hypothesized that the high incidence of cleft secondary palate in *Hoxa2* null embryos results from abnormal attachment of the hyoglossus muscle to the greater horn of the hyoid bone—a third branchial arch derivative. They reasoned that this defect would prevent the depression of the lateral edges of the tongue and create a physical barrier between the opposing palate shelves, thereby inhibiting their contact and fusion. However, a subsequent study by Ohnemus et al. (2001) reported that the hyoglossus is always properly inserted in the hyoid of *Hoxa2*$^{-/-}$ mutant mice regardless of the presence or absence of a cleft palate phenotype. This suggests the possibility that palatal clefting may instead be a primary defect in these embryos. Although *Hoxa2* is absent from the first branchial arch at early stages of morphogenesis, this does not preclude it from being expressed at later stages within the growing palatal shelves. Indeed, a previous study in our laboratory provided immunocytochemical data demonstrating Hoxa2 protein expression within both epithelial and mesenchymal cells of the developing murine secondary palate (Nazarali et al., 2000).

Our current study provides further evidence for a direct involvement of *Hoxa2* in the development of the murine secondary palate. Using quantitative real-time reverse transcriptase-polymerase chain reaction (RT-PCR), Western blot analysis and immunohistochemistry, we have confirmed and further characterized the endogenous expression of *Hoxa2* in the secondary palate throughout the period of murine palatogenesis. In addition, we observed that cell proliferation was elevated in the palatal shelves of *Hoxa2*$^{-/-}$ mice, indicating that genetic ablation of *Hoxa2* function can directly influence palatal growth. Moreover, the palatal tissue of *Hoxa2*$^{-/-}$ mice demonstrated increased expression of four putative *Hoxa2* target genes—*Ptx1*, *Barx1*, *Msx1*, and *Bmp4*. This provides further evidence that *Hoxa2* plays an intrinsic role within the palatal tissues by repressing expression of these downstream target genes.

Using an organ culture model in which the palatal shelves are cultured in the absence of the tongue, we further demonstrate that palates from *Hoxa2* null mice display significantly lower fusion rates than palates from heterozygous or wild-type embryos. Similarly, a knock down of *Hoxa2* expression in organ cultures of wild-type palates using antisense *Hoxa2* retroviral constructs also caused a significant decrease in palatal fusion rates. Collectively, these findings point to a direct role for *Hoxa2* in regulating murine palatogenesis.

RESULTS

Endogenous Hoxa2 Expression Within the Developing Palate

To determine whether the *Hoxa2* gene may be directly involved in regulating palate development, it was important to demonstrate that *Hoxa2* is expressed endogenously within the developing palate. Using quantitative real-time PCR and Western blot analysis, *Hoxa2* mRNA and protein, respectively, were detected in the developing palate of wild-type mice at E12.5, E13.5, E14.5, and E15.5 (Figs. 1, 3), which spans the period during which the palatal shelves emerge, elevate, and subsequently fuse. *Hoxa2* expression was highest at the two earliest time points, reaching an apparent peak at E13.5. By E14.5, *Hoxa2* mRNA expression decreased to a significantly lower level than at either E12.5 or E13.5 ($P < 0.05$), and it remained low at E15.5. As expected, *Hoxa2* transcripts were not detectable in palate tissues of *Hoxa2*$^{-/-}$ mice (Supp. Fig. S1, which is available online).

Immunohistochemical analysis of sections from the anterior, medial, and posterior regions of palates between E12.5 and E15.5 verified the presence of *Hoxa2* protein expression within the developing palate. Hoxa2

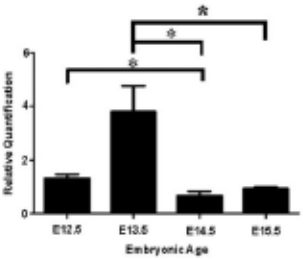

Fig. 1. Relative quantitative expression of the *Hoxa2* gene throughout murine palatogenesis. Relative *Hoxa2* expression levels in wild-type mouse palate shelves were determined by quantitative real time reverse transcriptase-polymerase chain reaction using Taqman primers and probes. Bars represent mean ± SEM, n = 3. *$P \leq 0.05$ between bars indicated by brackets.

was expressed in both the epithelium and the mesenchyme at E12.5 (Fig. 2a–c), and at increased levels by E13.5 (Fig. 2e–g). Hoxa2 expression appeared to generally decline throughout the palate by E14.5, with the highest expression observed in the midline epithelial seam (Fig. 2i–k). By E15.5, the contacted palate shelves had fused to mesenchymal confluence and low levels of Hoxa2 expression were persistent throughout the palate (Fig. 2m–o). In contrast, no Hoxa2 protein signal was detected in the palates of *Hoxa2* null mice confirming the specificity of the labeling (Figs. 2d,h,l,p, 3).

Altered Cell Proliferation in the Palatal Shelves of *Hoxa2*$^{-/-}$ Mice

To determine whether a loss of *Hoxa2* expression in the palate resulted in intrinsic changes in the growth of the palate primordial, we compared levels of cell proliferation and apoptosis within the anterior, medial, and posterior regions of the palate in wild-type and *Hoxa2* null palates at stages E12.5 through E15.5. Compared with normal wild-type *Hoxa2*$^{+/+}$ palates, a general trend toward increased cell proliferation rates was noted in the *Hoxa2* null palate shelves. In the anterior region, proliferation rates were significantly increased at E12.5, E14.5, and E15.5 ($P < 0.001$; Fig. 4a); in the medial (Fig. 4b) and posterior (Fig. 4c) regions, rates significantly in-

Developmental Dynamics

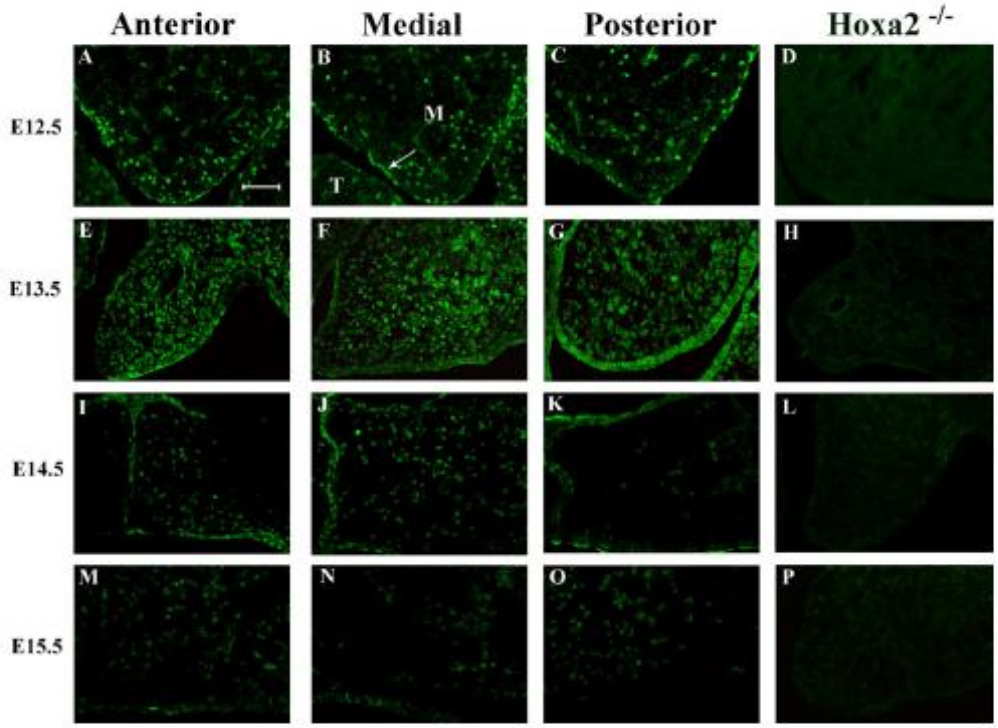

Fig. 2. Immunofluorescence staining of coronal sections from mouse embryos. Anterior, medial, and posterior palate sections are in the same orientation and from the same embryo. a–c, e–g, i–k, m–o: Green nuclear staining represents the expression of Hoxa2 protein at embryonic day (E) 12.5 (a–c), E13.5 (e–g), E14.5 (i–k), and E15.5 (m–o). d,h,l,p: Sections are from the respective anterior palatal region of *Hoxa2* null mice and show no staining. Arrow is pointing to the epithelium. M, mesenchyme; T, tongue. Scale bar = 5 μm.

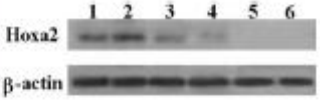

Fig. 3. Western blot analysis of protein extracted from palatal shelves of 12.5-, 13.5-, 14.5-, and 15.5-day-old mouse embryos. Proteins (30 μg) were separated on 10% polyacrylamide-sodium dodecyl sulfate gel and, after transfer to a polyvinylidene difluoride membrane, were probed with Hoxa2 antibody. Lane 1, embryonic day (E) 12.5; Lane 2, E13.5; Lane 3, E14.5; Lane 4, E15.5; Lane 5, E13.5 *Hoxa2*$^{-/-}$; and Lane 6, E14.5 *Hoxa2*$^{-/-}$.

creased at E12.5 and E14.5 ($P < 0.001$). A two-factor analysis of variance (ANOVA) of the proliferation data revealed a significant interaction between stage of development and genotype in all three palatal regions (anterior, medial, and posterior).

Palates were also examined for apoptosis at E12.5, 13.5, and 14.5 in both wild-type and *Hoxa2* null embryos. No difference in apoptosis was observed (Supp. Fig. S3).

Altered Gene Expression in the Palatal Tissue of *Hoxa2*$^{-/-}$ Null Mice

The expression of four genes known to be present in the palate—*Ptx1* (Lanctôt et al., 1997), *Barx1* (Welsh et al., 2007), *Msx1* (Zhang et al., 2002), and *Bmp4* (Zhang et al., 2002)—was analyzed at E12.5, E13.5, E14.5, and E15.5 using quantitative real time RT-PCR and Western blot analysis. Our results show *Ptx1* is expressed throughout palatogenesis in wild-type embryos (Figs. 5a, 6). *Hoxa2* null palates show a significant increase in *Ptx1* mRNA expression at E13.5 ($P < 0.01$), with levels equivalent to wild-type at E12.5, E14.5, and E15.5. Ptx1 protein also exhibited an increase in expression at E13.5 and E14.5 in the *Hoxa2* null palate shelves (Fig. 6).

Our results also demonstrate *Msx1* mRNA is expressed at all four ages in the wild-type palate (Fig. 5b). *Hoxa2* null palates exhibit a significantly higher expression of *Msx1* at E12.5 ($P < 0.01$), but have levels comparable to wild-type for the remainder of palatogenesis. Protein expression of Msx1 was also visibly increased at E12.5 as determined by Western blot analysis (Fig. 6). *Bmp4* is known to be downstream of *Msx1* in the palate (Zhang et al., 2002), so an increase in *Msx1* expression would be expected to be followed by an increase in *Bmp4* expression. As expected, *Bmp4* ex-

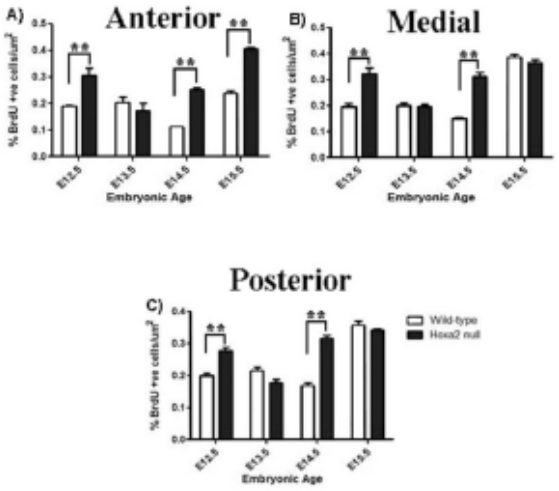

Fig. 4. Altered cell proliferation rates within *Hoxa2* null palates. Cell proliferation rates within the developing palate shown as mean percentage of cells that are 5-bromo-2'-deoxyuridine (BrdU) positive per μm^2 ±SEM. A–C: Sections from the anterior (A), medial (B), and posterior (C) regions of the palate from wild-type and *Hoxa2* null embryos were analyzed at E12.5, E13.5, E14.5, and E15.5 (n = 4). **P ≤ 0.001 between bars indicated by brackets.

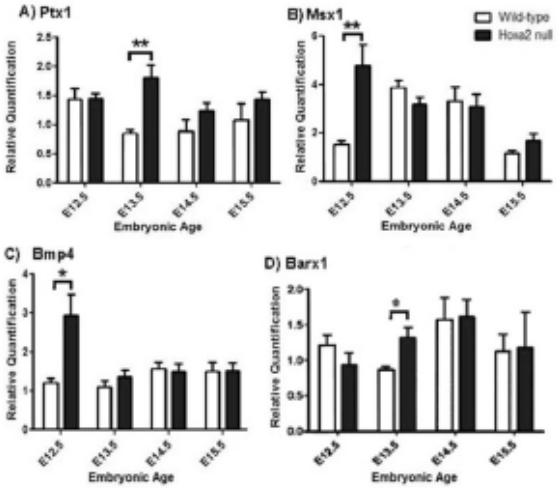

Fig. 5. Altered *Ptx1*, *Msx1*, *Bmp4*, and *Barx1* mRNA expression in *Hoxa2* null palate shelves. A–D: Relative quantitative expression of *Ptx1* (A), *Msx1* (B), *Bmp4* (C), and *Barx1* (D) throughout murine palatogenesis in $Hoxa2^{+/+}$ (wild-type) and $Hoxa2^{-/-}$ (knockout) embryos as determined by quantitative real-time reverse transcriptase-polymerase chain reaction using Taqman primers and probes. Bars represents mean ±SEM, n = 4. A single asterisk represents a significance $P \leq 0.05$, and a double asterisk represents a significance $P \leq 0.01$ between bars indicated by brackets.

pression increased at E12.5 in *Hoxa2* null palates ($P < 0.05$) with levels comparable to wild-type for the remainder of palate development (Fig. 5c). Bmp4 protein expression increased proportionally in the *Hoxa2* null palate shelves compared with wild-type at E13.5 and E14.5, representing a slight delay between increased mRNA message and an increase in the protein signal (Fig. 6).

In addition, an increase in the expression of *Barx1* mRNA was observed in the E13.5 *Hoxa2* null palates ($P < 0.05$) when compared with wild-type controls (Fig. 5d). Of interest, a similar increase in Barx1 was also observed at the protein level at E13.5 (Fig. 6).

Effects of *Hoxa2* Ablation on Palate Development and Fusion

Histological data comparing wild-type palatal development with that of the *Hoxa2* null mice (Supp. Fig. S2) indicates palatal shelves did not elevate in the *Hoxa2* knockout mice. An earlier study speculated that the occurrence of cleft palate in $Hoxa2^{-/-}$ mice is due to physical interference from the developing tongue resulting from abnormal attachment of the hyoglossus muscle to the greater horn of the hyoid bone (Barrow and Capecchi, 1999). However, we observed that the hyoglossus was properly attached to the hyoid in both wild-type and *Hoxa2* null embryos that exhibited cleft palate (Supp. Fig. S4), in agreement with the findings of Ohnemus et al. (2001). This suggests that the high incidence of cleft palate in $Hoxa2^{-/-}$ embryos is not merely a secondary defect due to abnormal positioning of the tongue. To determine whether genetic ablation of *Hoxa2* function might disrupt processes of palatal growth and fusion in a more direct intrinsic manner, we used an in vitro organ culture model in which whole palate explants were cultured in the absence of the tongue. Palates isolated from *Hoxa2* null embryos exhibited a high incidence of cleft defects even when cultured in the absence of the tongue (Table 1). Palate cultures from $Hoxa2^{-/-}$ embryos had significantly lower fusion rates

than cultured palates from either *Hoxa2*$^{+/-}$ or *Hoxa2*$^{+/+}$ animals ($P < 0.01$). In addition, more palates in *Hoxa2*$^{-/-}$ cultures either did not contact or contacted without fusion than in cultures of *Hoxa2*$^{+/-}$ or *Hoxa2*$^{+/+}$ palates.

In other experiments, *Hoxa2* expression was knocked down in palate cultures of wild-type embryos by infection with antisense *Hoxa2* retroviral particles at three different titers (Table 2) at both E12.5 and E13.5. The palates were assessed after 72 hr (E15.5). The fusion rates of *Hoxa2*$^{+/+}$ palates exposed to *Hoxa2* antisense retroviral particles were significantly lower than in wild-type palates infected with a control retroviral vector. Moreover, the low fusion rates of wild-type palates subjected to *Hoxa2* antisense knock down were comparable to those of cultured palates isolated from *Hoxa2*$^{-/-}$ mice. Quantitative real-time RT-PCR and Western blot analysis confirmed that the retroviral *Hoxa2* antisense infections effectively knocked down *Hoxa2* expression in the palate cultures (Supp. Fig. S5).

Palatal fusion rates were altered in the *Hoxa2* null embryos, but to determine whether loss of the *Hoxa2* gene led to inhibition of palatal fusion, E14 palate shelves from wild-type or *Hoxa2* null embryos were excised and arranged in pairs with their medial edges in contact and cultured for 72 hr (Shiomi et al., 2006; Nakajima et al., 2007). Fusion occurred with equal success in the *Hoxa2* null embryos at approximately 86% (Fig. 7; Table 3).

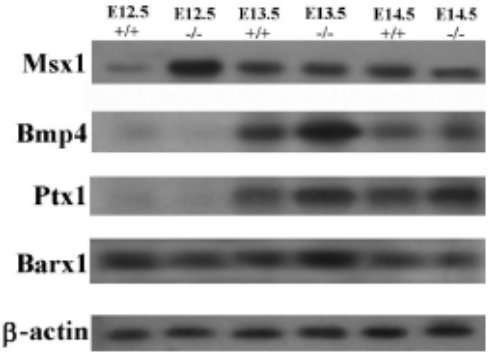

Fig. 6. Altered Msx1, Bmp4, Ptx1, and Barx1 protein expression in *Hoxa2* null palate shelves. Protein expression of Msx1, Bmp4, Ptx1, and Barx1 was analyzed by Western blot of palatal protein samples from *Hoxa2*$^{+/+}$ (wild-type) and *Hoxa2*$^{-/-}$ (knockout) at embryonic day (E) 12.5, E13.5, and E14.5.

DISCUSSION

Our data show that *Hoxa2* mRNA and protein are normally expressed throughout the palate in both the epithelium and mesenchyme during the critical periods of palatal shelf outgrowth, elevation, and fusion. Thus, although the *Hoxa2* gene is not expressed in the first branchial arch at stages before palatal process formation (Prince and Lumsden, 1994), its expression is activated within the palatal processes that subsequently emerge from the maxillary prominences of the first branchial arch. The intrinsic expression of *Hoxa2* in the palatal primordia suggests a possible role for *Hoxa2* in the regulation of early palatal growth. Moreover, we observed that genetic ablation of *Hoxa2* gene function in the *Hoxa2*$^{-/-}$ homozygous mice led to elevations in the rate of both cell proliferation within the palatal tissue as well as increases in the expression of putative *Hoxa2* target genes (*Msx1*, *Ptx1*, *Bmp4*, and *Barx1*). This suggests that the intrinsic action of *Hoxa2* within the palate is to regulate palatal tissue growth and patterns of downstream gene activation.

Barrow and Capecchi (1999) postulated that the cleft palate in *Hoxa2* null embryos is a secondary defect due to abnormal hyoglossus insertion to the greater horn of the hyoid bone leading to abnormal positioning of the tongue. However, our data indicate that the hyoglossus inserts properly into the hyoid regardless of the presence or absence of *Hoxa2* expression (Supp. Fig. S4), supporting similar findings by Ohnemus et al. (2001). Although other intrinsic or extrinsic factors could influence abnormal positioning of the tongue, our data raise the possibility that the malpositioning of the tongue may not be the primary cause of cleft palate in *Hoxa2* null embryos and are consistent with a more direct role for *Hoxa2* in palate development. Indeed, when palatal explants of *Hoxa2* null mice were cultured in the absence of the tongue, lower palatal fusion rates and lower contact rates were observed in comparison to palates from wild-type embryos. Furthermore, antisense retrovirus-mediated knock down of *Hoxa2* expression at E12.5 in wild-type palates resulted in decreased palatal fusion rates by E15.5 relative to controls, with *Hoxa2* antisense cultures resembling those of the *Hoxa2*$^{-/-}$ phenotype. The fusion rates for explant cultures of both *Hoxa2*$^{-/-}$ palates and palates with retroviral knock down of *Hoxa2* expression were in the range of 41–46%, which is considerably higher than the 20% reported for *Hoxa2* null embryos in vivo (Gendron-Maguire et al., 1993; Rijli et al., 1993; Barrow and Capecchi, 1999). Thus, interactions with the developing tongue could still play a role in contributing to the higher frequency of cleft palate seen in *Hoxa2* null embryos in vivo. Compared with wild-type embryos, *Hoxa2* null embryos may have disrupted synchrony between the rates of tongue and palate development, causing even a normally developed tongue to become a physical barrier between the rising palatal shelves. To demonstrate whether *Hoxa2* null palates were capable of fusion, E14 palatal explants were arranged in pairs with their medial edges in contact and in proper anterior–posterior orientation and allowed to culture for 72 hr (Shiomi et al., 2006; Nakajima et al., 2007). Palatal fusion was not impaired in *Hoxa2* null embryos (Fig. 7; Table 3), suggesting palatal growth

TABLE 1. Effects of *Hoxa2* Gene on Cultured Fetal Mouse Palates in Different Genotypes

Genotype of mouse embryos	Frequency of contacted but not fused palates	Frequency of fused palates	Frequency of non-contacted palates
Wild-type	10.0% (2/20)	90.0%** (18/20)	0%* (0/20)
Heterozygous	7.5%** (3/40)	78.7%** (37/47)	14.9% (7/47)
Hoxa2$^{-/-}$ Mutant	38.5%*** (5/13)	44.4%***,***** (8/18)	27.8%**** (5/18)

*$P \leq 0.05$, **$P \leq 0.01$ compared to *Hoxa2*$^{-/-}$ mutant, ***$P \leq 0.01$ compared to heterozygous.
****$P \leq 0.05$, *****$P \leq 0.01$ compared to wild-type.

TABLE 2. Effects of Retrovirus Infection on Wild-Type Cultured Mouse Palates

Virus and titer (cfu/ml)	Frequency of contacted but not fused palates	Frequency of fused palates	Frequency of non-contacted palates
Control			
0.016×10^5	5.3% (1/19)	81.8% (18/22)	13.6% (3/22)
0.08×10^5	0.0% (0/19)	86.4% (19/22)	13.6% (3/22)
0.8×10^5	0.0% (0/17)	77.3% (17/22)	22.7% (5/22)
Antisense *Hoxa2*			
0.016×10^5	0.0% (0/11)	45.8%* (11/24)	54.2% **(13/24)
0.08×10^5	10.0% (1/10)	40.9%** (9/22)	54.5% **(12/22)
0.8×10^5	10.0% (1/10)	45.0%* (9/20)	50.0% (10/20)

*$P \leq 0.05$, **$P \leq 0.01$ compared to respective control.

rate may be affected. Interestingly, we observed an overall increase in the rate of cell proliferation in the palatal shelves of *Hoxa2* null mice (Fig. 4), whereas apoptosis was not affected (Supp. Fig. S3). An increase in proliferation leading to a cleft palate phenotype was previously reported in mice lacking the Fgf antagonist *Spry2* (Welsh et al., 2007). The incidence of cleft palate penetrance in these animals is 83%, which is very similar to the frequency in *Hoxa2* null mice (81%).

Thus, although the in vitro knockout and knockdown organ cultures showed a decrease in the rate of fusion, mutant palate shelves appear to be capable of fusion if they are placed in close opposition as observed with the fusion organ cultures. The fusion organ cultures measure the ability of the palates to fuse with one another and eliminate any confounding issues that arise from the ability of the palate shelves to grow together and contact. The inability of the palate shelves to contact with one another properly (likely due to increased mesenchymal proliferation and altered palatal growth pattern) is believed to be the reason the in vitro knockout and knockdown cultures showed lower fusion rates.

Hoxa2 acts as a transcription factor and would presumably affect palatogenesis through regulating the expression of downstream targets. We have demonstrated that *Ptx1*, *Barx1*, *Msx1*, and *Bmp4* genes all exhibit altered expression profiles in the developing palates of *Hoxa2* null embryos compared with wild-type embryos, providing further support for a direct and intrinsic role for *Hoxa2* in palatogenesis. Through the regulation of these genes, *Hoxa2* might act to regulate cell proliferation within the developing palate.

Within the branchial arches, *Hoxa2* is known to activate *Msx1* expression (Santagati et al., 2005). However, our data suggest that *Hoxa2* represses *Msx1* expression in the developing palate. A significant increase ($P < 0.01$) in *Msx1* mRNA and protein expression was observed in E12.5 null mutants (Figs. 5b, 6). Cell proliferation in the anterior mesenchyme has been shown to be regulated by *Msx1* and its downstream targets including *Bmp4* (Zhang, et al., 2002). We found that *Bmp4* mRNA expression was increased at E12.5 together with *Msx1* (Fig. 5c). Bmp4 protein was also visibly increased at E13.5 and E14.5 and may indicate a delay in protein translation (Fig. 6). *Msx1* and *Bmp4* work within a feedback loop (Zhang et al., 2002), which might explain why mRNA levels return to wild-type levels by E13.5. Together, these data suggest that *Hoxa2* may influence cell proliferation and growth within the palate through regulation of *Msx1* and *Bmp4*.

Barx1 is expressed predominantly in the posterior regions of the palate shelves and is believed to play an important role in regulating cell proliferation in this region (Welsh et al., 2007). Increased expression of Barx1 in the *Hoxa2* null palate (Figs. 5d, 6) at E13.5 would, therefore, match the increased level of proliferation observed in the posterior regions of the palate.

Ptx1 is ectopically expressed within the second branchial arch of *Hoxa2* null embryos, and transgenic expression of *Hoxa2* in the first branchial arch is sufficient to block *Ptx1* expression. A partial reversion to the wild-type phenotype was observed in double mutants lacking both *Hoxa2* and *Ptx1* (Bobola et al., 2003). This suggests *Ptx1* is an im-

Developmental Dynamics

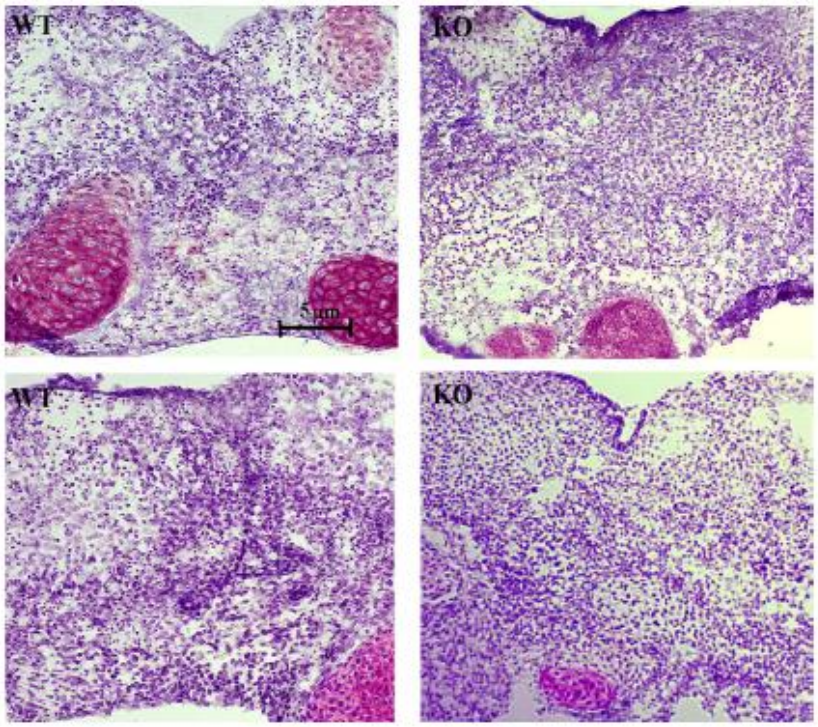

Fig. 7. Histological analysis for fusion of cultured palate shelves. After 72 hr in culture palate shelves were fixed, serial sectioned, and stained with cresyl violet to determine whether mesenchymal confluence was achieved. *Hoxa2* null and wild-type palates were equally capable of fusion.

TABLE 3. Effects of *Hoxa2* Gene on Cultured Fetal Mouse Palates of Different Genotypes

Genotype of embryo	No. of palates that fused	Total no. of palates cultured	% of fused palates
Wild-type	12	14	85.7
Heterozygous	14	15	93.3
Hoxa2$^{-/-}$ mutant	6	7	85.7

portant downstream target of *Hoxa2* in the second branchial arch. Our data show Hoxa2 also acts as a repressor of *Ptx1* in the developing palate. *Ptx1* expression is significantly increased in the *Hoxa2* null palates at E13.5 (Figs. 5a, 6) concurrent with peak *Hoxa2* expression in wild-type palates (Figs. 1, 3). This coincident expression could explain why *Hoxa2* appears to have a significant effect on *Ptx1* expression at this early stage. Thus, *Hoxa2* may block expression of *Ptx1* in the palate, similar to its role in the second branchial arch.

Our histological data indicates palatal shelves did not elevate in the *Hoxa2* knockout mice (Supp. Fig. S2). The mechanism of palate shelf elevation remains largely unclear and poorly defined at the present time. Various mechanisms have been put forward and these have not changed significantly from those reviewed by Lazzaro in 1940 and later by Ferguson in 1988. General consensus among researchers is that palate shelf elevation is a rapid process triggered by both intrinsic forces within the palate shelf and also influenced by other oral and craniofacial structures. Extracellular matrix was implicated by Lazzaro (1940) and studies have supported this and have identified progressive accumulation of hyaluronan to play an important role in palatal shelf elevation (reviewed in Ferguson, 1988). Collagen fibers, epithelial covering, and polarized alignment of mesenchymal cells have also been postulated to play a role in palatal shelf elevation (Ferguson, 1988). The neurotransmitter γ-aminobutyric acid (GABA) appears to play a role in palatal shelf elevation because it is reported that GABA agonists generate a cleft palate by inhibiting palatal shelf elevation, whereas GABA antag-

onist stimulate this process (Miller and Becker, 1975; Wee and Zimmerman, 1983). GABA as well as glutamic acid decarboxylase 67 (Gad 67), an enzyme important in GABA biosynthesis, is present in the palatal shelf (Wee et al., 1986; Asada et al., 1997; Hagiwara et al., 2003). It is possible that loss of *Hoxa2* which alters mesenchymal proliferation patterns affects GABA neurotransmitter signaling and changes the turnover of extracellular matrix which could contribute to delayed lifting of the shelves; however, this will have to await further studies.

In summary, we have demonstrated endogenous *Hoxa2* expression within the developing murine palate and have shown *Hoxa2* expression is necessary for normal palatogenesis. Although *Hoxa2* is not initially expressed within the first branchial arch, its expression appears to be switched on later in development within its derivative, the palate, where *Hoxa2* plays intrinsic roles in regulating both cell proliferation and gene expression during murine palatogenesis. Absence of *Hoxa2* did not inhibit the palatal fusion process; it does, however, induce an increase in mesenchymal cell proliferation, which will alter the palatal growth pattern and likely affect palatal elevation, preventing the palatal shelves from coming together for fusion.

EXPERIMENTAL PROCEDURES

Hoxa2 Transgenic Mice

Hoxa2$^{+/+}$, *Hoxa2*$^{+/-}$, and *Hoxa2*$^{-/-}$ C57 black mice were obtained by timed heterozygous matings. They were staged according to Kaufman (1992) and were considered E0 days pregnant on the day the vaginal plug was found. *Hoxa2*$^{+/+}$, *Hoxa2*$^{+/-}$, and *Hoxa2*$^{-/-}$ mice genotypes were confirmed by PCR analysis (Gendron-Maguire et al., 1993). CD-1 mice were used for wild-type palatal organ cultures treated with *Hoxa2* antisense retroviral particles.

Whole Palatal Organ Culture

Whole mouse palatal organ cultures were established according to the protocol outlined by Abbott et al. (1999) with modifications as indicated below. Pregnant females at embryonic stage E12.5 were anesthetized by halothane (MTC Pharmaceuticals). Fetuses were aseptically removed from the uterus in Hanks' balanced solution (Sigma). The maxillary regions were dissected by removing the mandible and tongue as well as the brain and the spinal cord from the posterior region of the palate. Palates were placed, intact, in sterile 60-ml glass bottles containing 10 ml of Richter's Improved Zinc MEM Option and F12 Nutrient Medium (Invitrogen) (1:1), supplemented with 1% fetal bovine serum, 6 mg/ml bovine serum albumin, 10 μg/ml transferrin, 10 ng/ml selenium, 50 μg/ml sodium ascorbate, 2.4 mg/ml glucose, 0.6 mg/ml L-glutamine, 50 μg/ml streptomycin, and 50 units/ml penicillin (Sigma). Bottles were flushed with 50% O_2, 45% N_2, and 5% CO_2 for 2 min and then incubated at 37°C, circulated at 12–15 rpm. Every 24 hr the media was changed, flushed with the same gas mixture, and cultures incubated as indicated above. After 72 hr (E15.5), the palates were assessed and relevant parameters such as frequency of contacted but not fused, frequency of noncontacted palates, and frequency of fused palates were measured with a micrometer under a dissecting microscope.

Cell Proliferation Assay

Cell proliferation was assessed by intraperitoneal injection of timed-pregnant mice with 5-bromo-2′-deoxyuridine (BrdU) at a concentration of 100 mg/kg body weight. BrdU is a thymidine analogue that is taken up and incorporated into the DNA of proliferating cells, including those in the developing embryos. One and a half hours after injection, mice were killed, and the harvested embryos fixed and sectioned as described in the Immunohistochemistry section. Sections were immunohistochemically stained with a monoclonal anti-BrdU antibody (Sigma) and the Mouse on Mouse staining kit (Vector Laboratories) to detect proliferating cells, using a modified procedure as follows: briefly, the sections were pretreated by rehydrating the tissue sections in phosphate buffered serum (PBS) 0.1% Triton X-100 before being exposed to 1 N HCl on ice for 10 min and then 2 N HCl for 10 min at room temperature followed by a 40 min incubation at 37°C. Sections were neutralized with 0.1 M sodium borate, followed by three 5-min washes in PBS-1% Triton-X100. Endogenous biotin and avidin was blocked using the Avidin-Biotin blocking kit (Vector Laboratories) as per the manufacturer's protocol. After incubating the section in the blocking reagent overnight at 4°C, the remainder of the procedure was as per the manufacturer's protocol. Finally, sections were counter stained with Hoescht and mounted in Prolong (Molecular Probes). Sections from the anterior, medial and posterior regions of wild-type and *Hoxa2* null embryos at E12.5, E13.5, E14.5, and E15.5 were analyzed. The mitotic index was only calculated for the mesenchyme region of the palate due to an inability to gain accurate total cell counts from the epithelium. The percentage of total cells that were BrdU positive per unit area was used as the mitotic index.

TUNEL Assay

Cell survival and apoptosis was measured using the DeadEnd Fluorometric TUNEL (terminal deoxynucleotidyl transferase-mediated dUTP nick-end labeling) System (Promega) as per the manufacturer's protocol. Tissue from the anterior, medial, and posterior regions of wild-type and *Hoxa2* null embryos at E12.5, E13.5, and E14.5 were examined for apoptotic cell death.

RNA Isolation and Reverse Transcription

Total RNA was isolated from excised wild-type and *Hoxa2* null embryo palate shelves using the RNeasy Protect Mini Kit (Qiagen) as per the manufacturer's protocol. RNA concentration was determined by optical density. First-strand DNA synthesis was performed using the SuperScript first-strand synthesis system for RT-PCR (Invitrogen) and random decamer primers, as per the manufacturer's protocol. The final concentration of RNA for all RT reactions was 20 ng/μl.

Quantitative Real Time RT-PCR

Gene expression was quantified using the Taqman primers and labeled probe system and the ABI 7300 (Ap-

plied Biosystems). Wild-type and *Hoxa2* mutant embryo palates at E12.5, E13.5, E14.5, and E15.5 were tested for *Msx1*, *Bmp4*, *Barx1*, and *Ptx1*; only wild-type tissue was tested for *Hoxa2*. All reactions were performed using the Taqman Universal Master Mix (2X), FAM-labeled Taqman Gene Expression assays for gene of interest, VIC-labeled Taqman Endogenous Control β-actin, and 10 ng of cDNA. All reactions were run in replicates of 4, with n = 4. Thermocycling parameters were as follows: 2 min at 50°C, 10 min at 95°C, 40 cycles of 15 s at 95°C, plus 70 s at 60°C.

Immunohistochemistry

The *Hoxa2* rabbit polyclonal antibody was generated using oligopeptide SPLTSNEKNLKHFQHQS (Hao et al., 1999; Nazarali et al., 2000). Time staged embryos were fixed in 4% paraformaldehyde followed by immersion in 20% sucrose in PBS. Frozen embryos in embedding medium were sectioned (8 μm thick), and tissue sections were collected on gelatin-coated coverslips. Coverslips were dried for 2 hr at room temperature before being subjected to immunohistochemical analysis with TSA #22 (Invitrogen) using the following modified procedure. Coverslips with tissue sections were incubated twice in PBS, 5 min each time, followed by a 1-hr incubation in a 3% hydrogen peroxide solution. This was followed by two 5-min washes in PBS and then 30 min in the manufacturer provided block solution. After blocking, sections were incubated overnight at 4°C with the *Hoxa2* specific antibody at a dilution of 1:5,000 in the block solution. Sections were rinsed in PBS twice (5 min each) and then incubated in biotinylated anti-rabbit secondary antibody (Vector Laboratories) at 1:100 dilution for 1 hr at room temperature. Sections were then washed twice (5 min each) in PBS, followed by a 30-min incubation in the avidin-horseradish peroxidase antibody at 1:100 dilution. The sections were washed twice in PBS for 5 min each, then incubated in the Alexa Fluor 488-conjugated tyramide diluted to 1:200 in the amplification buffer for 10 min, and then counterstained with Hoechst before being mounted in Prolong (Molecular Probes).

Western Blot Analysis

Protein was isolated from wild-type and *Hoxa2* null mutant embryonic palatal shelves by lysis in RIPA buffer (150 mM NaCl, 10 mM Tris, 0.1% sodium dodecyl sulfate [SDS], 1% Triton X-100, 1% deoxycholate, 5 mM ethylenediaminetetraacetic acid). Protein was quantified using the Bio-Rad Detergent Compatible Protein Assay kit (Bio-Rad) to ensure equal loading on gel. Samples were then boiled for 20 min with loading buffer and loaded on a 10% polyacrylamide-SDS gel. After separation the proteins were transferred to a PolyScreen PVDF membrane, which was blocked overnight in 3% skim milk in PBS (SM-PBS) at 4°C. The membrane was then exposed to primary antibody for 1 hr at 28°C (*Hoxa2*, 1:1,000; Ptx1, goat polyclonal, Santa Cruz, 1:100; Msx1, rabbit polyclonal, Developmental Studies Hybridoma Bank, 1:500; Bmp4, goat polyclonal, Santa Cruz 1:200; Barx1, goat polyclonal, Santa Cruz, 1:200). This was followed by 3 consecutive washes of 10 min each in PBS with 0.08% Tween-20. After the washes were complete, the membrane was incubated with the secondary antibody, goat anti-rabbit IgG horseradish peroxidase conjugate (Bio-Rad) in SM-PBS at a dilution of 1:3,000 for 1 hr at 28°C. After 3 washes of 40 min each in PBS-Tween-20 the membrane was exposed with a chemiluminescent reagent (DuPont NEN) and signal was detected by exposing to X-ray film. The membrane was then washed overnight in PBS at 4°C before being incubated with the anti–β-actin at a dilution of 1:1,000, and incubated for 1 hr at room temperature, followed by 3 washes in PBS with 0.08% Tween-20. After the washes, the membrane was exposed to the anti-mouse IgM horseradish peroxidase conjugate (Bio-Rad) in SM-PBS at a dilution of 1:1,500, washed and membrane exposed to X-ray film as indicated above.

Hoxa2-Antisense Retroviral Particles

Hoxa2 cDNA was restriction digested from the recombinant plasmid pRSV-D0C-*Hoxa2* with *Hind*III and *Xho*I (Tan et al., 1992) and used as a template to PCR amplify the *Hoxa2* antisense sequence using the following primers: forward 5-ggctcgagccatgaattacgaatttgagcg-3, reverse 5-ggaagctttttagtaattcagatgctgtaggtcg-3. The *Hoxa2* antisense DNA was then cloned into a retroviral vector pLECFP-C1 (BD Biosciences Clontech) at the same two restriction enzyme sites; the sequence of the pLEGFP-*Hoxa2* antisense construct was confirmed with an ABI PRISM system. The EcoPack2-293 packaging cell line (BD Biosciences Clontech) was cultured as per the manufacturer's instructions, and the recombinant retrovirus expressing *Hoxa2* antisense was generated by transfecting the recombinant construct pLEGFP-*Hoxa2* antisense into the packaging cells using SuperFect reagent (Qiagen). Desired transfection efficiency was verified by EGFP protein expression. Subsequently, a selection of stable retrovirus producer cells were harvested from a medium containing 400 μg/ml of G418 (Sigma) after 14 days. The retrovirus producer cells were then cultured to 90% confluence, and the supernatant containing retroviral particles collected. Viral stocks were centrifuged and filtered through a 0.45-μm filter and stored at −80°C. Viral titer was determined by infecting NIH-3T3 cells.

Transduction of Palatal Organ Culture

Viral stocks were added to a palatal organ culture medium to reach final concentrations of 10^5, 10^4, and 10^3 cfu/ml at both E12.5 and E13.5. The palates were assessed after 72 hr (E15.5) and measured for the same parameters as the whole palatal organ cultures above. The desired transduction effect was verified by observing EGFP expression using confocal microscopy. The ability of the antisense retroviral construct to knock down *Hoxa2* expression was confirmed by quantitative real time RT-PCR and Western blot analysis.

Fusion Cultures

Pregnant CD-1 mice (E14) were killed by cervical dislocation after anesthesia with Halothane (MTC Pharmaceuticals) and the embryos were aseptically removed in Hanks' Balanced Salts solution (Sigma-Aldrich). The palate shelves were aseptically dissected and palate shelf cultures set up as previ-

ously described (Shiomi et al., 2006; Nakajima et al., 2007) with two modifications: the addition of 1 M HEPES (4-(2-hydroxyethyl)-1-piperazineethanesulfonic acid) to a final concentration of 20 mM and addition of a penicillin–streptomycin antibiotic solution to a final concentration of 0.1% (Sigma-Aldrich). In brief, the E14.0 palate shelves were excised and arranged in pairs with their medial edges in contact and in proper anterior–posterior orientation on Nucleopore Polycarbonate Track-Etch filters (8.0 μm pore; Whatman, Inc.). Two filters were floated in a 35-mm tissue culture dish containing 1.4 ml of BGJb medium (Invitrogen), supplemented as indicated above, and incubated with 5% CO_2 at 37°C for 72 hr. After 72 hr incubation, cultures were observed under a light microscope to determine whether the palate shelves fused. Cultured palatal shelf explants were sectioned in a coronal plane and stained with cresyl violet to ensure that the midline epithelial seam was degraded. Fusion rates were compared between wild-type, heterozygous, and *Hoxa2* null mutant embryos.

Histological Analysis

The *Hoxa2*$^{-/-}$ and wild-type newborn palate specimens were fixed in Bouin's solution, embedded in paraffin, then 4-μm-thick sections were stained with hematoxylin and eosin.

Statistical Analysis

Statistical analysis on quantitative real-time RT-PCR data was performed using a Student's *t*-test between wild-type and *Hoxa2* null palate shelves at each stage. A Chi-square paired-sample test was applied to compare the frequencies of contacted and fused palates. Cell proliferation data were analyzed statistically by comparing mean values using two-way ANOVA and Bonferroni post-tests for comparing groups. A significant P value of less than or equal to 0.05 was adopted for all comparisons.

ACKNOWLEDGMENTS

We thank Dr. Filippo Rijli for his review of our manuscript. A.J.N. was funded by a grant from the Natural Sciences and Engineering Research Council of Canada.

REFERENCES

Abbott BD, Held GA, Wood CR, Buckalew AR, Brown JG, Schmid J. 1999. AhR, ARNT, and CYP1A1 mRNA quantitation in cultured human embryonic palates exposed to TCDD and comparison with mouse palate in vivo and in culture. Toxicol Sci 47:62–75.

Akin ZN, Nazarali AJ. 2005. Hox genes and their candidate downstream targets in the developing central nervous system. Cell Mol Neurobiol 25:697–741.

Alasti F, Sadeghi A, Sanati MH, Farhadi M, Stollar E, Somers T, Van Camp G. 2006. A mutation in HOXA2 is responsible for autosomal-recessive microtia in an Iranian family. Am J Hum Genet 82:982–991.

Asada H, Kawamura Y, Maruyama K, Kume H, Ding R-G, Kanbara N, Kuzume H, Sanbo M, Yagi T, Obata K. 1997. Cleft palate and decreased brain gamma-aminobutyric acid in mice lacking the 67-kDa isoform of glutamic acid decarboxylase. Proc Natl Acad Sci U S A 94:6496–6499.

Barrow JR, Capecchi MR. 1999. Compensatory defects associated with mutations in Hoxa1 restore normal palatogenesis to Hoxa2 mutants. Development 126:5011–5026.

Bobola N, Carapuço M, Ohnemus S, Kanzler B, Leibbrandt A, Neubüser A, Drouin J, Mallo M. 2003. Mesenchymal patterning by Hoxa2 requires blocking Fgf-dependent activation of Ptx1. Development 130:3403–3414.

Ferguson MW. 1988. Palate development. Development 103(suppl):41–60.

Gendron-Maguire M, Mallo M, Zhang M, Gridley T. 1993. Hoxa-2 mutant mice exhibit homeotic transformation of skeletal elements derived from cranial neural crest. Cell 75:1317–1331.

Grammatopoulos GA, Bell E, Toole L, Lumsden A, Tucker AS. 2000. Homeotic transformation of branchial arch identity after Hoxa2 overexpression. Development 127:5355–5365.

Hagiwara N, Katarova Z, Siracusa LD, Brilliant MH. 2003. Nonneuronal expression of the GABA(A) beta3 subunit gene is required for normal palate development in mice. Dev Biol 254:93–101.

Hao Z, Yeung J, Wolf L, Doucette R, Nazarali A. 1999. Differential expression of Hoxa-2 protein along the dorsal-ventral axis of the developing and adult mouse spinal cord. Dev Dyn 216:201–217.

Kaufman MH. 1992. The atlas of mouse development. New York: Academic Press. p 1–512.

Lanctôt C, Lamolet B, Drouin J. 1997. The bicoid-related homeoprotein Ptx1 defines the most anterior domain of the embryo and differentiates posterior from anterior lateral mesoderm. Development 124:2807–2817.

Lazzaro C. 1940. Sul meccanismo di chiusura del palato secondario. Monit Zool Ital 51:249–273.

Miller RP, Becker BA. 1975. Teratogenicity of oral diazepam and diphenylhydantoin in mice. Toxicol Appl Pharmacol 32:53–61.

Nakajima A, Ito Y, Asano M, Maeno M, Iwata K, Mitsui N, Shimizu N, Cui X-M, Shuler CF. 2007. Functional role of transforming growth factor-beta type III receptor during palatal fusion. Dev Dyn 236:791–801.

Nazarali A, Puthucode R, Leung V, Wolf L, Hao Z, Yeung J. 2000. Temporal and spatial expression of Hoxa-2 during murine palatogenesis. Cell Mol Neurobiol 20:269–290.

Nazarali A, Kim Y, Nirenberg M. 1992. Hox-1.11 and Hox-4.9 homeobox genes. Proc Natl Acad Sci U S A 89:2883–2887.

Ohnemus S, Bobola N, Kanzler B, Mallo M. 2001. Different levels of Hoxa2 are required for particular developmental processes. Mech Dev 108:135–147.

Pasqualetti M, Ori M, Nardi I, Rijli FM. 2000. Ectopic Hoxa2 induction after neural crest migration results in homeosis of jaw elements in Xenopus. Development 127:5367–5378.

Prince V, Lumsden A. 1994. Hoxa-2 expression in normal and transposed rhombomeres: independent regulation in the neural tube and neural crest. Development 120:911–923.

Rijli FM, Mark M, Lakkaraju S, Dierich A, Dollé P, Chambon P. 1993. A homeotic transformation is generated in the rostral branchial region of the head by disruption of Hoxa-2, which acts as a selector gene. Cell 75:1333–1349.

Santagati F, Minoux M, Ren S-Y, Rijli FM. 2005. Temporal requirement of Hoxa2 in cranial neural crest skeletal morphogenesis. Development 132:4927–4936.

Shiomi N, Cui X-M, Yamamoto T, Saito T, Shuler CF. 2006. Inhibition of Smad2 expression prevents murine palatal fusion. Dev Dyn 235:1785–1793.

Tan DP, Ferrante J, Nazarali A, Shao X, Kozak CA, Guo V, Nirenberg M. 1992. Murine Hox-1.11 homeobox gene structure and expression. Proc Natl Acad Sci U S A 89:6280–6284.

Wee EL, Zimmerman EF. 1983. Involvement of GABA in palate morphogenesis and its relation to diazepam teratogenesis in two mouse strains. Teratology 28:15–22.

Wee EL, Norman EJ, Zimmerman EF. 1986. Presence of gamma-aminobutyric acid in embryonic palates of AJ and SWV mouse strains. J Craniofac Genet Dev Biol 6:53–61.

Welsh IC, Hagge-Greenberg A, O'Brien TP. 2007. A dosage-dependent role for Spry2 in growth and patterning during palate development. Mech Dev 124:746–761.

Zhang Z, Song Y, Zhao X, Zhang X, Fermin C, Chen Y. 2002. Rescue of cleft palate in Msx1-deficient mice by transgenic Bmp4 reveals a network of BMP and Shh signaling in the regulation of mammalian palatogenesis. Development 129:4135–4146.